Alma Mater Studiorum – Università di Bologna

DOTTORATO DI RICERCA IN

Ingegneria elettronica, telecomunicazioni,
e tecnologie dell'informazione

Ciclo XXIX

Settore Concorsuale di afferenza: 09\F2

Settore Scientifico disciplinare: ING-INF\03

Network Coding Strategies for Satellite Communications

Presentata da: **Ala Eddine Gharsellaoui**

Coordinatore Dottorato

Prof. Alessandro Vanelli-Coralli

Relatore

Prof. Daniele Tarchi

Correlatori:

Prof. Alessandro Vanelli-Coralli

Dr. Samah A. M. Ghanem

Esame finale anno 2017

To my loving family . . .
To my mother: *whatever I do, can not even repay a small fraction of her sacrifices.*
To my father: *for his kindness heart.*
To my brothers and sisters: *for their encourage and trust.*
. . . **To my respected Supervisors** . . .
To Daniele: *for his continuing and patient assistance.*
To Samah: *for her huge efforts and thoughts.*
To Alessandro: *for his unlimited trust and support.*
. . . **To my colleagues** . . .
Who were my companions through PhD journey.

Declaration

I hereby declare that except where specific reference is made to the work of others, the contents of this dissertation are original and have not been submitted in whole or in part for consideration for any other degree or qualification in this, or any other university. This dissertation is my own work and contains nothing which is the outcome of work done in collaboration with others, except as specified in the text and Acknowledgements.

Ala Eddine Gharsellaoui
April 2017

Abstract

Network coding is one of the technologies by which the network services are almost optimal, in terms of reliability, latency and data rate. The main advantage of network coding structure is to reduce the necessity for re-transmissions of packets. Satellite Communications (SatComs) are one of the potential applications that can leverage on the benefits of network coding due to their challenging fading environments and high round trip times.

In order to extend the network coding gains, the physical layer-awareness is taken into consideration in an adaptation mechanism. In this thesis, we propose different rate and energy efficient adaptive network coding schemes for time variant channels. We compare our proposed physical layer adaptive schemes to physical layer non-adaptive network coding schemes for time variant channels. The adaptation of packet transmissions on the basis of the channel variations over time, and their corresponding time-dependent erasures, allows proposed schemes to achieve significant gains in terms of throughput, delay and energy efficiency. A trade-off between energy efficiency and delay-throughput gains is also highlighted to demonstrate the favor of adaptive approaches to the less transmissions under high erasures, and hence, they may cause a rise in delay and lower throughput gains compared with non-conservative approaches that favor more transmissions to account for high erasures. It shows that these schemes are robust for large and small size of packets. Although, the energy per bit is affected, a similar rate and energy gains can be arise. However, the performance gains are not motivated by the packet size, but through duty cycle silence of transfer packets.

In this thesis, virtual schemes are also proposed to solve an open literature problem in the network coding. The objective is to find a quasi-optimal number of coded packets to multicast to a group of independent wireless receivers suffer from a different channel conditions. In particular, we propose a virtual network that allows for the representation of a group of receivers as a multicast group to be visible as one receiver and single channel. This approach allows for the transmission system to be adapted to the all receivers presented in the multicast group as it adapts to the virtual channel. To this regard, two different visualization plans have been proposed. The first scheme plan is to benefit from “ erase Max package ” in order to create a virtual reference for the network channel. The second scheme plan is taking the maximum completion time “ Max CT ” as a maximum time standard of the worst

reception channel, then implementing such virtual channel as a reference for all receivers in the multicast group. These schemes are applied to LEO/MEO/GEO satellite scenarios. It demonstrates remarkable gains compared to that strategy in which the adaptation depends only on one receiver point-to-point.

Publications

[1] A. E. Gharsellaoui, S. A. M. Ghanem, D. Tarchi, and A. Vanelli- Coralli, “Adaptive network coding schemes for satellite communications,” in 2016 8th Advanced Satellite Multimedia Systems Conference and the 14th Signal Processing for Space Communications Workshop (ASMS/SPSC), Sept 2016, pp. 1–7.

[2] A. E. Gharsellaoui, S. A. M. Ghanem, D. Tarchi, and A. Vanelli-Coralli, “Energy efficient adaptive network coding schemes for satellite scenarios,” in 8th EAI International Conference on Wireless and Satellite Systems (formerly PSATS), Cardiff, UK, Sep. 2016.

[3] S. A. M. Ghanem, A. E. Gharsellaoui, D. Tarchi, and A. Vanelli-Coralli, “Network coding channel virtualization schemes for satellite multicast communications,” in IEEE GLOBECOM (submitted), Singapore, December 4-8, 2017.

[4] S. A. M. Ghanem, A. E. Gharsellaoui, D. Tarchi, and A. Vanelli-Coralli, “Physical layer aware adaptive network coding schemes for satellite communications (submitted),” International Journal of Satellite Communications and Networking, 2016.

Table of contents

List of figures

List of tables

Chapter 1

Introduction

1.1 State of the art on 5G and satellite techs

The coming years will be characterized by the introduction of a novel standard, often referred as 5G, aiming at defining a set of techniques for enabling the future of the wireless transmissions. Differently from the previous standards, like LTE, 3G, one of the main novelty of the 5G is to drive the wireless communications towards a single and unique standard enable to support different scenarios and requirements. Some key changes are required in the structure of current generation in order to move towards the next for mobile radio communications systems " 5G ".

Nowadays, many organizations all over the world have already launched the operations to develop new standards towards 5G visions. Where it reached to the need for dense network of small cells operating in the millimeter wave bands that are adaptable and software-controlled structure.

However, the role of satellite in 5G vision could have several potential places, such as the extension of coverage, content distribution, flexibility to use the spectrum integrated with other systems, broadcasting and reliability. While in the past most of the expectancy was toward high throughput communication systems, the last years have been characterized by an increasing request of low throughput techniques for supporting the Internet of Things scenarios. Those techniques may include the reduction in latency and energy consumption, and the administration ability of the massive number of objects as the case of (Internet of Things). In addition to that the management of high data rate traffic could also be considered as one of the new big challenges of the next generation.

In paper [2], the authors expose the possibility of using the satellite links within the emerging standards of 5G as flexible back-haul in the Internet future. Indeed, their analysis on effects, benefits and opportunities for the integration of satellite links was devised based on studies conducted in the framework of the European Space Agency ARTES 1 "to provide integrated services via satellite and terrestrial networks in order to provide a flexible backhaul links in 5G.

Not so far from the previous paper, the paper [3] has drawn a strategy for satellites in 5G that has been done under some work of the "Working Group Satellite" in the European technology platform NETWORLD2020. the author has first reviewed 5G visions and their drivers as specified by 5GPPP Association through the mobile terrestrial mobile society. Then the paper identifies how to integrate the satellite technology within 5G system and the difficulties which may face the expected contributions of satellite by 2020.

The paper [4] expects number of characteristics to be at the high-end in order to meet the next generation of telecommunications. Those features include: connectivity everywhere, extremely low latency, very high-speed data transfer, the spectrum utilization, and device diversity. Actually, satellite technology could provide some of them, and yet need the collaboration with the terrestrial networks. However, the paper also specifies the challenges to such achievements in terms of energy optimization, device flexibility, handling interference, high reliability, mobility and hand-off, security and the privacy for end users. Then the authors conceive the applications that need the advanced features of the 5G, as in the case of, heath care systems, smart grids, and D2D communication.

In paper [5], the authors gave an architecture of a hybrid satellite terrestrial network, where the satellites collaborate with terrestrial femtocells for providing functionality to the plane. Based on the feasibility of the proposed network structure, the "dual connectivity" feature, it enables transmission of U-plane and C- plane to be simultaneous from the different nodes. In addition, the authors depict cognitive ability of the satellites and their intelligence to maximize the utilization of resources and radio link performance. Such as, the location information of UEs and femtocells within their coverage, which enables UEs connecting to femtocells more appropriate. In typical, satellite offers significant reduction in physical infrastructure and maintenance cost since it has the ability to cover and control an entire country.

Other vision of integrating satellite into the terrestrial network is carried out through [6], where the authors defined some main functions that should be developed such those in the current protocols to facilitated for example the handover procedures. Other changes to be done in the management structure in order to harmonize the network procedures for the emergency cases. In addition, authentication, security, billing, load balancing and QoS are all necessary for expected services such as peer-to-peer and near video on demand. Based on the rapid growth of small satellites, a different role has been proposed in [7]. This role has been considered as a result of the advances in modern manufacture which enables to miniaturize the electronics components and so to the size of those machines. However, the main interesting advantage is their suggestion of new modulator that uses the Software Defined Radio(SDR) architecture in the context of 5G systems. In which, the different broadcasting technologies, such as Gaussian Minimum Shift Keying (GMSK), phase shift keying (PSK) and orthogonal frequency division multiplexing (OFDM) can be deployed quickly under the care of SDR.

Another foretelling of which satellite service could be the most promising is the multimedia content delivery. This adoption has been carried out in [8]. Where the authors designed a new algorithm for the management of radio resources in order to optimize multicast multimedia transmission. Their approach has used the experienced channel qualities to form an index called multicast subgrouping-maximum satisfaction (MS-MSI) to divide the muticast terminals into different subgroups, and hence provides the best tradeoff between user throughput and equity. Another promising satellite service in 5G is the vehicle positioning using mmWave signals [9]. The approach examined the mmWave capabilities and concluded with finding out a tradeoff between ranging accuracy and computational complexity. Moreover, this tradeoff is based on the choice of using between the energy detector or correlation receiver. However, some conditions that can not be avoided and can attenuate energy signal, and hence, make it difficult for the design system to achieve the intended results [10]. Especially, for the case of mmWave signals where the deployment of mmWave communication systems requires a wide knowledge of the characteristics of the mmWave propagation channel, and to know the main challenges, as well as the solutions and benefits associated with the use of mmWaves [11].

The participation between satellite and 5G small cells has gained an importance attention among the researcher communities. In particular, a study [12] has been conducted to figure out the possibility of the coexistence of 5G small cells with fixed satellite systems (FSSs), with analyses of the interference resulted by FSS radiation over the base stations (BSs). According to their results of using realistic FSS parameters and radiation pattern, combined with very recent channel, that the co-channel deployment of 5G small cells with FSS earth stations is a possible option for 5G systems, taking into account a large number of antennas with a proper distance between the FSS and BS cellular, as well as a different deployments of mobile transmitters.

The strength of a signal is reduced as a natural consequence of signal transmission over long distances. Attenuation is caused by different factors like the path loss which causes power loss to the signal. The path loss depends on the travelling path distance of the signal and the clearance of this path. Path loss is typically modelled as a (single-slope or multi-slope) power-law dependency on distance plus a log-normally distributed shadowing attenuation [13]. Another factor is the free space loss which is a loss in signal strength resulted by the propagation of electromagnetic waves in the space. However, antenna systems play an important role to accurate the evaluation of the noise temperature, particularly if the specifications of the antenna alone are a few Kelvins as in applications for radio astronomy [14]. Also, receiver sensitivity and system characteristics are of great importance, since for a certain performance the receiver may have a minimum RF signal power level. In addition, Effective Isotropic Radiated Power (EIRP) which represents the transmitted output power minus cable loss plus the transmitting antenna gain.

In reality, fading phenomena has a big concern since it happens by other factors such as, multipath propagation. The transmitted signals may travel in different path having different length, attenuation and delays. Then, at the receiver they may be summed and resulting an attenuated signal. In the study of multipath propagation [14], the challenge was to estimate the fading coefficients for uncorrelated sources. In this study some high-resolution algorithms are utilized to estimate the fading coefficients of a challenging environment containing many correlated signals. Another reason for fading phenomena is of the line of sight (LOS) having some obstacles around it. LOS describes the imaginary straight line that connect the receiver antenna with the transmitter antenna. As an example, LOS component dominates the fading of millimeter-wave (mmWave) communication at 60GHz [15], because of the characterization scarcity of high-GHz frequencies by Rayleigh or Rician distribution. Weather conditions and forecasts have also an important source of fading such as rain and wind. However, there are some techniques that may deal probably with rain attenuation characteristics, a type of antenna called “Lune-Q antenna” for terrestrial digital broadcasting system [16]. The Lune-Q antenna shows performance against rain attenuation compared to the parabolic antenna about 1/10 times better. This performance is due to the design of Lune-Q to be as multi-path reception, the feed horn position, and the polarization effects, etc.

In telecommunications, the signal maybe modified or disrupted along the channel between the source and the receiver. This kind of disruption caused by additional signals to the original one and it is called the signal interference. The main example of interference is the electromagnetic interference (EMI), or radio-frequency interference (RFI) which is defined according to the International Telecommunication Union’s (ITU) as: «the effect of unwanted energy due to one or a combination of emissions, radiations, or inductions upon reception in a radiocommunication system, manifested by any performance degradation, misinterpretation, or loss of information which could be extracted in the absence of such unwanted energy» [17]. This disturbance reduces the performance of the data transmission along the channel path, hence, it increases the error rate or even to cause a total loss in the transmitted data [18].

The most well-known classification for satellite orbits uses the altitude, i.e., how much far the satellite evolving above the earth. Each orbit has its own perspective that has valuable characteristics than the others. For example, the distinctive one is the geostationary orbit (GEO) because it is fixed above a certain point on the earth's surface, and hence, it is suitable for application such as television broadcasting. GEO orbit has an altitude of 35,786 kilometers. At this altitude the orbit period is the same as the Earth's rotation period around its self. The propagation time for a radio signal to travel from a ground station to the satellite and back again to the station is about 239.6 milliseconds (ms) [19]. Therefore, the total delay for transmitting a signal and its corresponding reply (one round-trip time or RTT) could be at least 558 ms. There is also an additional delay time such like the time used for transmission time or buffering the data inside a system.

Another kind of orbits is the Low Earth orbit (LEO) where its altitude is ranging from 0.428 km to 2,000 km. These types of satellite are usually used for weather forecast or for Global Positioning (GPS) system or for many other applications like research satellites and high quality communication services for mobile users [20]. Because of the continuity in the movement of LEO satellites constellation and switch the connection among them, the propagation delay to a LEO orbit ranges from several milliseconds when communicating with a satellite directly overhead, to as much as 80 ms when the satellite is on the horizon [19].

Between LEO and GEO orbits, there is Medium Earth orbit (MEO), i.e., their attitude is above 2,000 km and under 35,786 km. For example, O3b Networks MEO constellation orbits at 8,062 km, the RTT latency is of approximately 125 ms [21].

1.2 State of the art on network coding

5G wireless systems aim to 1000 fold capacity gains with 1 ms maximal latency, high quality of experience, seamless connectivity for users and global ubiquity. Such goals put forth challenges on introducing key enabling technologies to be integrated with wireless communications systems.

Network coding is a transmission technique that, by performing algebraic operations across transmitted packets rather than relying on packet repetition or replication, allows to reliably transmit with lower end to end delays in a communication system.
Network coding was firstly introduced in [22] as a promising technique that can achieve the min-cut capacity in wired networks i.e., multicast capacity. Given the noiseless assumption of wired networks, adaptation techniques become less relevant. Therefore, network coding provides a key enabling technology to systems that exhibit high latency and challenging wireless conditions.

Thereafter, there have been several contributions that aim to study the performance gains of using network coding in different applications including wireless networks, associated with challenging characteristics that are relevant to proposals of adaptive schemes.

Network coding has been defined as a key enabling technology in Fifth Generation (5G) wireless networks [23]. In particular, Random Linear Network Coding (RLNC) is a promising solution for current and future networks as is proven to provide increased throughput, security and robustness for the transfer of data across the network.

Moreover, the study of network coding for wireless networks need to take into consideration different aspects in the wireless medium like noise, interference, and fading. However, several efforts are going towards standardizing such technology to current protocols and systems in practice, e.g., design some mechanisms to manage heterogeneous packet lengths for data packets and video data which can reduce the overhead. When the wireless network is impaired by more challenging channel characteristics, like deep fading, or interference, they can be used as a network code, the diversity benefits introduced by network coding can be utilized [24].

Furthermore, from the decoder perspective, the authors in [25] proposed ZigZag decoding that is based on interference cancellation, requiring a precise estimation of channel coefficients for each packet involved in a collision.
Network coding proved that it can be innovative and so to be involved in many recent applications. For example, in [26] an opportunistic network coding approach was introduced, where the codewords are generated in real time according to snoop on all communications over the wireless medium and hence adapting to the receiving information from the neighbors. In [27], the authors show that non-adaptive network codes without channel state information (CSI) cannot achieve min-cut under current channel state. However, they proved for relay networks, that adaptive network codes at intermediate nodes (relays) with one bit global CSI have lower erasure probability than the codes without CSI.

Physical layer aware adaptive network coding strategies are driven by CSI estimation at the receiver side, however, such strategies are usually limited to packet erasure channel model, that is a two-state Markov model of Gilbert-Elliott channel, in which a packet is whether dropped with a certain probability or received without error (see [28, 29]). In [28], the authors developed a rate-controlled multipath strategy using network coding. They showed that such strategy can provide throughput performance comparable to multipath flooding of the network while utilizing bandwidth nearly as efficiently as single-path routing.

Additionally, network coding mechanisms are key enablers to energy efficient communications. Due to the steady increase in energy consumption and energy costs in mobile communication systems, more efficient schemes are required.

In particular, with higher reliability obtained via network coding, less re-transmissions are required. Consequently, more energy savings can be achieved [30].

In [29], the authors studied the delay and energy performance under bursty erasures. They proved that channel-aware policies reduce delay by up to a factor of 3 and significantly increase the network's stable throughput region compared to a simple queue-length driven policy. Within many, network coding offers a unique technique to multicast communications where a common information is shared among a set of receivers in a one-to-many fashion. Multicast communications are fundamental to many practical applications, including Satellite TV broadcast, content delivery and interactive communications, such as in multimedia conferencing, across wired or wireless medium.
In [31] it is shown that an explicit construction of a code that achieves multicast network capacity is a linear network code.

The Random Linear Network Coding (RLNC) is a network coding forms that proved its optimality in many applications. RLNC is based on the concept of considering terminals as algebraic entities to which packets are combined algebraically via random coding coefficients drawn from a Galois field of pre-defined size.

In [32] (RLNC) was proposed for multicast, a distributed network coding approach with nodes independently and randomly selecting linear coding coefficients from inputs onto output links over a Galois field, that achieves capacity with very high probability. In [1], the author proposed adaptive and non-adaptive network coding schemes for time variant channels relying on physical layer awareness, where potential gains where proved to be achieved. In [33], a RLNC scheme that utilizes forward error correction (FEC) at the physical layer is proposed to mitigate packet erasures. Additionally, some proposed schemes go beyond the physical layer; for instance, in [34], a cross layer RLNC scheme is proposed where delay optimization is based on the tradeoff between codeword lengths on physical and network layers.

The potential of network coding in all its forms, non-adpative or adaptive, as XOR NC or as a RLNC was shown to achieve great benefits in SatComs [35]. The works [1, 36, 37] propose a set of physical layer adaptive network coding schemes aiming to be rate and/or energy efficient for satellite applications. In [1], the author shows how adaptive network coding schemes can be of particular importance if used to mitigate the rain fading in Ka-band satellite. In [36], the authors utilize the framework in [1] to propose adaptive schemes that modify its packet transmission and modulation scheme according to the channel erasures, providing gains in terms energy efficiency compared to the rate efficient schemes proposed in [1]. In [37], energy efficient schemes have been proposed, exhibiting self tuning features to adapt transmission to the channel variations over time.

In wireless networks, owing to their broadcast nature, multicasting on wireless links suffering different channel behavior, noise, and interference levels becomes a challenge. Since there are no explicit models that express a wireless network capacity, this is considered as an open problem; thus, the characterization of optimal approaches, that jointly minimize the system completion time to several entities, is yet an open problem.

Since then, network coding has shown many benefits in wireless mesh networks. The applicability of network coding was firstly demonstrated from some practical network coding schemes include COPE, a XOR-form [38], or MORE, an RLNC-form [39], of random mixing of packets, or a combination of both forms [40]. In general, the promising gains introduced by network Coding makes it of potential interest for several practical applications [41, 42]. One of the most interesting application scenario is the satellite communications, whose trends are going towards a global coverage with high-throughput and low-latency services to the end users [43]. SatComs represent also a challenging scenario due to their large latencies (especially in case of Geostationary Earth Orbit (GEO)), relatively high packet erasure rates, and high deployment costs. As part of the 5G global heterogeneous network, SatComs allow for a ubiquitous coverage [44].

Additionally, in P2P networks, network coding shows significant benefits in content distribution [45] and streaming [46]. In [47] multicast network coding capacity was shown to be inversely proportional to the connection probability among the receiving nodes in the multicast.

Moreover, when the network coded schemes are specifically designed for enhancing their awareness with respect to the system characteristics, higher performance gains can be achieved in terms of delay, throughput or energy efficiency [1], [36]. One of the most important issue to be considered in satellite communications is energy efficiency. In [48], several factors that have a direct impact on energy efficiency of satellite and mobile terminals have been discussed, including dynamic spectrum access and cross layer design. In [1] and [49], the authors show that channel-aware transmission schemes jointly with network coding, can serve to reduce the delay and allow for energy performance gains. In [36], the authors propose novel adaptive network coding schemes and show a clear trade-off between energy-driven channel-aware schemes, that remain silent when channel encounter high erasures, and rate-driven channel-aware schemes that chose to transmit more to account for erasures.

Further, the authors in [50] explored the timing nature of coding across packets over time division duplexing channels. They proposed a network coding scheme that reduces the end to end completion time. However, they considered time invariant channels, i.e., with fixed erasure probability, thus time independence between erasures is inherent. Of practical relevance is the study of channel variation and fading over time. Despite the fact that random linear network coding (RLNC) inherently adapts its rate to variations of the channel, however, in fading channels, the packet erasures become time dependent. The goal is to exploit the channel variability on the fly to adapt the strategy of transmission of packets allowing for delay-throughput performance gains and energy efficiency which can mitigate the effects of the high Round Trip Time (RTT) of the satellite communications.

With respect to the model and schemes proposed in [1], herein an optimization of network coding transmission/retransmission patterns is considered to improve the end-to-end energy efficiency that is applied for adaptive RLNC schemes.

Moreover, an adaptive modulation is also introduced to the adaptive RLNC as a method that allows on one hand, to minimize the energy consumption. On the other hand, it allows for maximizing the data rate, by exploiting the inherent tradeoff between number of packets to be transmitted/retransmitted, adapting to the time dependent channel probability of erasures, and packet length parameters. This is attributed to the fact that an adaptive modulation system, with higher modulation order corresponds to a higher data rate and a smaller size packets (i.e., lower energy). Additionally, this work considers a realistic satellite channel model resorting to a Land Mobile Satellite (LMS) channel model, in an open area scenario [51].

The work by Ghanem in [1] stands as a milestone towards modeling coded and uncoded packet transmission over time varying channels and allows for proposals of network coding schemes that rely on the channel variation awareness and prediction to define strategies of packet transmission that allows for significant delay and throughput gains.

The proposed approaches aim to provide practical and efficient schemes applicable to the satellite scenario, where rate and energy efficiency are main goals. These goals are particularly important in both broadband and broadcast applications, where the satellite should meet a certain QoS. Besides having a QoS target that is driven by data rate demand, it should also maintain minimal end-to-end delay in order to avoid huge energy consumption. The benefits obtained via the proposed schemes provide a direction towards adopting adaptive RLNC schemes for the satellite scenario or for other future communications systems exhibiting similar fading environments and service demands. The contributions of this work can be summarized as the followings:

1. A proposal of a novel rate efficient physical layer aware adaptive RLNC scheme with joint adaptive modulation, i.e., ANCM.

2. A proposal of two novel energy efficient physical layer aware adaptive RLNC schemes, i.e., ANCEF and ANCMEF.

3. Delay utilization and throughput approximations to simulate Low Earth Orbit (LEO), Medium Earth Orbit (MEO) and Geostationary Earth Orbit (GEO) satellite scenarios characterized by different RTTs, establishing the fact that there is a clear trade-off between the packet size per transmission and energy efficiency or delay-throughput performance in the satellite scenario addressed.

4. Establishing the fact that smart channel aware adaptive transmission strategies can be switched on and off alternatively to allow, through transmitter silence or larger batches of coded transmission, less delays, higher throughput and better utilization of the physical channel by inherent reduction of retransmissions.

5. Analysis of the packet length effect is included, by considering both the effect of having larger batches of coded packets, and, at the same time, the effect of different packet time durations.

6. Characterize schemes that can jointly design the number of coded packets to multicast to a set of multicast group receivers encountering different time variant channels. In particular, the direction is to find the optimal number of coded packets to transmit to all receivers of a multicast wireless network group.

Chapter 2

Core Model

2.1 Introduction

This section explains the basic elements and composition units that has been adopted by the structure of the proposed strategies. Knowing the main components structure is very important in the realization and following the methodology. In this framework, the transmission link is a forward link of three satellite types, i.e, LEO, MEO, and GEO. The satellite performs on the board RLNC before transmission in the line network [32].

During propagation, the signal suffers from variable attenuation depending on time, geographical position and movement, multipath propagation, obstacles affecting the wave propagation, and radio frequency. Therefore, the channel gain between the transmitter and the receiver is not constant but varying over time. In particular, for representing the shadowing and fading effects associated to such scenario, the work resort to the Land Mobile Satellite (LMS) model in [51], by focusing on the open area environment. This model is based on a joint exploitation of a state based and a Loo based distribution [52] that allows to efficiently reproduce the shadowing and fading effects of a forward link satellite channel under mobile terminal assumptions.

2.2 Model Properties

2.2.1 Channel Model

The open area environment is modeled by resorting to the Land Mobile Satellite (LMS) model in [51], that is one of the most known in the literature. This model is based on a joint exploitation of a state based and a Loo based distribution [52] that allow to efficiently reproduce the shadowing and fading effects of a forward link satellite channel under mobile also

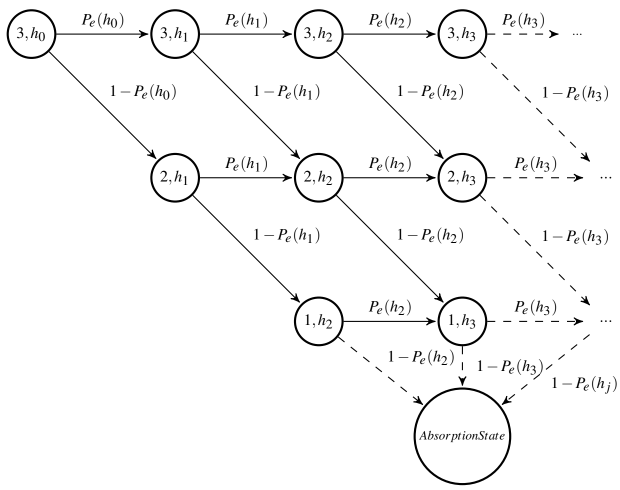

Fig. 2.1 Time Varying Channel Model of 3 Packets Transmission in [1]

terminal assumptions. The work capitalizes on the channel model has been proposed in [1], which is time-variant channel model and it has been used to express the end-to-end delay in the addressed line network. This model expresses the RLNC problem in a closed form, and provide a baseline to the proposed schemes in this work. Fig. 2.1 shows the Markov chain of a 3 packets transmission over time variant channel proposed in [1].

Consider to have, in general, N packets or degrees of freedom (dof) to be transmitted. The Network Coding (NC) scheme can be exploited in such a transmission system by supposing the receiver able to send an ACK packet requesting the lost dofs. This, in turn, can be exploited at the transmitter side for transmissions of successive batches of packets whose length is equal to the remaining dofs, yet required at the receiver side to allow for correct decoding of the native packets. Hence, if N_i is the number of coded packets to be sent in batches for combining i dofs, the transmission scheme will work for sending at each step $N_i \geq i$ packets, where i is the number of dofs to be sent, corresponding to the number of independent linear combinations required to recover the transmitted packets via performing Gaussian elimination to solve the resulting linear system. The process is repeated until all coded packets are transmitted. Such scheme capitalizes on the proposed packet transmission Markov model for time varying channels in [1], where each state is represented by the couple (i,h_j) that stands for i the number of dofs to be sent and the channel state h_j, whose value can change during time.

Each two successive states are characterized by the transition probabilities between them, i.e., $p_{(i,h_j)\to(l,h_k)}$, that corresponds to the probability of correctly sending $i-l$ dofs, and the following state is $k-j$ time slots after the starting state. This means that $k-j$ corresponds to the number of channel variations along the transmission of the dofs which is $k-j \leq N_i$ and equals to N_i+1 if ACK is considered. The probability of each path outgoing from a certain state depends on several parameters, such as the modulation type, the channel gain, and the length of the packets.

We can build one step transition probability matrix P, having a size equal to the number of states considered in the Markov chain, whose components are defined through two transition probability components, $p_{(i,h_j)\to(i,h_{j+N_i})}$ and $p_{(i,h_j)\to(l,h_{j+N_i})}$ $\forall l < i$. The one step transition probabilities are:

$$p_{(i,h_j)\to(i-1,h_{j+1})} = 1 - P_e(h_j), \tag{2.1}$$

and

$$p_{(i,h_j)\to(i,h_{j+1})} = P_e(h_j), \tag{2.2}$$

where $P_e(h_j)$ is the packet erasure probability when the channel $h(t) = h_j$ for the duration of the packet transmission, and the probability of transitioning from the channel state and back to itself equals zero due to channel variation over time.

2.2.2 End to end mean completion time

The expression of expected time required to deliver N_i coded packets that proposed in [1] is a summation of the first transmission time, the waiting time to have acknowledgment, and the transmission time of the lost dofs. The ACK packet includes the information of the lost dofs, during which the channel process evolves until a new transmission takes place at the new channel state. Therefore, the expected time to deliver N_i coded packets is given as:

$$T(i,h_j) = T_d(N_i,h_j) + \sum_{l=1}^{i} P^{N_i}_{(i,h_j)\to(l,h_{j+N_i})}\, T(l,h_{j+N_i+1}), \tag{2.3}$$

where T_d is the required time for delivering a block of size N_i coded packets. It includes also the waiting time T_w for the acknowledgement, and can be expressed by:

$$T_d(N_i,h_j) = N_i T_p + T_w,$$

where T_p is the length packet time, the transition probability $P_{(i,h_j)\to(l,h_{j+N_i})}$, from state (i,h_j) to state (l,h_{j+N_i}) corresponds to transmitting a batch of N_i coded packets. Such probability can be extracted from the Markov model transition matrix P. The power N_i describes how many times the chain is revisited due to transmission in batches, in turn,

$$\left(\prod_{i=1}^{N_i} P\right)_{(i,h_j)\to(l,h_{j+N_i})} = P^{N_i}_{(i,h_j)\to(l,h_{j+N_i})}, \tag{2.4}$$

The addition of 1 in the state $j+N_i+1$ appears due to considering the timing of one acknowledgment packet of a minimum size of T_p, due to no erasure in the feedback link.

The proposal of Markov chain, as considered in [1], assumes a finite number of time slots to allow the transmission and reception of a given number of packets. Thus, the approximation of delay resorting to this model inherently constraints the number of re-transmissions of packets, but has sufficiently large number of slots for precise approximation.

By doing an example, represented in Fig. 2.1, where we suppose to transmit 3 packets, the first packet transmission at state $(3,h_0)$ will be either successfully delivered at channel state h_0 with probability $1-P_e(h_0)$ causing a transition to occur to state $(2,h_1)$. However, the failure in its transmission corresponds to a probability $P_e(h_0)$ causing a transition to state $(3,h_1)$. In the following events the transition will occur either to state $(3,h_2)$ or to state $(2,h_2)$ in case of packet delivery failure or success, respectively. After a certain number of time slots, if the last packet at state $(1,h_k)$, $k\geq 3$ is delivered successfully, the process will be absorbed at a terminal state of the Markov chain, corresponding to end of transmission/reception process.

2.2.3 Average number of transmitted packets

The average number of transmitted packets has several considerations in terms of satellite efficiency. First of all, the complexity of the algorithms used and the amount of computational operations, which are directly related to the consumed energy on the board of the satellite, as we will see next later. Secondly, knowing how many packets injected in the transport channel and thus estimate how efficient use of radio resources available in the communication channel. Another consideration is calculating the latency which gives the time needed to complete the transition of the data. In this work, the average number of transmitted packets can be calculated by resorting to the expected transmission delay formula, by taking into account the overall transmission delay except the time needed for the ACK round trip.

Therefore, the average number of transmitted coded packets to be can be calculated as,

$$N_P(i,h_j) = \frac{T(i,h_j)_{T_w=0}}{T_p}. \tag{2.5}$$

where $T(i,h_j)_{T_w=0}$ corresponds to the expected time for transmission when the waiting time for ACK is zero, i.e., corresponding solely to the amount of time spent in packets transmission/retransmission.

2.2.4 Average consumed energy

Apart from the fuel needed to lunch the satellite on its orbit, the issue regarding as the fuel consumption of orbit optimization is of great importance constraint [53]. In general, the fuel on the satellite board is mainly chemical and it is used to maintain its pointing towards earth. On the other hand, the electrical power generated from solar panels to power all the on-board electronics and to power the radio receivers/transmitters that are typically the main part of the satellite payload. Therefore, the power transmission is one of crucial criterion, i.e., the power of the downlink signal has to be strong enough to ensure the quality of service [54]. It also needs to be able to capture solar energy sufficient to operate the on-board electronics for the transmitter, telemetry and control once it is operational. In particular, the satellite receives very weak signals from one sender at the end of the link, amplify them, and re-transmit them on very high energy to the receiver at the other end of the link. Moreover, the available on board power is limited, as is the power output of the transmitter. Hence, lowering the operational energy requirements is of great intention among the researchers, as it also affects the lifetime of batteries which may be used to store energy also limit the satellite's lifetime. Therefore, the motivation is to minimize the operational energy requirements.

Similarly the average consumed energy can be evaluated by resorting to the average number of transmitted packets. Indeed, by resorting to (2.5), the average energy consumed for i dofs at the receiver side during the expected transmission time $T(i,h_j)$ is given by,

$$E(i,h_j) = N_P(i,h_j)E_bN_b \tag{2.6}$$

where N_b is number of bits per packet, and E_b is the energy per bit. E_b can be derived for a given E_b/N_0 ratio and a given noise spectral density N_0.

2.2.5 Average throughput

The key factor of the new generation of high throughput satellites (HTS) systems require to estimate the forward and return capacity [55]. In particular, many elements involved in forming this key factor such as the effective isotropic radiated power (EIRP) and the gain over noise temperature (G / T) cumulative densities, the carrier-to-inference (C / I) estimations and the capacity assessment for the forward and return links.

The average throughput is measured as the reciprocal average completion time multiplied by the maximum number of coded packets to transmit within this completion time.

$$\eta(i,h_j) = \frac{N_i}{T(i,h_j)} \tag{2.7}$$

Chapter 3

Rate efficient adaptive network coding in line sat network

3.1 Introduction

Technology of today is developing to meet the 5G standard as it is expected to begin their services in 2020. The 5G cellular and satellite networks will primarily contain the Quality of Service (QoS) parameters (e.g. delay, loss rate, throughput . . . etc.). The key challenge of 5G technology is to include the minimum bandwidth and maximum delay constraints. The big challenge in optimizing traffic flows is of great importance demand in broadcasting the multimedia where the wireless channel has properties that is time-varying. In this section, we learn about network coding (NC) and familiarize it to improve the transmission delay and the corresponding throughput over time-varying wireless channels. In general, the performance of throughput and delay over time-varying erasure channels could be optimized and improved within broadcasting systems that uses the NC more than those are using uncoded packets [56, 57].

In the following we will explore network coding (NC) without any adaptive roles to be considered as a basic standard measure for comparison with the other proposed schemes. Therefore, the number of packets combinations, i.e., "window size" or "batch size" will be predefined manually as a fixed block size. To this regard, we show the performance of non-Adaptive NC in various fading channels, i.e., Rayleigh, Rician, and realistic Land Mobile Station (LMS) channel model. The evaluation will be the results of the corresponding transmission delay, throughput, average number of the transmitted packets, as well as the average consumed energy. Then we show the development of an Adaptive NC (ANC) scheme that adapts the window packets size according to the channel erasure probabilities varying over time, the scheme adjusts the block size window to maximize the system throughput. In addition, another adaptive NC scheme will be presented and it is called Adaptive NC and Modulation (ANCM) scheme which selects the available and appropriate modulation scheme.

3.2 Non-adaptive network coding

In the technique of linear network coding, the relay nodes of a network generally don't only relay the informative packets as they receive them, but combine among them and then transmit the packets combinations instead of the primary received ones. In particular, it optimizes the multicast mechanisms of the information at the source nodes to other nodes on the network in the multihop fashion, in which the network flow will be max and optimum [31]. Moreover, this technique proves a development in the network flows in terms of throughput, efficiency, and it is robust against hacking attacks.

However, if a multicast network has no linear solution over any finite field, then there is no finite commutative ring with identity will give any linear solution. Moreover, there is no asymptotic solution for linearity as the network coding capacity of such network is greater than the maximum linear coding capacity over any finite field [58]. Therefore, many attentions and efforts to find the optimal solutions for network coding have been done in general network problems with arbitrary demands.

The non-adaptive network coding scheme relies on the use of Random Linear Network Coding (RLNC) [59]. This coding scheme has many benefits such as allowing improving the throughput in the broadcasting schemes and the linear dependency among coefficients vectors which can reduce the number of innovative encoded blocks. In particular, the transmitter generates coded packets by properly selecting randomly the coding coefficients from a Galois field with a size large enough to reduce the probability of generating linearly dependent packets. However, the challenge of the RLNC is when a receiver obtains an insufficient number of coded packets; it is severely difficult that they can recover any of the original packets. However, yet, we cannot avoid the time dependency between packets due to considering time variant channels. From a timing perspective, if the transmission of N_i coded packets over $h_j, \dots, h_{j+N_i}$ was not successfully decoded for all N_i coded packets, it will be addressed by sending additional random linear combinations until the receiver obtains the appropriate number of packets and it will be considered as an additional amount of time needs to be considered for transmitting the lost dofs.

In the following two sections, first we present the essential physical layer aware adaptive network coding scheme (ANC) proposed in [1], and then modulation enhanced scheme which is called adaptive network coding and modulation scheme (ANCM) that proposed in [36]. Both schemes fulfill one of the fundamental goal in future satellite communications which is rate efficiency demand. In general, rate efficient schemes are defined by their capability to adapt to the awareness of the channel variation over time within a certain fixed time-window. Such schemes favor more transmission over being silent, to account in advance for expected erasures in the channel. The system adapts the number of packets per transmission/retransmission and also the modulation scheme.

3.3 Adaptive Network Coding (ANC)

Adaptive coded transmission scheme in [1] relies on awareness of the physical layer. Such assumption involves in sensing the variation over time of a wireless channel and then predicting the packet erasure probabilities. Due to the predicted rate erasures given by $P_e(h_j)$, transmitter can interact with the channel variation and follow a suitable strategy for optimizing the transmitted batch size. Hence, the transmitting system can adapt number of coded packets inside each successive batch ready to transmit. Therefore, the strategy determines how many packets the receiver could successfully decode, i.e., $1-P_e(h_j)$ packets. According to those parameters and further aim performance, the adaptive system process can instantly build batches, which their sizes could achieve the final purpose of the transmission process. Therefore, the adaptive transmission strategy takes into account the lost packets or dofs, via the transmission of coded packets.

The following equation presents the most promising adaptive throughput strategy,

$$\sum_{s=j}^{N_i}(1-P_e(h_s)) = i, \tag{3.1}$$

The aim of this equation is to find the number of coded packets N_i need to be transmitted to allow for successful reception of i dof. Thus, the sum in (3.1) expresses a counting process of how much packets can pass through a time variant erasure channel such that the sum equals i. The integer number of times the channel is visited equals the number of adaptive coded packets N_i to be transmitted. In turn, $j = 0$ is the initial time state of the counting process. This adaptive scheme provides the optimal number of coded packets to transmit/retransmit at each SNR. The implication of this process on the time is that the transition matrix should span up to N_i. Therefore, we adaptively transmit accounting for packet erasures caused by channel variations over time as well as the dof of the receiver. Notice that the adaptation is controlled by the SNR level.

Therefore, the time when switching on or off adaptation is of particular importance to the process. In fact, adaptation is more required at the low-SNR regime. Furthermore, it is worth noticing that such adaptive scheme is of hybrid nature, through which it might sometimes behave as a selective repeat ARQ scheme when erasures are almost equivalent across all transmission/retransmission process or when the N_i is constrained to a certain maximum value per transmission.

3.4 Adaptive Network Coding and Modulation (ANCM)

The rate efficient adaptive scheme we are considering here is based on the exploitation of different modulation schemes as foreseen in the most modern communication standards (e.g., DVB-RCS, RCS2, LTE). By resorting to the adaptation rule exploited in the Adaptive Network Coding (ANC) scheme, our idea is to include an adaptation of the modulation scheme.

The rationale is, on the one hand, a higher modulation order is more efficient, allowing for transmitting the same amount of information in shorter packets; on the other hand, due to the higher bit and symbol error probability, a higher number of packets could be needed to be sent. This introduces a trade-off between the packet length and the number of coded packets for a given modulation scheme. The proposed strategy is shown in the following equation:

$$\sum_{s=j}^{\min(N_i,N_i^*)} (1 - P_{e_m}(h_s)) = i, \tag{3.2}$$

where $P_{e_m}(h_s)$ is the erasure probability of the m-th modulation order that can be derived as:

$$P_{e_m}(h_s) = 1 - (1 - P_{b_m}(h_s))^B \tag{3.3}$$

where P_{b_m} is the bit error probability for the same m-th modulation order while B is the number of bits within one packet, that we consider as constant for fair comparison. N_i corresponds to the number of coded packets to be sent in each transmission, which is optimized, and N_i^* constraints the number of retransmissions to a value that does not increase the delay. The value of N_i^* is higher than N_i at high SNR, and limited to a maximum of N_i at low SNR, where, in the latter SNR regime, erasures are vanishing, hence, N_i is equal to i almost surely.

Therefore, the transmission strategy at low SNR adapts the maximum batch size to be transmitted using the most reliable modulation scheme to deal with the higher erasure probability. On the other hand, the strategy is for utilization a higher modulation order as channel conditions improve, i.e., for higher SNR. Hence, the maximum batch size is increased and so on for the number of coded packets when the conditions of the wireless channel improve.

In general the equation (3.2) adapts maximum batch size according to some following parameters:

1. Packet erasure probabilities that are varying over time and over different modulation schemes.

2. Missing degrees of freedom at the receiver side.

3. Maximum number of coded packets inside the batch size that is varying due to the selected modulation scheme. Higher modulation order allows for m-th more coded packets inside the window size.

Indeed, the aim of proposed scheme is to find the optimal number of coded packets to transmit/re-transmit and assure successful reception of a given number of i dof. Since a different modulation order corresponds to a different packet duration, the aim is to select the modulation order that allows for minimizing the end to end transmission time.

In the following section we will expose the properties of adaptive proposed schemes by testing and simulating them under the same channel environments. Then show the results of all proposed schemes at the same curves in order to figure out performance of each scheme compared to the others.

3.5 Properties of the proposed schemes

We shall now present a set of illustrative results that cast further insights into the adaptive proposed schemes and their gains with respect to rate efficiency, in a manner where we compare the performance of the adaptive network coding schemes to the performance of non-adaptive network coding scheme. In particular, the proposed schemes are evaluated for GEO, MEO, and LEO satellite scenarios with Rayleih fading, Rician fading or with single mobile terminal with $1\,\mathrm{m/s}$ or $10\,\mathrm{m/s}$ speed in an open area environment modeled as in [51].

We suppose that the satellite utilizes adaptive RLNC. When the adaptive number of coded packets is devised. The RLNC step operates by generating new packets which are linear combinations of the original data packets, multiplying them by random coefficients drawn from a Galois Field of a certain size. The satellite transmits the adaptive coded data appended with the coding coefficients. Then, the receiver performs Gaussian elimination across the coded packets transmitted and retransmitted back to back until all the data packets are reliably decoded.

The LMS model considered is the one introduced in [51]. Among several propagation scenarios, we focus on a scenario having the following parameters:

- The ground receiver is located in an open-area environment, rural area with no trees; The elevation angle of the satellite equals 40°;
- The average multipath power, $MP = [-22.0;\ -22.0;\ -21.2]$ dB;
- The direct signal is assumed to be log-normally distributed with mean $\alpha = [0.10;\ -1.0;\ -2.25]$ dB relative to Line of Sight (LOS) and standard deviation $\Psi = [0.37;\ 0.5;\ 0.13]$ dB, corresponding to the LOS, intermediate shadow and deep shadow propagation states, respectively.

We consider a medium length of 5 data packets to be transmitted in order to build the simulation environment; following this, the batch length in terms of number of coded packets per transmission/retransmission is limited or lower bounded by double the dofs, i.e., the adaptive strategy of ANC will produce for each SNR a set of possible maximum number of coded packets to be transmitted N_i is equal to 10, and for ANCM the maximum optimal number that could be transmitted N_i^* is equal to 40 coded packets when the selecting of the modulation type is 16QAM.

Moreover, we consider to have one single beam with a transmitting power equal to 65 W and that the transmission bandwidth is 36 MHz.

The performance of the proposed rate efficient adaptive schemes has been evaluated for the main key performance indicators, which are: the delay, throughput, average number of transmitted packets and average energy consumption. The number of bits per packet is considered to be equal to 1000, thus, if the maximum number of packets per batch is 10, this corresponds to a maximum number of bits per batch equal to 10000 bit. Moreover, it is worth to note that for taking into account practical QoS levels in terms of error probability we consider in the following that an acceptable bit error rate threshold is 10^{-5} [1]. The used modulation scheme is BPSK in case of NC and ANC, while ANCM exploits four possible modulation schemes, i.e., BPSK, QPSK, 8PSK and 16QAM.

3.5.1 Average number of transmitted packets for the proposed rate efficient schemes

The Figs. 3.1, 3.2, and 3.3 depict the performance in terms of average number of transmitted packets for GEO, MEO, and LEO satellite scenarios, respectively. Each figure considers a

[1] The acceptable bit error rate, as proposed by the ITU ranges between 10^{-3} to 10^{-6} based on the rate and service expected at the mobile terminal.

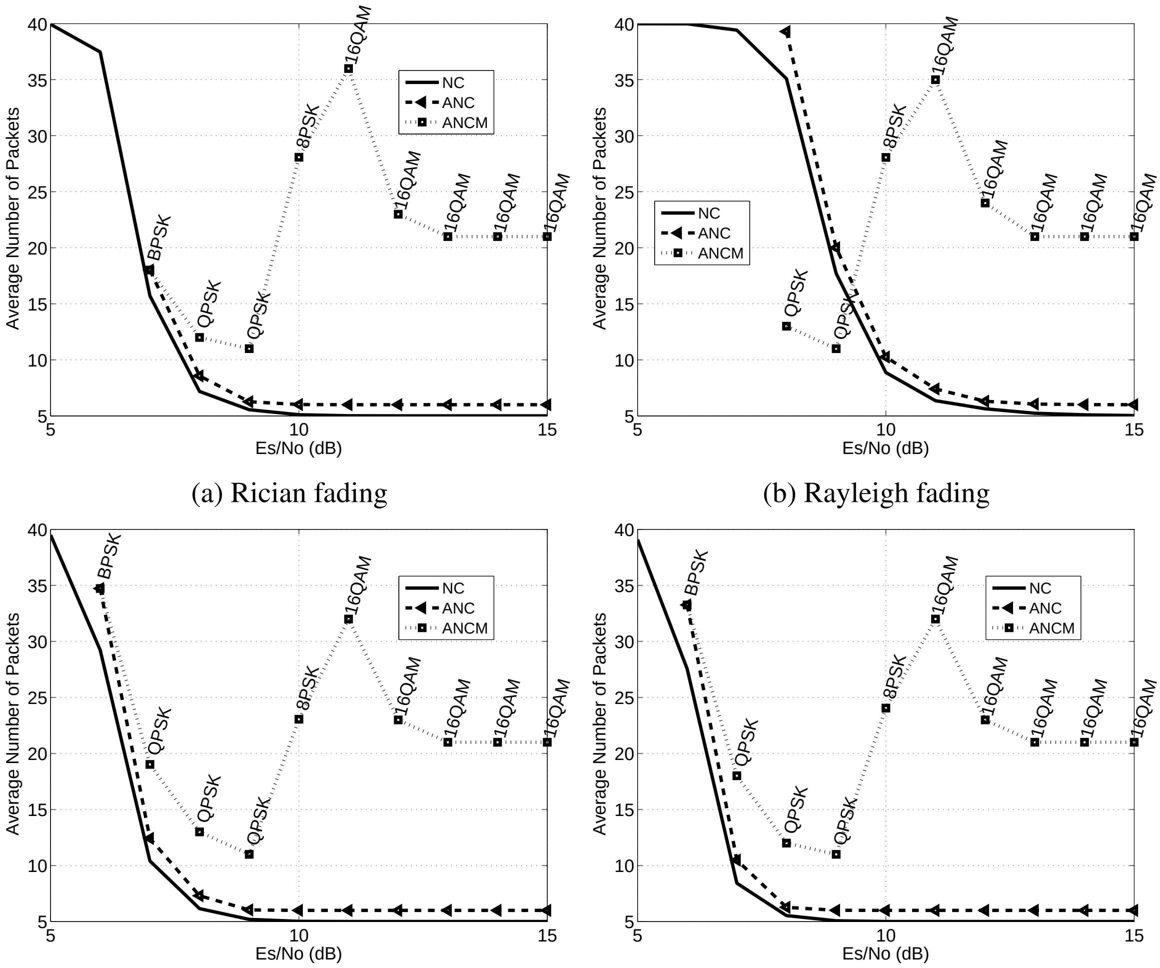

(a) Rician fading (b) Rayleigh fading

(c) LMS fading model with 1 m/s mobile speed (d) LMS fading model with 10 m/s mobile speed

Fig. 3.1 Average number of transmitted packets in GEO satellite scenario for variable E_s/N_0 values and within various fading models.

various fading model, i.e., Rician, Rayleigh, LMS model 1 m/s, or LMS model 10 m/s. It's worth to mention that in case of non-adaptive network coding scheme, the number of coded packets are fixed along the transmission/retransmission with no adaptation, while in case of adaptive network coding schemes the number of coded packets for each batch depends on the missing dofs and on the time dependent erasure probabilities at a set of estimated channel states.

In general, we can see in Fig. 3.1 which describes the GEO satellite scenario, that the average number of packets for all the schemes at low SNR, i.e., $E_s/N_0 \leq 9$ dB, is greater than those at high SNR due to the higher probability of re-transmission at low SNR. However, it is possible to see that the ANCM scheme has the higher number of transmitted packets, since it has been designed for transmitting N_i packets whose value increases for higher modulation order.

Moreover, ANCM at low SNR values employs the most robust modulation method (in terms of error probability), i.e., BPSK, leading to the same performance of the ANC that instead uses always the BPSK modulation scheme. This is evident in Fig. 3.1a, 3.1c, and 3.1d, while in Fig. 3.1b at low SNR, the first transmission attempt does not begin with BPSK modulation, but it starts with QPSK immediately when the signal improves enough for transmission.

This is because of the Rayleigh fading has no line of sight signal, which is supposed to be more stronger than the other signal paths. But instead, this fading makes a scarcity in the signal and leads to make a shift in the initial SNR transmission point for ANC and ANCM. Moreover, with Rayleigh fading it is possible to see that the curve is shifted to the right compared to other types of fading. For instance, to compare the performance among different schemes and scenarios, it is useful to consider a standard value of average transmitted packets equals 10. So, as we can see that all fading models allow for schemes to reach less than 10 packet at the SNR lower than 8 dB except the case of Rayleigh fading.

It's worth to mention that ANCM gradually uses higher modulation as SNR gets improved, i.e., it starts with the modulation type BPSK at low SNR, QPSK at moderate condition, then 8PSK and finally 16QAM when the channel becomes quite perfect. The diverse use of modulation orders is for achieving higher throughput and better quality, thus increasing the number of packets when the channel conditions allow this.

The aforementioned reason can explain two main observations; the first is why the performance of ANC and ANCM does not match at this moderated range of SNR values. Second, it can explain the sudden increase of ANCM curve, i.e., exhibits an intermediate maximum in the curve.

For ease explanation, we intend to add the modulation scheme name selected by ANCM transmission strategy beside each corresponding point of SNR values. For the earlier observation of intermediate maximum in curve and the associated modulation types, we denote that using different types of modulation allows in a certain point of channel improvements to select a higher modulation order that it sometime increases the average number of packet used at that stage of SNR value. The increment point means a better channel condition with a higher modulation order that leads to more average number of packets to transmit. That is not abide to decrease by converging to a certain value at higher SNR.

In other words, if we imagine by dividing ANCM curve into multiple sub curves. So the last sub curve, i.e., that is only presented by 16QAM points, shows same general behavior compared to NC and ANC. It begins with higher value then it converges at higher SNR to a close value product of m-th and dofs.

Indeed, for higher SNR, corresponding to lower packet erasure probability, the average number of packets in NC and ANC decreases by converging to the number of dof required at the receiver.

Not further from Fig. 3.1 which describes the GEO satellite scenario and the related average number of transmitted packets, Fig. 3.2 illustrates the MEO satellite scenario and the related average number of packets. It is obvious that the four fading models having more or less the same effects on MEO as the previous manner on GEO satellite scenario. But, we can see a minor difference between the two. In particular, for the LMS fading model and between the two speeds, i.e., $1\,\mathrm{m/s}$ and $10\,\mathrm{m/s}$. The notation tells that when the terminal speed is $10\,\mathrm{m/s}$ at MEO satellite scenario, it makes the channel having more sharp erasure probabilities than those at speed of $1\,\mathrm{m/s}$. That effects on the average number of transmitted packets using ANCM can be seen more in the different selection of modulation schemes. For instance between Fig. 3.2c and Fig. 3.2d at 7 dB, ANCM at speed of $10\,\mathrm{m/s}$ prefers using a better robust modulation type BPSK, while at the speed of $1\,\mathrm{m/s}$ it uses QPSK with a corresponding average of 12 packets and 18 packets, respectively.

The behavior of average number of transmitted packets for LEO satellite scenario is shown in Fig. 3.3. It is almost the same performance as GEO and MEO scenarios, especially for the case of Rician and Rayleigh fading.

However, the curve of average transmitted number becomes more flat in case of LMS model at mobile speed equals $1\,\mathrm{m/s}$ and $10\,\mathrm{m/s}$, i.e., Fig. 3.3c and Fig. 3.3d, respectively. Reason behind its flatness is the less effect of LEO fading scenario that experiences a short distance between the satellite and terminal. Hence, ANC scheme achieves its final transmission goal for sending 5 dofs required at the receiver side by only transmitting 6 coded packets at the very first trial for each SNR value.

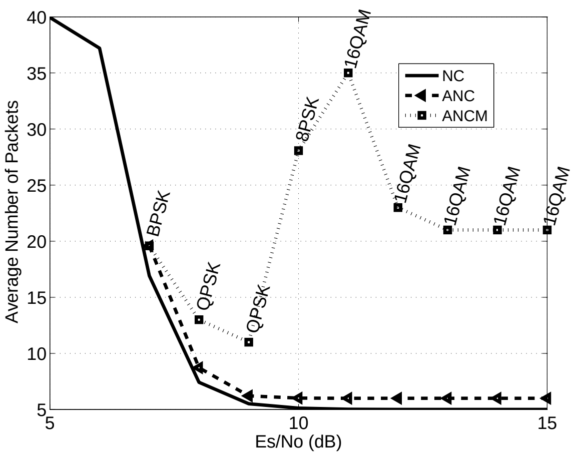

(a) Rician fading

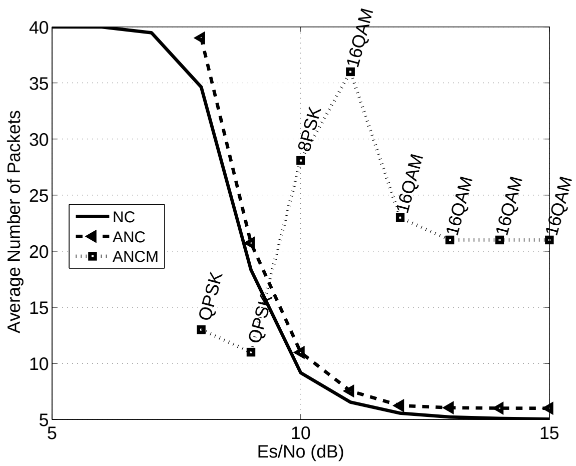

(b) Rayleigh fading

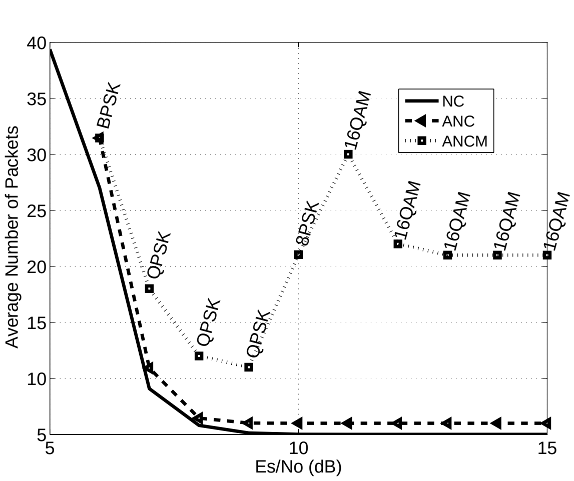

(c) LMS fading model with 1 m/s mobile speed

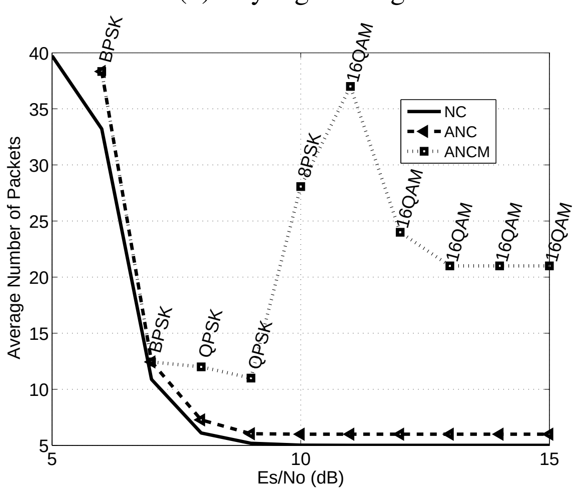

(d) LMS fading model with 10 m/s mobile speed

Fig. 3.2 Average number of transmitted packets in MEO satellite scenario for variable E_s/N_0 values and within various fading models.

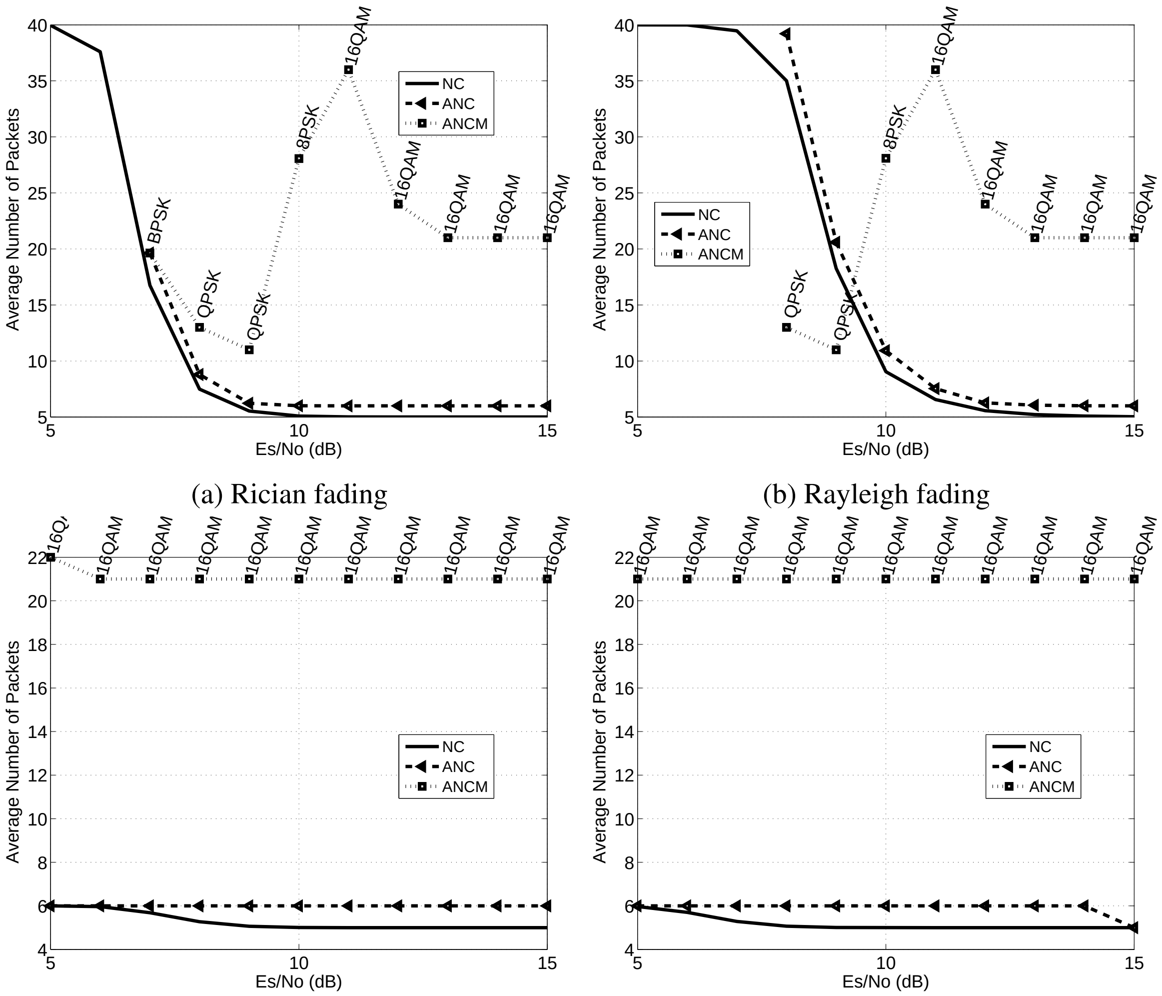

(a) Rician fading

(b) Rayleigh fading

(c) LMS fading model with 1 m/s mobile speed

(d) LMS fading model with 10 m/s mobile speed

Fig. 3.3 Average number of transmitted packets in LEO satellite scenario for variable E_s/N_0 values and within various fading models.

The same case is also reported for ANCM scheme in which the channel conditions allow to use directly the modulation type 16QAM. Hence, it sends 21 coded packets at every first trail resulting in a reception of the required 5 dofs for each SNR value.

Moreover, it is possible to see the effect of terminal speed on ANC curve in both Fig. 3.3c and Fig. 3.3d. There are two SNR values in which the average number of coded packets for ANC is emerged with NC. The first one is equal to 14 dB when the terminal in LMS fading has a speed of 1 m/s, the second equals 15 dB for higher speed of 10 m/s. In reality, this behavior is considered as a normal performance because of more speed the terminal has, more erasure probabilities over time the channel suffers.

3.5.2 End to end completion time for the proposed rate efficient schemes

In Figs. 3.4, 3.5, and 3.6 we can see the behavior in terms of end to end transmission delay for the proposed adaptive rate efficient schemes in GEO, MEO, and LEO satellite scenarios, respectively. Each scenario is simulated using four different fading environments; Rician, Rayleigh, LMS fading model with 1 m/s mobile speed, and LMS fading model with 10 m/s.

It is possible to note in Fig. 3.4 as the other figures of delay performance using the adaptive rate and network coding schemes, that there are considerable gains in terms of end to end completion time. In particular, Fig. 3.4a, Fig. 3.4c, and Fig. 3.4d at low SNR values, i.e., $E_S/N_0 \leq 9$ dB show considerable improvements. However, there is a negligible delay gain in ANCM over ANC, since it adds the complexity of modulation adaptation, and this case is common among most delay performance figures and precisely at SNR equals 8 dB.

Moreover, Fig. 3.4b shows the delay performance within Rayleigh fading, in which a special case of performance using ANCM scheme is reported. The initial trial for transmitting the required dofs begins at 8 dB and the selected modulation scheme is QPSK resulting in 0.7 s gain over ANC and 2 s over non-adaptive NC.

After a certain SNR value, in particular after 14 dB, the majority performance curves of adaptive and non-adaptive schemes are similar. Because, each batch size N_i nominated by rate efficient schemes (i.e., ANC and ANCM) is shorten and converged to the number of dofs/coded packets i required at the receiver side in the non-adaptive NC scheme. It is worth mentioning that ANCM is not an exception since a normalization on the average number of transmitted packets with $\log m$ matches the dof for such length of dofs required at the receiver side. Furthermore, it is straightforward to understand the delay convergence of all the schemes to its minimal value for high SNR values.

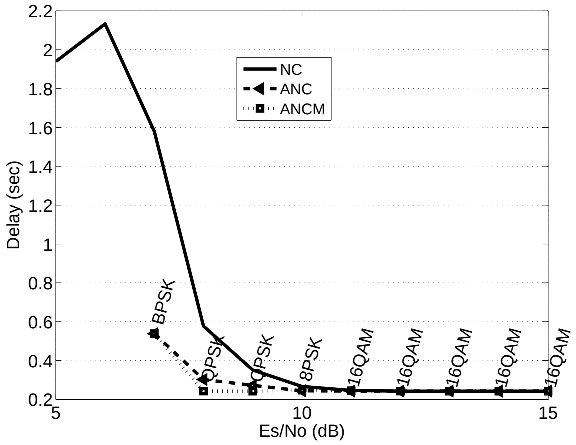

(a) Rician fading

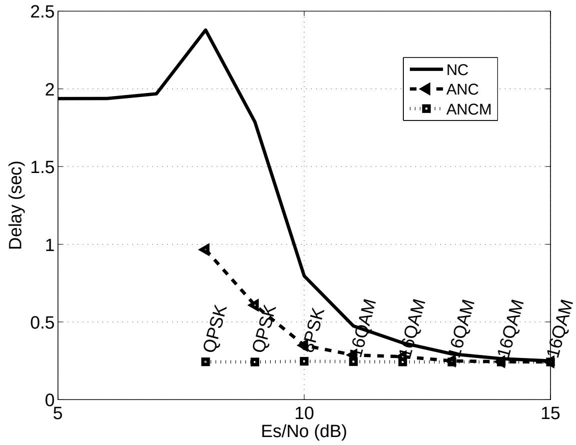

(b) Rayleigh fading

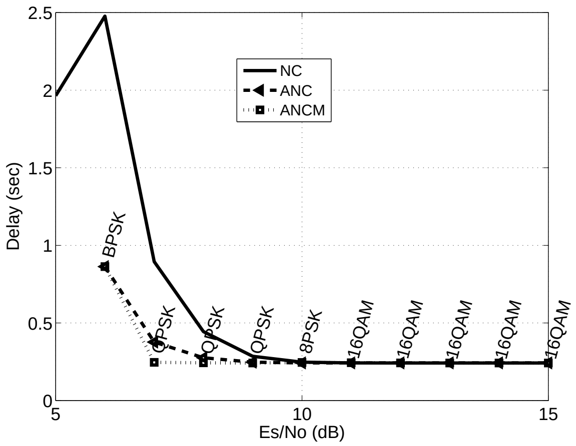

(c) LMS fading model with 1 m/s mobile speed

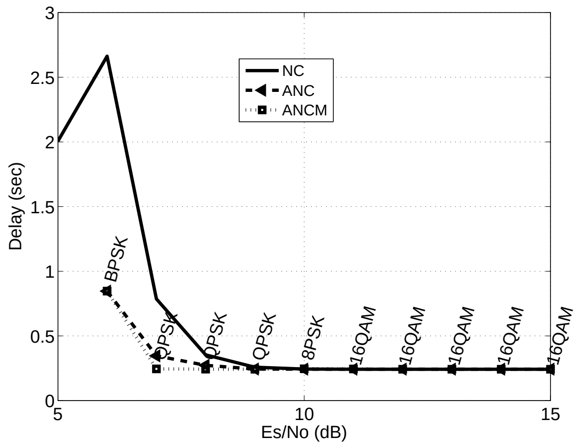

(d) LMS fading model with 10 m/s mobile speed

Fig. 3.4 Expected end to end completion time in GEO satellite scenario for variable E_s/N_0 values and within various fading models.

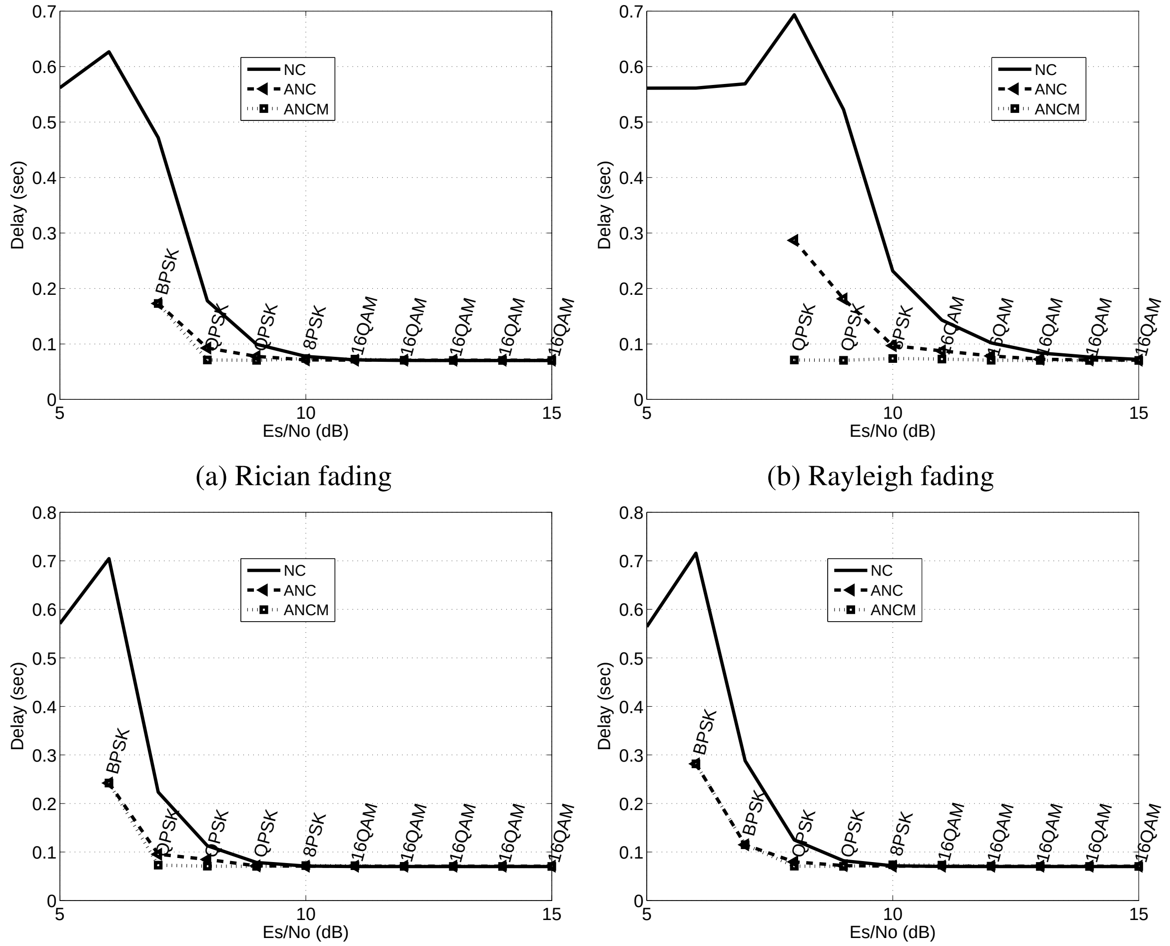

(a) Rician fading

(b) Rayleigh fading

(c) LMS fading model with 1 m/s mobile speed

(d) LMS fading model with 10 m/s mobile speed

Fig. 3.5 Expected end to end completion time in MEO satellite scenario for variable E_s/N_0 values and within various fading models.

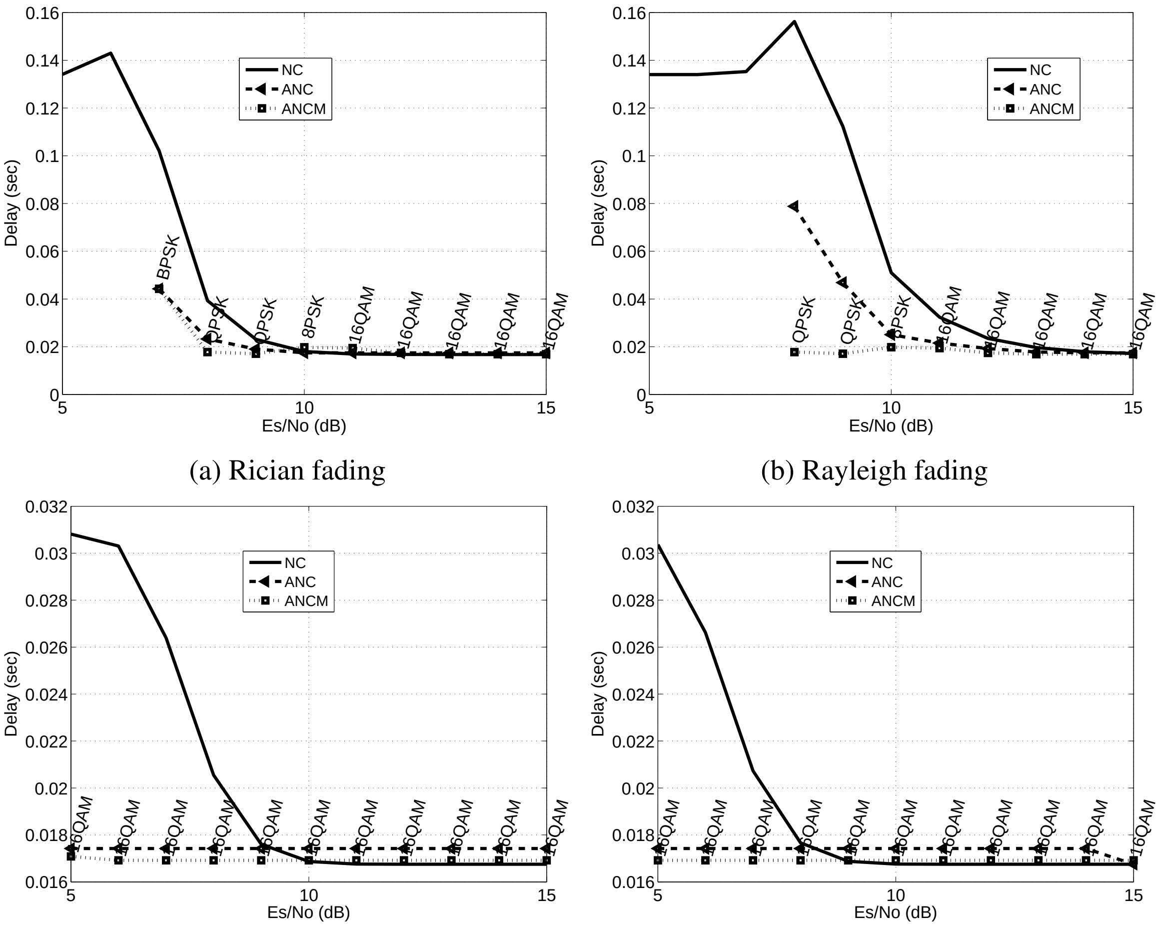

(a) Rician fading

(b) Rayleigh fading

(c) LMS fading model with 1 m/s mobile speed

(d) LMS fading model with 10 m/s mobile speed

Fig. 3.6 Expected end to end completion time in LEO satellite scenario for variable E_s/N_0 values and within various fading models.

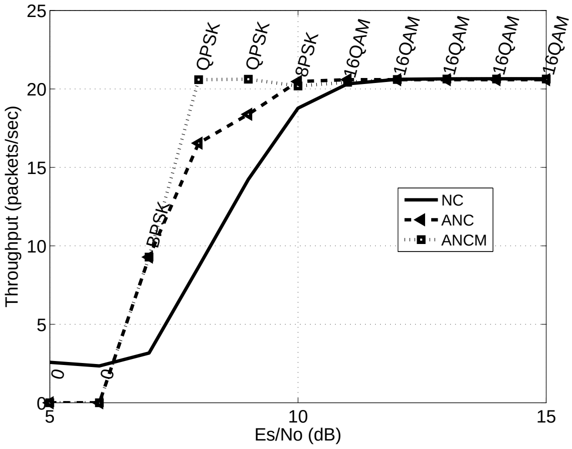

(a) Rician fading

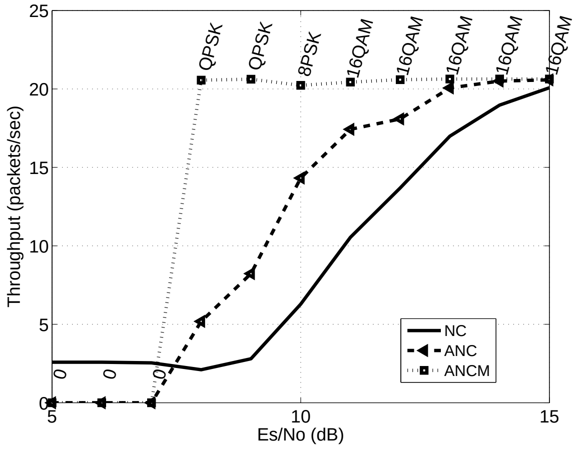

(b) Rayleigh fading

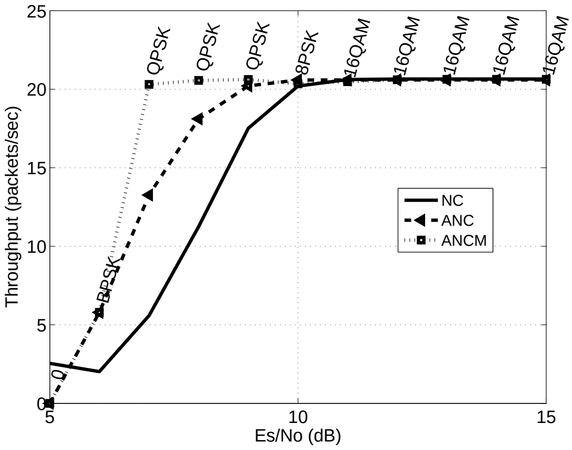

(c) LMS fading model with 1 m/s mobile speed

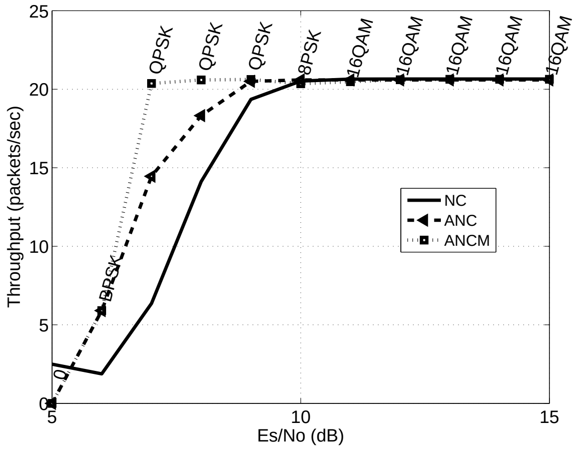

(d) LMS fading model with 10 m/s mobile speed

Fig. 3.7 Average throughput in GEO satellite scenario for variable E_s/N_0 values and within various fading models.

3.5.3 Average throughput for the proposed rate efficient schemes

In Figs. 3.7, 3.8, and 3.9 the throughput performance is shown for the three satellite scenarios; GEO, MEO, and LEO, respectively. For each scenario, the adaptive schemes; ANC and ANCM, and non-adaptive NC are simulated under various fading models; Rician, Rayleigh, LMS with 1 m/s mobile speed, and LMS with 10 m/s mobile speed.

In aforementioned figures at low and intermediate SNR values, ANC and ANCM curves show remarkable achievements over the non-adaptive network coding scheme NC in terms of throughput. Additionally, it is possible to see that the ANCM scheme, by utilizing different modulations schemes, can gain in terms of throughput in comparison to the other schemes; ANC and NC. The Rayleigh fading impacts differently on the schemes of network coding, since the signal received within Rayleigh fading can be considered as a result of reflection over multiple paths and it will vary randomly, or fade, according to a Rayleigh distribution. However, it's worth to observe that at a certain SNR, all the schemes converge to maximum throughput value. Moreover, the impress of the various fading on the throughput among the simulated schemes is almost the same with delayed or ahead of each other. For instance but not limited to, the schemes in Figs. 3.7a, 3.7c, and 3.7d are converging at a value of SNR equals 12 dB. While, in Fig. 3.7b the convergence is happening after 15 dB.

Furthermore, the Figs. 3.9c and 3.9d show that when the channel is improved enough above 8 dB for the case of Fig. 3.9c and above 9 dB for the case of figurename 3.9d, non-adaptive network coding scheme NC could perform better than those of adaptive schemes. Hence, it would be preferable to switch of the adaptation and be dispensable when the channel has sufficiently improved. However, in Fig. 3.9b of Rayleigh fading, this exchange between adaptation and non-adaptation whether or not to use has a long delayed than the other types of fading.

3.5.4 Average consumed energy for the proposed rate efficient schemes

The final criteria in analyzing the rate efficient schemes is the expected average of the consumed energy, in which Figs. 3.10, 3.11, and 3.12 show the results in terms of the total energy consumption for GEO, MEO, and LEO satellite scenarios; with the four fading models we have already. To this aim we suppose that power spectral density of the noise component N_0 is equal to $-107\,\mathrm{dBm}$. It is possible to note that all the proposed adaptive schemes may have increment in terms of energy consumption with respect to the standard non-adaptive network coding NC. It is straightforward to observe that along the variation of SNR, ANC has a reasonable average of energy consumption over NC and it is roughly between $1 \times 10^{-5}\,\mathrm{mW\,Hz^{-1}}$ and $6 \times 10^{-5}\,\mathrm{mW\,Hz^{-1}}$, see Fig. 3.10a, Fig. 3.11a, and

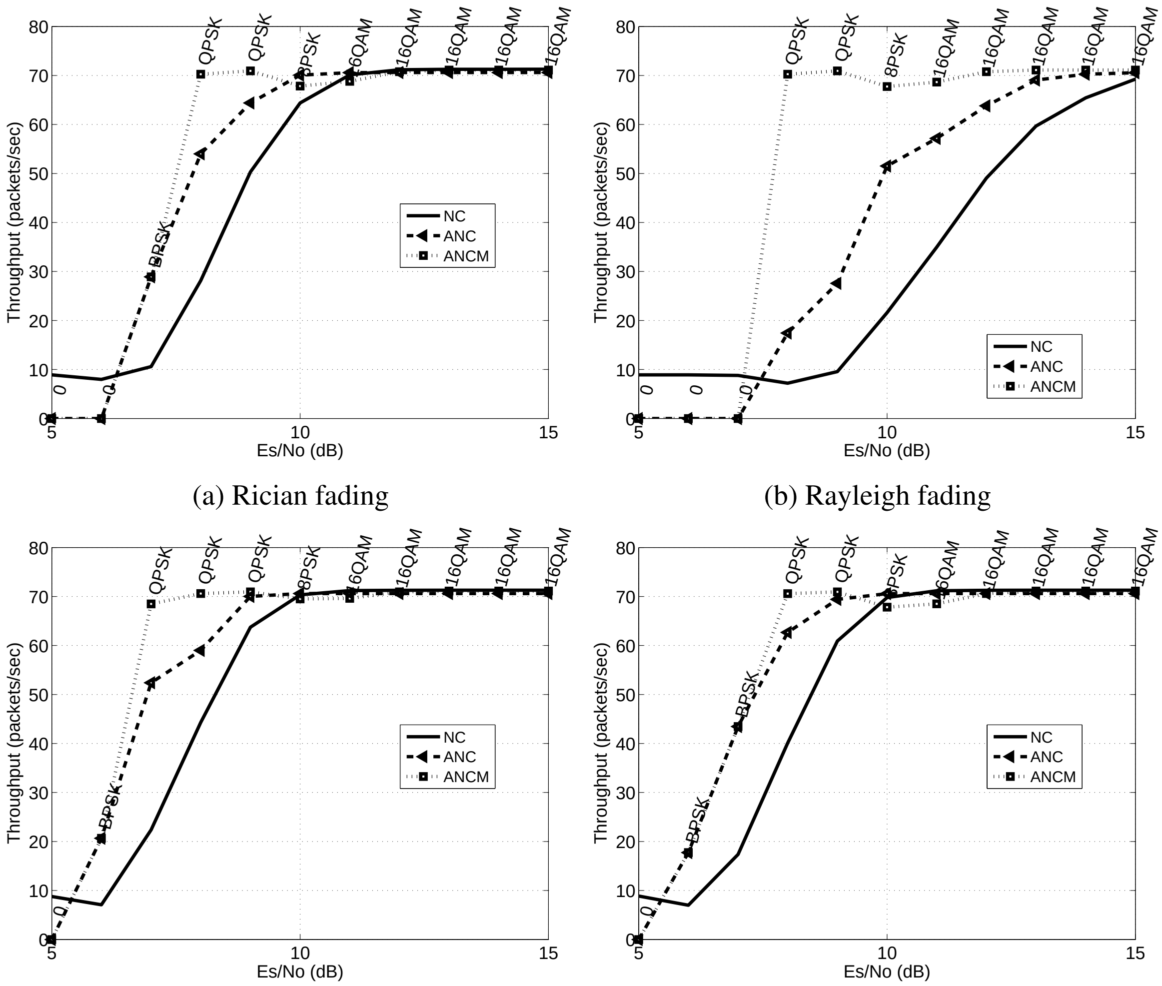

(a) Rician fading

(b) Rayleigh fading

(c) LMS fading model with 1 m/s mobile speed

(d) LMS fading model with 10 m/s mobile speed

Fig. 3.8 Average throughput in MEO satellite scenario for variable E_s/N_0 values and within various fading models.

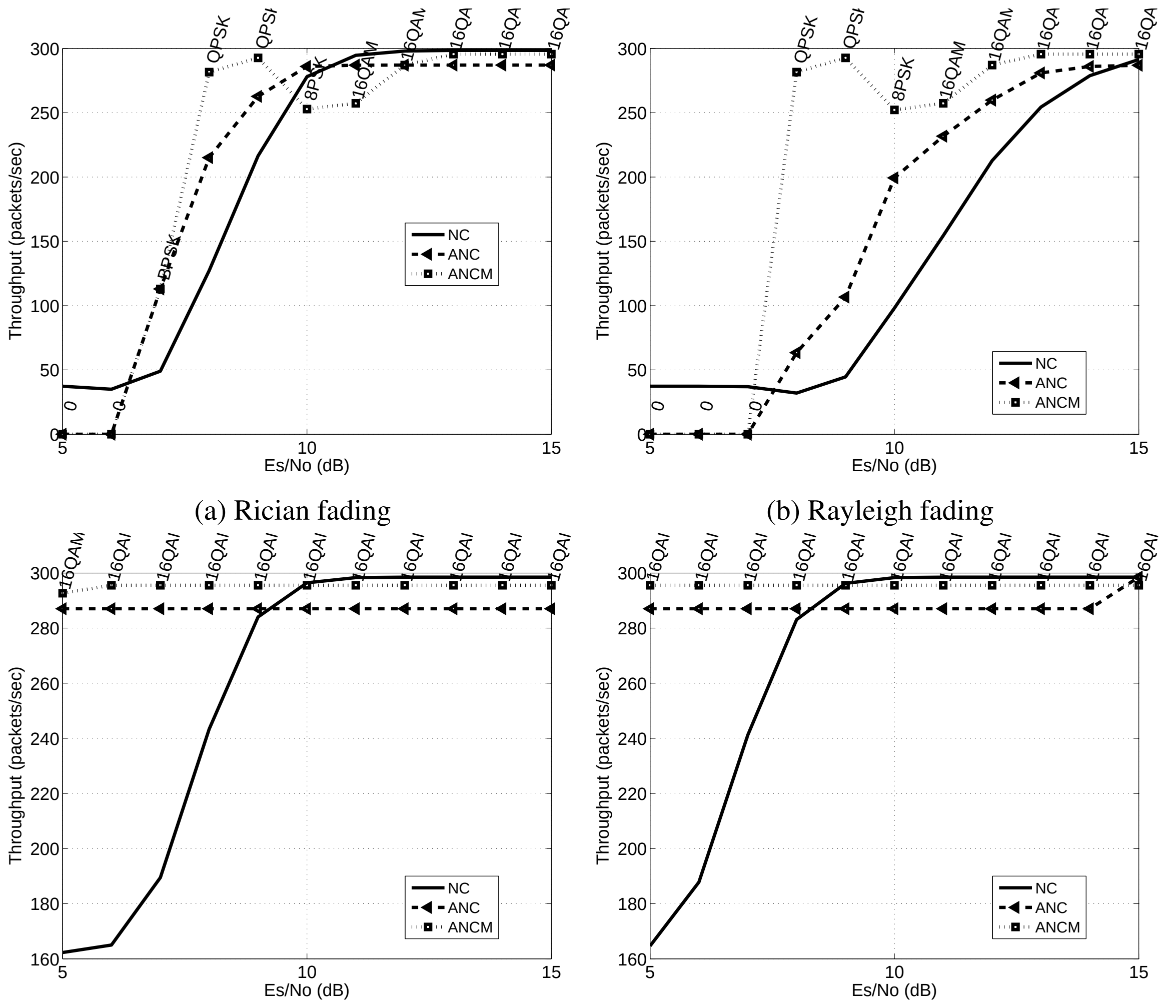

(a) Rician fading

(b) Rayleigh fading

(c) LMS fading model with 1 m/s mobile speed

(d) LMS fading model with 10 m/s mobile speed

Fig. 3.9 Average throughput in LEO satellite scenario for variable E_s/N_0 values and within various fading models.

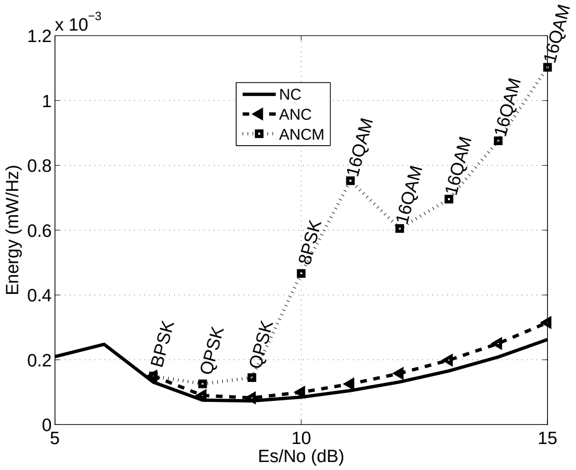

(a) Rician fading

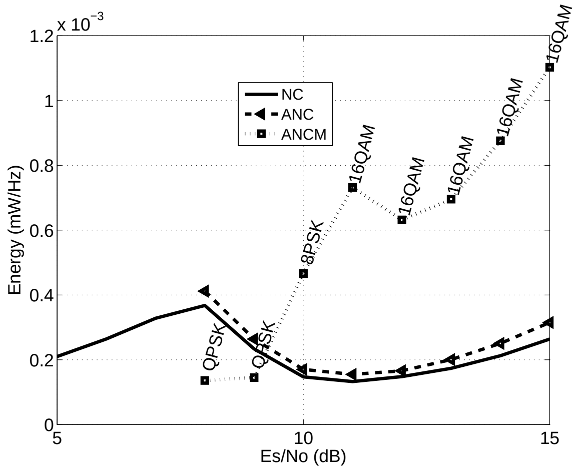

(b) Rayleigh fading

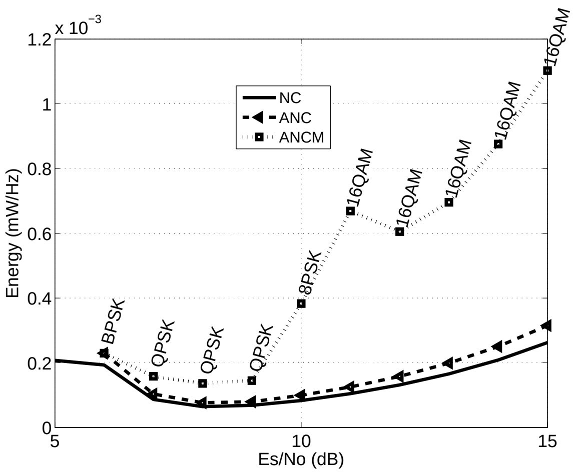

(c) LMS fading model with 1 m/s mobile speed

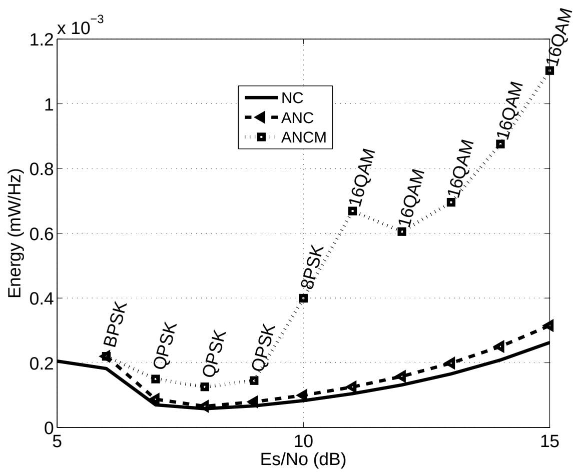

(d) LMS fading model with 10 m/s mobile speed

Fig. 3.10 Average consumed energy in GEO satellite scenario for variable E_s/N_0 values and within various fading models.

Fig. 3.12a for examples. It is worth to mention that it corresponds for a transponder operating at 36 MHz in Ka-band. However, ANCM scheme has a remarkable excess in average energy consumption over other schemes and its value varies between $1 \times 10^{-5}\,\mathrm{mW\,Hz^{-1}}$ at low SNR to $8 \times 10^{-4}\,\mathrm{mW\,Hz^{-1}}$ at high SNR. In addition, ANCM has a small gain in terms of average energy consumption for Rayleigh fading at SNR range 8 to 9 dB. This gain range is about $1 \times 10^{-4}\,\mathrm{mW\,Hz^{-1}}$ to $2 \times 10^{-4}\,\mathrm{mW\,Hz^{-1}}$ which can be observed for all simulation over Rayleigh fading model; Figs. 3.10b, 3.11b, and 3.12b. Moreover, it is interesting to note that for the increasing SNR values, the increased modulation order is associated with a increase in the number of transmitted packets, thus with a increased energy consumption.

Beyond a certain SNR, a leakage in energy exists suggesting no further benefits out of increasing the SNR, when the number of packets converges to minimum, thus the energy consumption increases almost exponentially. In addition, this suggests that for energy consumption purposes, the adaptation is no more convenient to be used when the SNR is getting too high, by achieving the global minimum, as depicted in Fig. 3.12c and Fig. 3.12d.

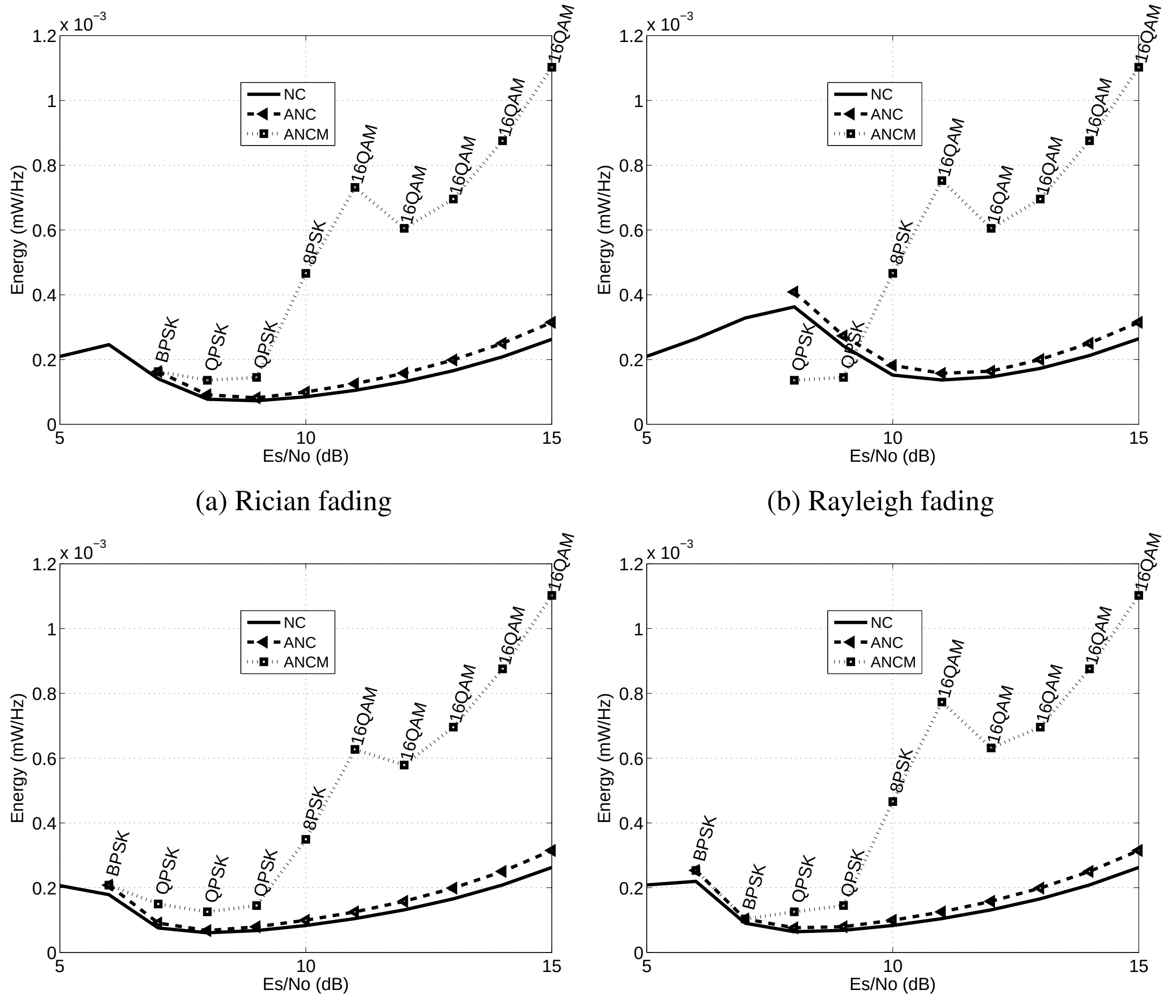

(a) Rician fading

(b) Rayleigh fading

(c) LMS fading model with 1 m/s mobile speed

(d) LMS fading model with 10 m/s mobile speed

Fig. 3.11 Average consumed energy in MEO satellite scenario for variable E_s/N_0 values and within various fading models.

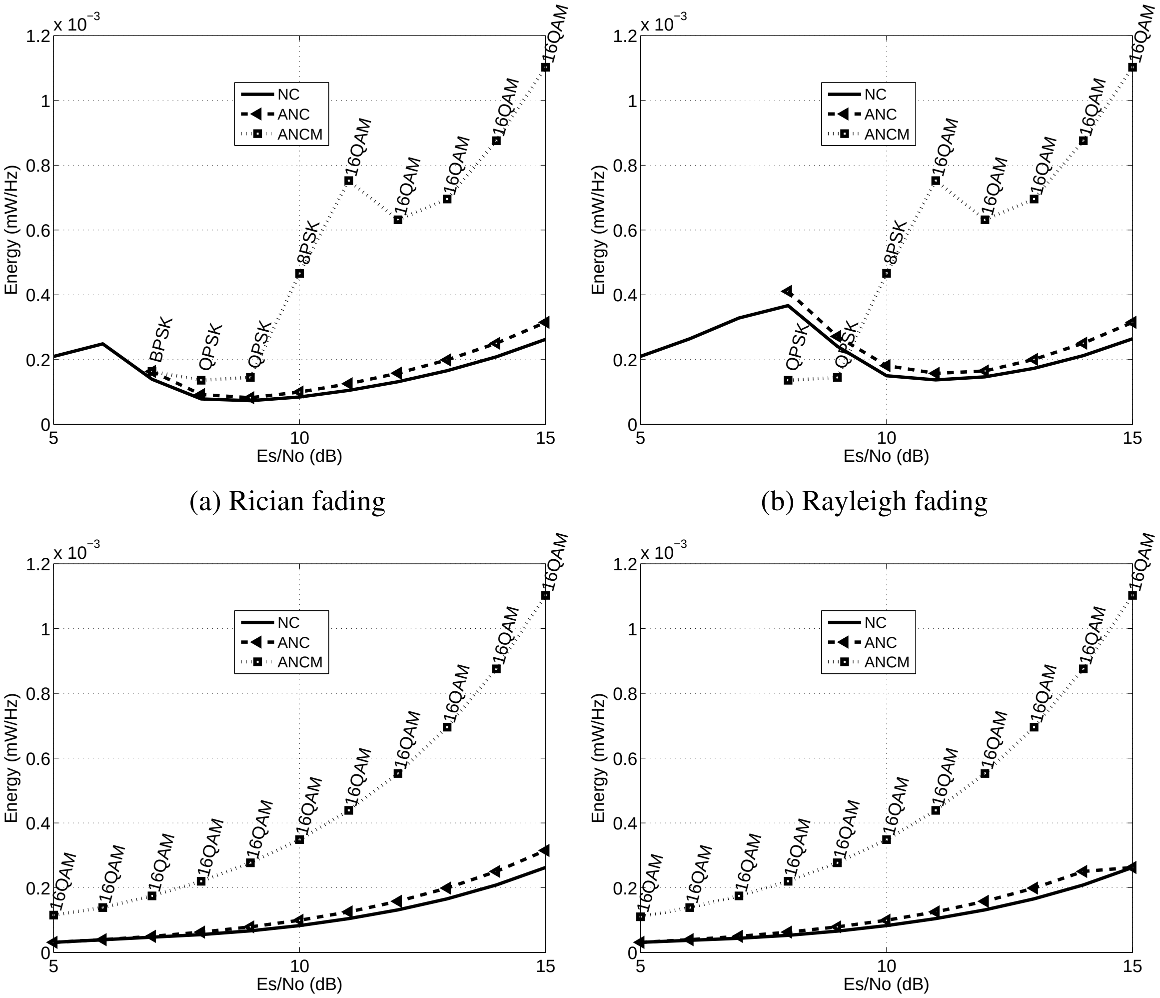

(a) Rician fading

(b) Rayleigh fading

(c) LMS fading model with 1 m/s mobile speed

(d) LMS fading model with 10 m/s mobile speed

Fig. 3.12 Average consumed energy in LEO satellite scenario for variable E_s/N_0 values and within various fading models.

Chapter 4

Energy efficient network coding in line sat network

4.1 Introduction

The transmission technique of network coding allows to reliably transmit with lower end to end delays in a communication system. Additionally, network coding mechanisms are key enablers to energy efficient communications. Usually, NC can be obtained by performing algebraic operations across transmitted packets rather than relying on packet repetition or replication. However, there is a general steady increase in energy consumption and energy costs in mobile communication systems, thus more energy efficient schemes are required. In particular, less re-transmissions can be achievable obtained via network coding with higher reliability. Moreover, more approaches of network coding can control and limiting energy consumption [60]. Network coding schemes can be designed for specific purposes for enhancing their awareness to the system characteristics and the channel variation over time, thus higher performance gains can be achieved in terms of delay and throughput or in terms of energy efficiency [1], [36], [37]. Energy efficiency is of great importance issue to be considered in satellite communications, since the satellite batteries have a dedicated life time and the fuel cells is limited [61]. A reduction in energy consumption gains can be achieved through integration between channel-aware transmission and network coding schemes, e.g., [1] and [49]. The proposed adaptive schemes in [36] show a relation between energy-driven and channel-aware schemes, in which the schemes remain silent or send very few when channel encounter high erasures. In this chapter, various aspects of energy efficiency using network coding and modulation schemes are proposed. The schemes are evaluated in the three common satellite scenarios, i.e., GEO, MEO, and LEO. In addition, the simulation has considered four various fading models. Then to describe the characteristics of the proposed schemes, we will show the simulation results to demonstrate the performance of the energy efficiency. We highlight that adaptation through channel-aware policies allows for silence periods or less transmissions which leads to significant energy savings compared to non-adaptive network coding or adaptive network coded schemes that are rate efficient.

4.2 Adaptive Network Coding with Energy efficiency (ANCEF)

In general, the proposed energy efficient schemes adapt to the channel variations over time within a certain fixed time-window with the aim of reducing the energy consumption. Such schemes favor silence or less transmission under worse channel conditions, to account in advance for expected energy losses when erasures in the channel enforces a definite retransmission. The system adapts the number of packets per transmission/retransmission.

This scheme (ANCEF) adapts the transmission for achieving the energy efficiency, by following the observation of the channel erasure; the strategy is to transmit small batches of coded packets if the observation of channel erasure is high (applies to low SNR), and to transmit larger batches of coded packets if erasure is low (applies to high SNR). Through this, the system can reduce the number of transmissions and re-transmissions and save energy accordingly. The following equation illustrates the number of coded packets N_i required to be sent at the channel state h_j when i dofs are required at the receiver,

$$N_i = \sum_{s=j}^{j+i-1} (1 - P_e(h_s)). \tag{4.1}$$

It is worth mentioning that N_i is required to be rounded to the nearest decimal or integer number, because it represents the number of coded packets. Moreover, the sum is expressed with a shifted start of the state of measurements. This is due to the channel evolution over time, thus, a new round of transmission/re-transmission is associated to shift in the channel window. When erasures are high (at low SNR) such sum vanishes to zero corresponding to no transmission. However, when erasures are very low (at high SNR) such sum converges to the transmission of i degrees of freedom almost surely.

4.3 Adaptive Network Coding and Modulation with Energy efficiency (ANCMEF)

In this scheme, we integrate adaptive modulation to the ANCEF scheme. The rationale behind this, is that, on the one hand, a higher modulation order m allows for transmitting the same amount of information in shorter packets due to the concatenation of more bits in the real and imaginary spaces. On the other hand, a higher modulation order is associated with higher energy per symbol, and less energy per bit, i.e. $E_b/N_0 = E_s/(N_0 \cdot \log m)$. Thus, a higher bit error probability suggests that higher number of packets need to be sent due to adaptation. Such trade-off between the packet length and the number of coded packets for a given modulation scheme is of particular interest to address when taking into account energy efficiency. ANCMEF transmission strategy of coded packets N_{i_m} is given by,

$$N_{i_m} = \sum_{s=j}^{j+i\cdot\log m-1} (1 - P_{e_m}(h_s)), \tag{4.2}$$

Resorting to the energy efficiency of the proposed scheme, the lower bound on random linear network coding, with $N_{i_m} \geq i$, i.e. with equality, is used; this was reflected in the sum range, by scaling the degrees of freedom i by a factor $\log m$ that unifies the energy per symbol for each modulation scheme. $P_{e_m}(h_s)$ is the erasure probability of that modulation which can be derived as

$$P_{e_m}(h_s) = 1 - (1 - P_{b_m}(h_s))^B,$$

where P_{b_m} is the bit error probability for the given modulation order m, and B is the number of bits per packet.

Indeed, the aim of the scheme is to find the optimal number of coded packets N_{i_m} for a given modulation order m to be transmitted/re-transmitted for assuring successful reception of a given number of i dof along the way with energy efficiency; hence, when P_{b_m} of m-th modulation order is derived, for fair energy comparison among the different modulation schemes, E_s is supposed to be constant for each modulation scheme, such unified energy per symbol on each modulation reflects on the packet length at each modulation scheme during adaptation.

4.4 Properties of the proposed schemes

We shall now provide a set of illustrative results that cast further insights to the proposed schemes with respect to energy efficiency. Particularly, we focus on GEO, MEO, and LEO satellite scenarios simulated along with four various channel fading models, i.e., Rician, Rayleigh and LMS models. considering GEO satellite with delay T_w equals 0.2388 s, equals 0.0668 s in MEO satellite, and for LEO satellite equals 0.0134 s. LMS model will be simulated in an open area with a mobile terminal having two speed values; the first speed is equal to $1\,\mathrm{m\,s^{-1}}$ and the second speed is equal to $10\,\mathrm{m\,s^{-1}}$. Moreover, it is worth to note that for taking into account practical QoS levels in terms of error probability we consider in the following that an acceptable bit error rate threshold is 10^{-5} [1]

The benchmark scheme is considered to be non-adaptive network coding scheme NC for time variant channels that was presented in [1]. In the non-adaptive network coding scheme, it is clear that the number of coded packets are fixed along the transmission/re-transmission with no adaptation considered. Contrary to the non-adaptive network coding scheme, the the proposed schemes adapt the number of coded packets for each batch of transmission based on the missing dof and on the channel erasures at a given window of estimated channel.

The modulation scheme considered is the BPSK in case of NC, and ANCEF, while the ANCMEF exploits four possible modulation schemes, i.e., BPSK, QPSK, 8PSK and 16QAM, in order to efficiently exploit the channel behavior. The selection of modulation order is driven by SNR level, i.e., E_s/N_0.

The number of bits per packet is considered to be 1000, and since the maximum number of packets per batch equals 10, the maximum possible batch of packet size equals 10000 bits. This number of bits corresponds to the same, the half, the one-third, and the one-forth number of samples in BPSK, QPSK, 8PSK, and 16QAM, respectively.

To construct the simulation environment, we consider to transmit data of 5 coded packets/dof. As mentioned previously, the maximum batch length due to channel adaptation of the schemes is constrained to 10 coded packets/dof, so the number of transmission/re-transmission trials to be fairly constrained and satisfied to the case that is requiring the highest possible number of states, i.e., number of states, equals 44. This corresponds to a transition matrix of maximum size equals 221×221 including one additional slot for absorption state, which changes entries and size according to the transmitted packets [2].

[1]The acceptable bit error rate, as proposed by the ITU ranges between 10^{-3} to 10^{-6} based on the rate and service expected at the mobile terminal.

[2]The transition matrix size is depending on the maximum number of states required upon the strategies of the proposed schemes $max(N_{states})$; we should count it for the higher modulation 16QAM in the case of ANCM and ANCMEF that will count $max(m) = 4$, and for our maximum batch that equals $max(N_i) = 10$ coded packets. In particular, it should be applied on the last remaining original packet/dof of the transmitted vector [5 4 3 2 1] required at the receiver side, i.e., [.... 1]. Hence, it should be added to the number of the required states. Therefore, the maximum number states for each transmitted packet can be given by,

$$max(N_{states}) = max(m) * max(N_i) + i - 1 \tag{4.3}$$

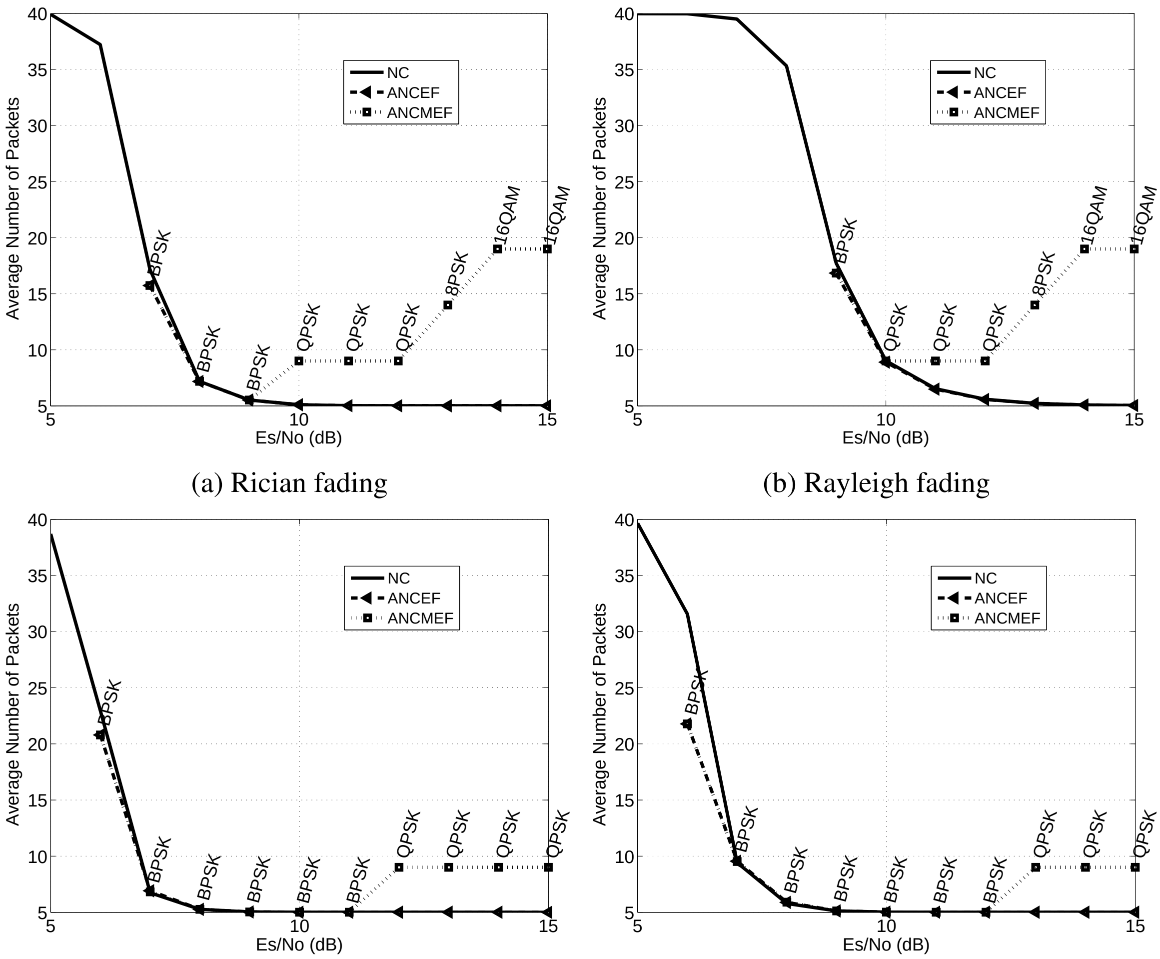

(a) Rician fading

(b) Rayleigh fading

(c) LMS fading model with 1 m/s mobile speed

(d) LMS fading model with 10 m/s mobile speed

Fig. 4.1 Average number of transmitted packets in GEO satellite scenario for variable E_s/N_0 values and within various fading models.

The performance of proposed schemes is compared in terms of the average number of transmitted packets, end to end compilation time, average throughput, and average energy consumption.

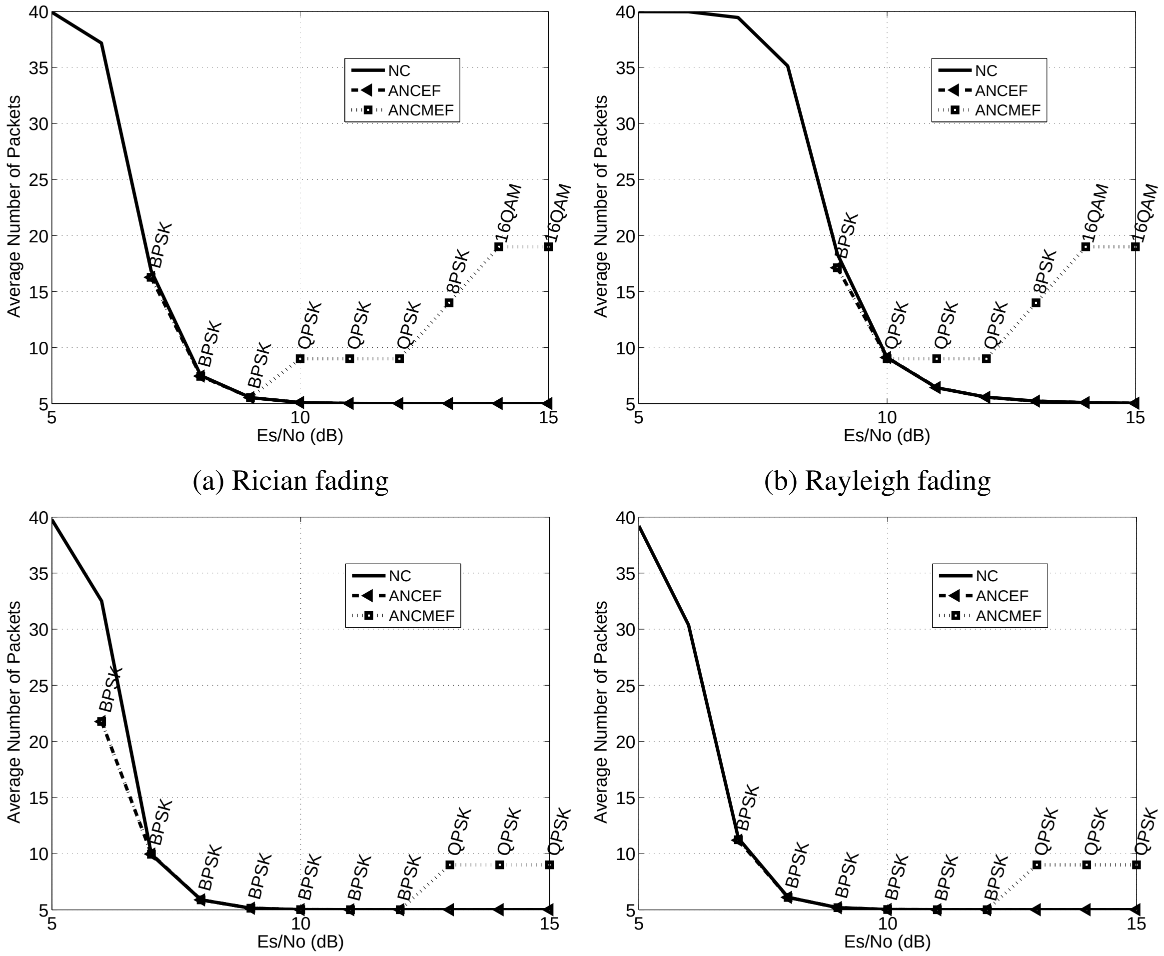

(a) Rician fading

(b) Rayleigh fading

(c) LMS fading model with 1 m/s mobile speed

(d) LMS fading model with 10 m/s mobile speed

Fig. 4.2 Average number of transmitted packets in MEO satellite scenario for variable E_s/N_0 values and within various fading models.

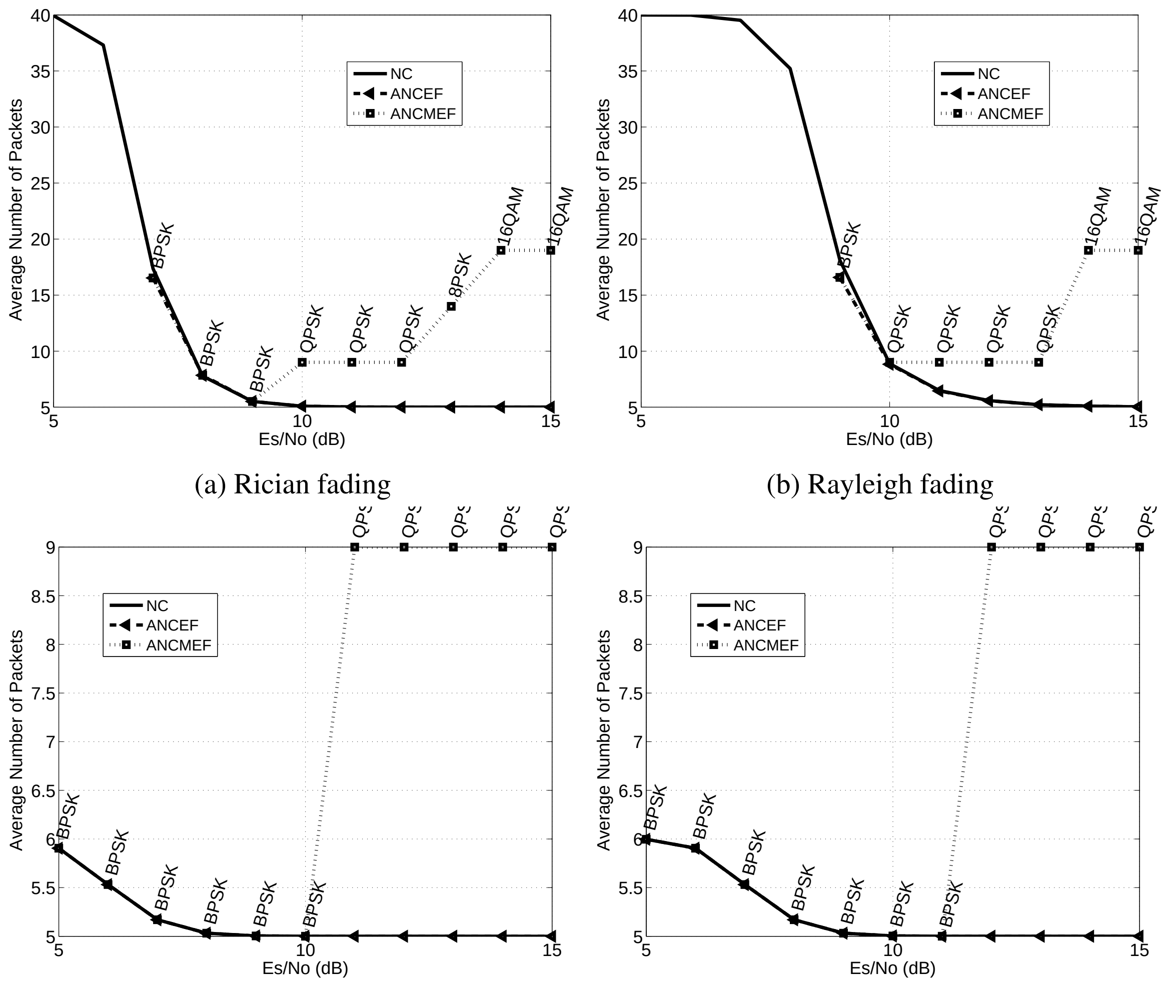

(a) Rician fading

(b) Rayleigh fading

(c) LMS fading model with 1 m/s mobile speed

(d) LMS fading model with 10 m/s mobile speed

Fig. 4.3 Average number of transmitted packets in LEO satellite scenario for variable E_s/N_0 values and within various fading models.

4.4.1 Average number of transmitted packets for the proposed energy efficient schemes

Here, the average number of coded packets sent back to back for the different schemes is compared; under different SNR values and with four various fading models, i.e., Rician, Rayleigh, and LMS mobility model ($1\,\mathrm{m\,s^{-1}}$ and $10\,\mathrm{m\,s^{-1}}$.) This can be seen in GEO, MEO, and LEO satellite scenarios in Figs. 4.1, 4.2, and 4.3.

In general, we can see that the average number of packets for all the schemes at low SNR is greater than those at high SNR due to the higher probability of re-transmission at low SNR. In particular, NC scheme which has a fixed number of dof to be transmitted can illustrate the initial pick in the average number, while both ANCEF and ANCMEF, and due to the minimum acceptable QoS, will have an initial transmission has been started after a silent period.

Moreover, due to energy efficiency rule, the average number of packets will be as much small as to commensurate with the higher erasure probability at low SNR or E_s/N_0 values, since they are designed to limit the number of sent packets in case of bad channel conditions i.e., there is no need to spend more energy in such low chance of delivery.

The tendency of the proposed schemes ANCEF and ANCMEF to send less packets than NC at low SNR values can be seen clearly, for example in: Fig. 4.1b, Fig. 4.1c, and Fig. 4.1d. While in others such as 4.1a, Fig. 4.2a, and Fig. 4.3a can be seen with difficulty, since Rician fading at low SNR values provide better channel conditions to the proposed schemes, in such a way their strategies will tend to initiate the transmission with number of coded packets as much close to NC as possible.

For ANCMEF scheme, the behavior of increase in average number of packets when $E_b/N_0 > 9$ dB is due to selecting higher modulation order. When the channel improves to allow for better modulation scheme, the average number of packets increases due to the ability of that modulation order in sending more packets for same window size. Hence, the availability to increase number of transmitted packets inside same window size is related to the availability of using higher modulation order, that in turns related to channel improvements.

It is possible to see also that ANCEF for upper and intermediate SNR sticks with NC due to the energy consumption strategy which does not favor to increase the throughput when a sufficient dofs is being already satisfied. Such like, Fig. 4.2a-Fig. 4.2d.

By applying the previous equation to find $max(N_{states}) = 44$, and then finding the product with i, we can exactly have the dimension of transition matrix has been used, i.e., $max(N_{states}) * i = 220$. Not exactly, because we should add one extra slot for the absorption state and so the dimension is equal to 221 in constraints of our simulation.

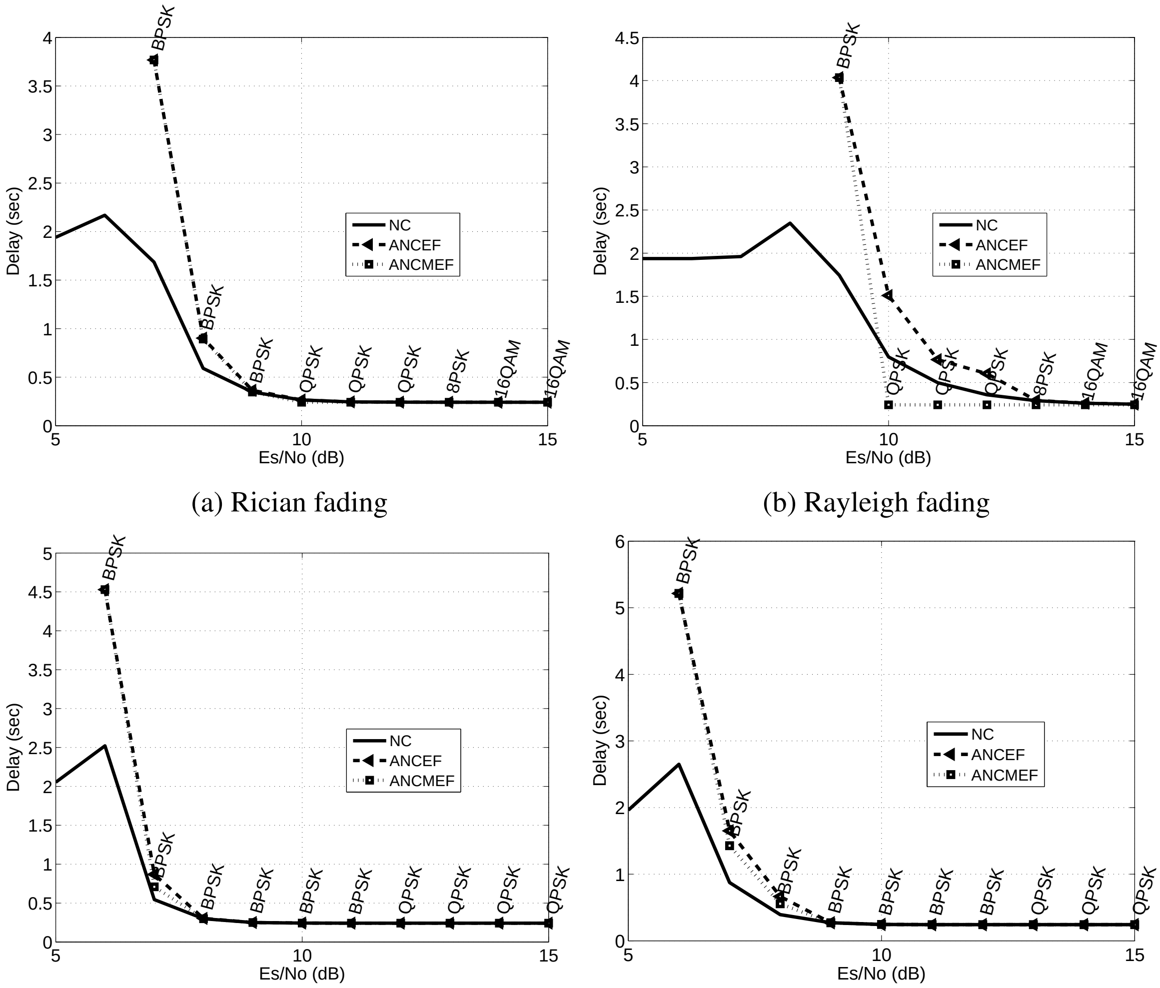

(a) Rician fading

(b) Rayleigh fading

(c) LMS fading model with 1 m/s mobile speed

(d) LMS fading model with 10 m/s mobile speed

Fig. 4.4 Expected end to end completion time in GEO satellite scenario for variable E_s/N_0 values and within various fading models.

4.4.2 End to end completion time for the proposed energy efficient schemes

Figs. 4.4, 4.5, and 4.6 illustrate the behavior in terms of transmission delay mainly for the efficient energy proposed schemes in GEO, MEO, and LEO satellite scenarios, respectively. Each scenario simulated in four different fading channels, i.e., Rician, Rayleigh, and LMS model.

The proposed schemes (ANCEF and ANCMEF) have the higher delay for low SNR values; this is due to the fact that the energy efficient adaptive schemes adapt its transmission to small size batches at the low E_s/N_0 that associated with high erasures. Therefore, the transmission suffers from extra waiting times for acknowledgment at the end of each short

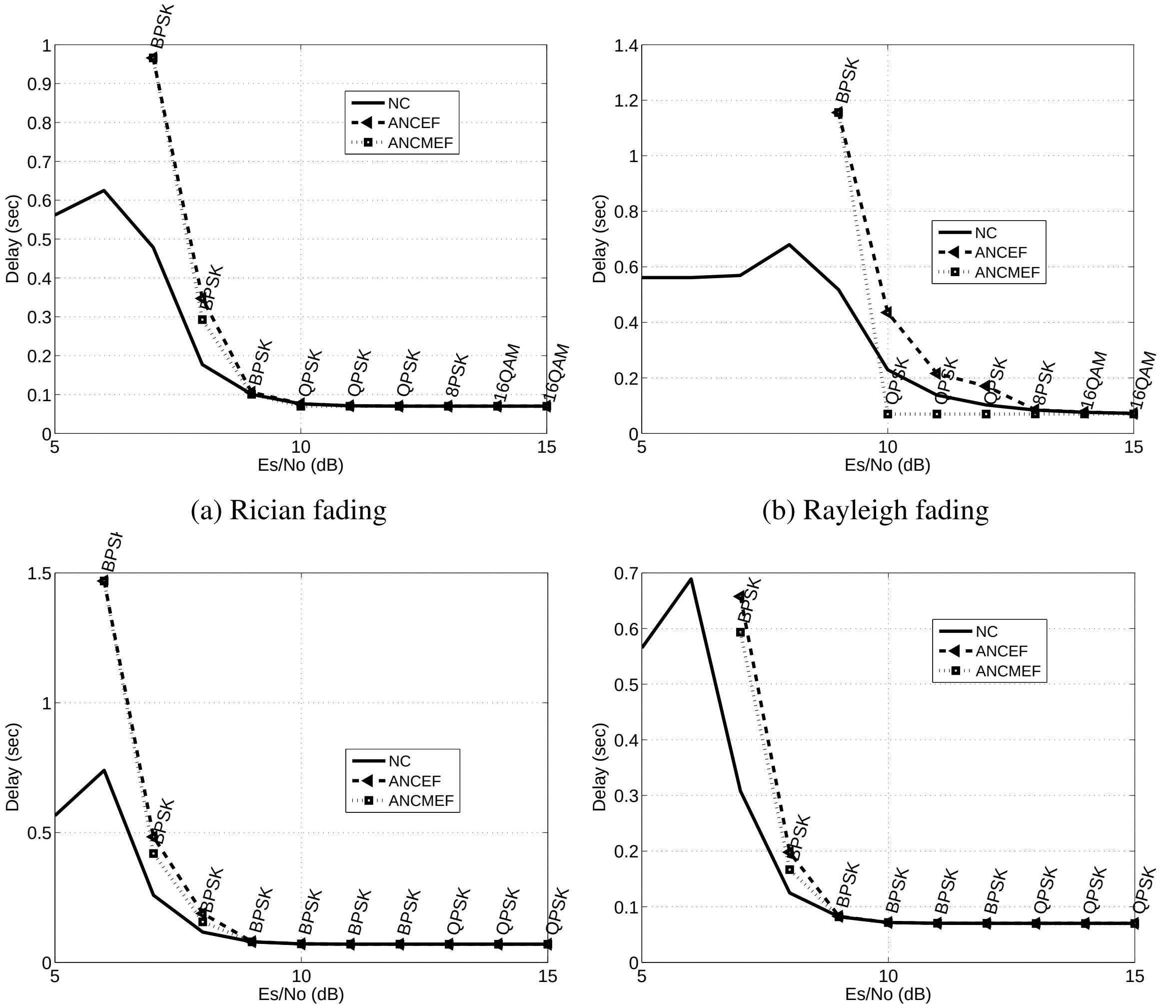

(a) Rician fading (b) Rayleigh fading

(c) LMS fading model with 1 m/s mobile speed (d) LMS fading model with 10 m/s mobile speed

Fig. 4.5 Expected end to end completion time in MEO satellite scenario for variable E_s/N_0 values and within various fading models.

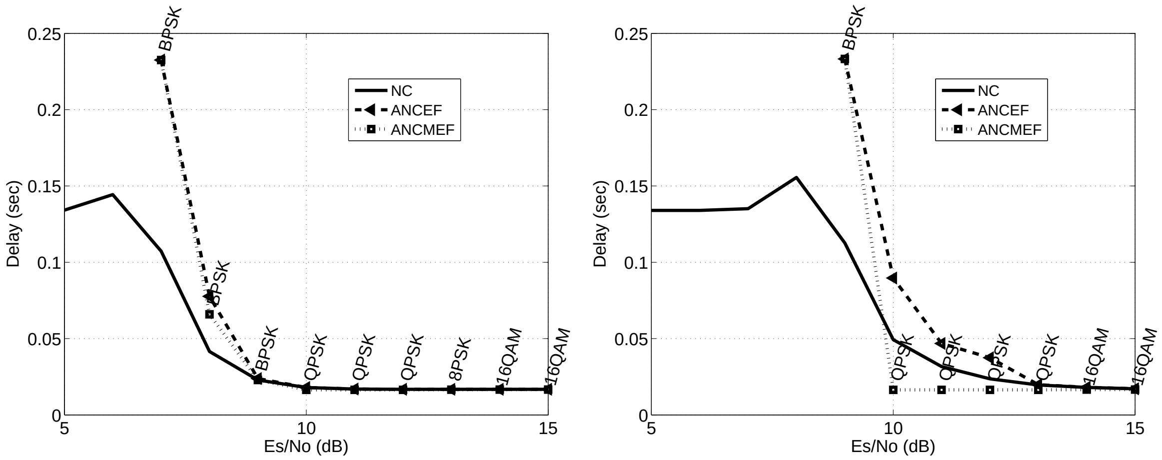

(a) Rician fading (b) Rayleigh fading

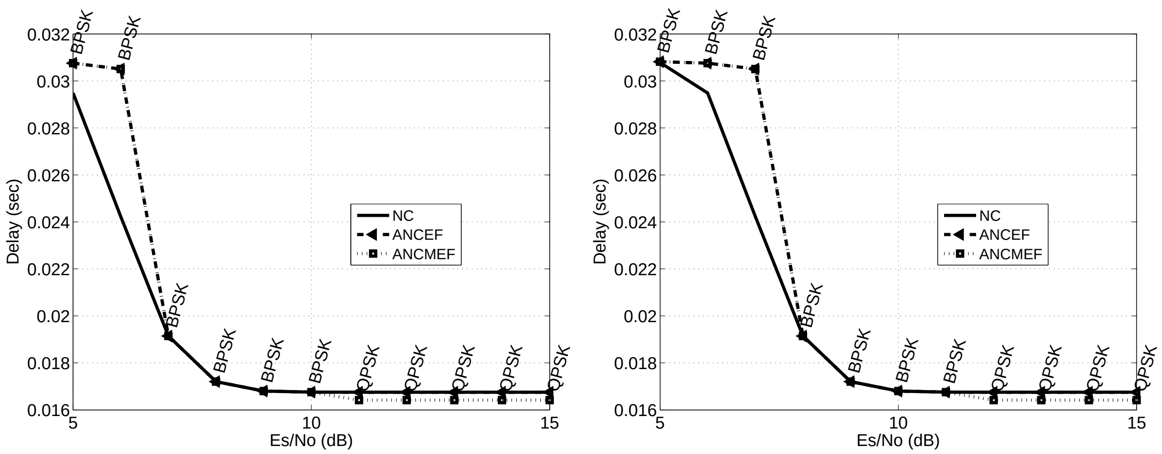

(c) LMS fading model with 1 m/s mobile speed (d) LMS fading model with 10 m/s mobile speed

Fig. 4.6 Expected end to end completion time in LEO satellite scenario for variable E_s/N_0 values and within various fading models.

batch. Thus, taking Fig. 4.4a as example for explanation, the time spent waiting for acknowledgment using ANCEF and ANCMEF is very long compared to the time of delivering the coded packets, i.e., the time has been taken using the proposed scheme is higher than using NC by 1.8 s to 0.3 s. Hence, the expected consumed time to deliver one coded packet using ANCEF and ANCMEF is about 0.7 s per packet and 0.18 s per packet at $E_s/N_0 = 7$ dB and $E_s/N_0 = 8$ dB, respectively. In contrary, using NC, the time is about 0.7 s per packet and 0.18 s per packet at the same previous SNR values.

Therefore, the delay performance of the proposed schemes at low SNR within Rician, Rayleigh and most LMS fading (except LEO scenario) is relatively higher than the delay value obtained when using NC. While in Figs. 4.6c, and 4.6c, by looking to the packets vectors promoted by ANCEF and ANCMEF, the delay difference of proposed schemes in the opposite NC is relatively small because of the fading nature of the short distance, i.e., LEO satellite scenario, as well as having the shortest delay time among the others.

However, some results of ANCMEF scheme have some exception since a normalization on the average number of packets with $\log m$ matches with the dof for such shorter length packets. The end to end compilation time results shown in, 4.4b, 4.5b, 4.6b, 4.6c, and 4.6d, can be clarified by resorting to the nature of Rayleigh fading or mobility LMS fading and also to the proposals of packets vectors for ANCMEF strategy where the selection of QPSK was much more convenient than BPSK used in the other schemes (NC and ANCEF). Thus, some time gain within a range of SNR about 10 to 12 dB that could be varied between 0.1 s and 1 s in GEO satellite scenario and between 10 ms and 100 ms.

After a certain E_s/N_0 value, the schemes have similar performance due to the number of packets in each batch that has been increased and then converged to the exact dof value of the non-adaptive NC scheme. Then finally, it is indeed straightforward to understand the delay saturation of all schemes to its minimal value at the high SNR.

4.4.3 Average throughput for the proposed energy efficient schemes

In Figs. 4.7, 4.8, and 4.9 present the throughput behavior also for three satellite scenarios, i.e., GEO, MEO, and LEO. The simulation has been done considered various fading environments, i.e., Rician, Rayleigh, and LMS mobility model.

The general view of all throughput figures and for low or sometimes for intermediate SNR values, i.e., $E_s/N_0 < 8$ dB or sometimes < 9 dB, both proposed schemes ANCEF and ANCMEF don't have any gains or even less than NC in terms of the average throughput. This can be explained by resorting to the proposed energy efficient methods that is limiting and reducing the number of coded packets when the channel characteristics suffer from high erasure probabilities.

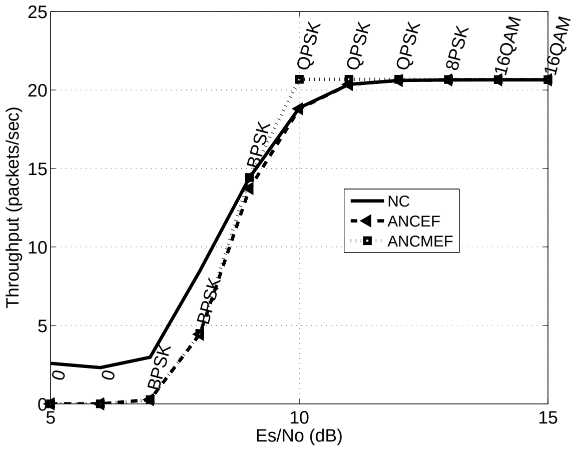

(a) Rician fading

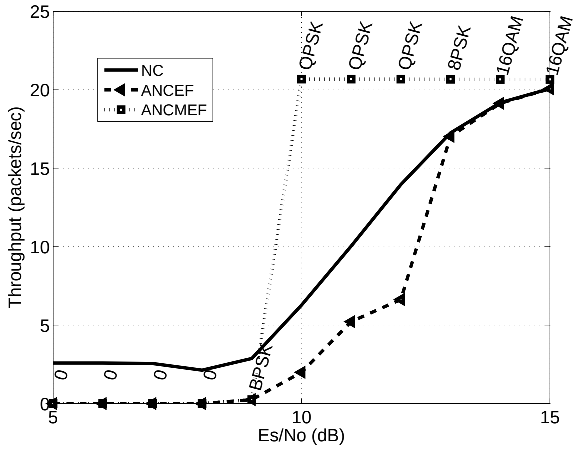

(b) Rayleigh fading

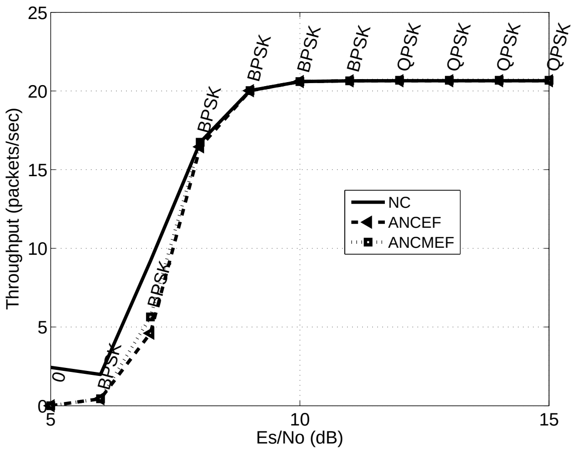

(c) LMS fading model with 1 m/s mobile speed

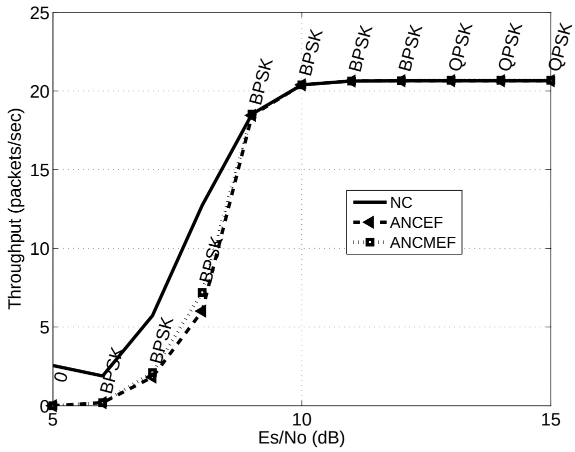

(d) LMS fading model with 10 m/s mobile speed

Fig. 4.7 Average throughput in GEO satellite scenario for variable E_s/N_0 values and within various fading models.

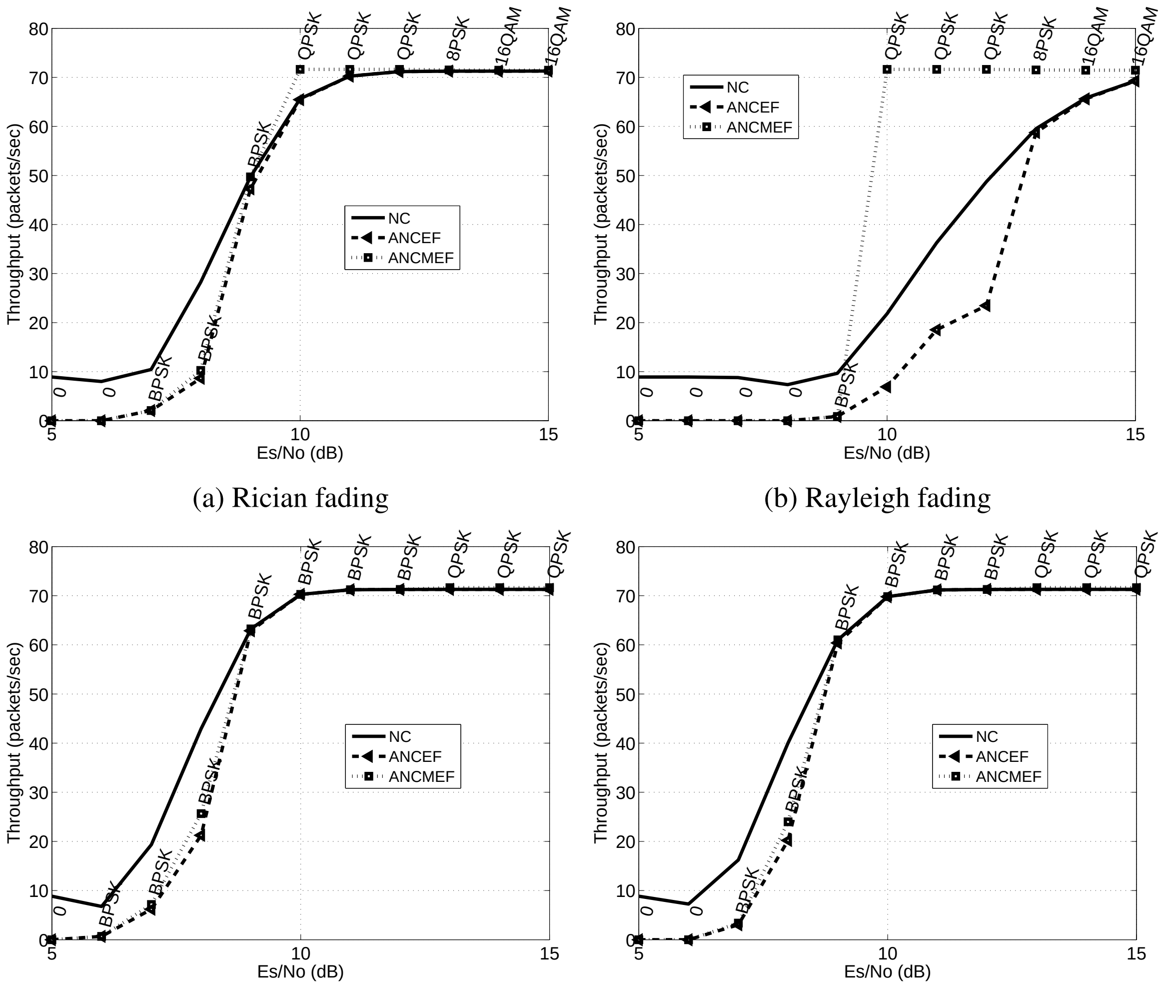

(a) Rician fading

(b) Rayleigh fading

(c) LMS fading model with 1 m/s mobile speed

(d) LMS fading model with 10 m/s mobile speed

Fig. 4.8 Average throughput in MEO satellite scenario for variable E_s/N_0 values and within various fading models.

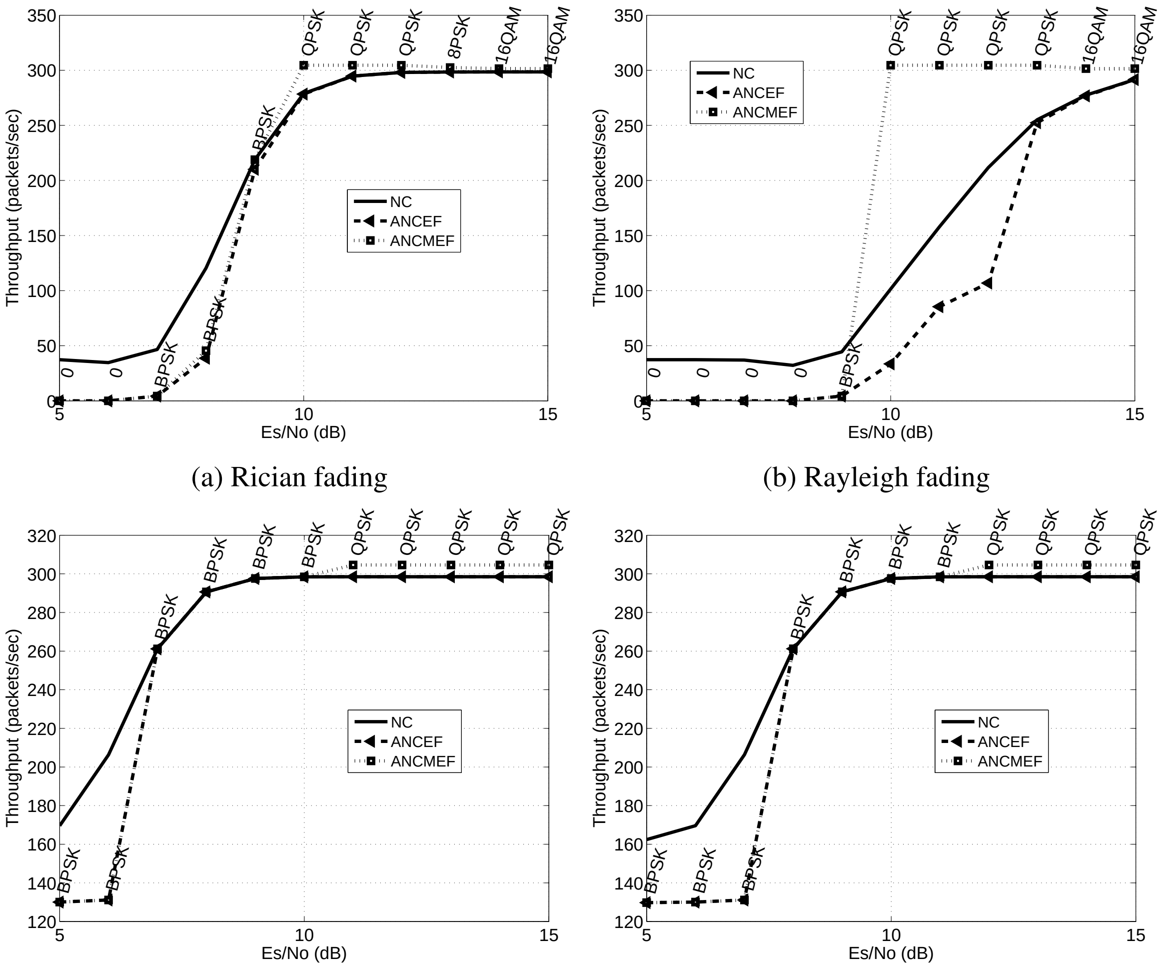

(a) Rician fading

(b) Rayleigh fading

(c) LMS fading model with 1 m/s mobile speed

(d) LMS fading model with 10 m/s mobile speed

Fig. 4.9 Average throughput in LEO satellite scenario for variable E_s/N_0 values and within various fading models.

It is worth to emphasize that the main aim of these schemes is to avoid any source of energy consumption that rise due to bad channel conditions, hence, such schemes remain silent in these conditions, hence, our schemes favors to be silent from transmission, than consuming energy by limiting the transmitted packets, and its utilization to adaptive coding techniques allows for reliable transmission and less energy due to decreased re-transmissions encountered. Furthermore, its worth to observe that at a certain E_s/N_0, all the schemes converge to maximum saturation throughput independent of fading model, mobile speed or channel variation.

While, some results of ANCEF and ANCMEF almost coincide in the behavior of the throughput performance, by improving the channel conditions and swapping among the fading models the picture will be change to be having a sort of throughput difference between NC and ANCEF on one hand and ACNMEF on the other hand. When SNR is getting better and improved enough, ANCMEF will use higher modulation types (QPSK, 8PSK, and 16QAM) which will give a sort of remarkable achievements in terms of the average throughput. These can be seen clearly in the whole output of the Rayleigh fading figures such as Fig. 4.7b, Fig. 4.8b, and Fig. 4.9b. While these throughput improvements can be hardly seen in the output of the LMS mobility model, especially when round trip time is relatively high, i.e., GEO and MEO satellite scenarios like in Figs. 4.7c, 4.7d, 4.9c, and 4.9d.

Furthermore, it's worth to observe that, for each satellite scenario and each fading model, the performance at a certain SNR of all the schemes (NC, ANCEF, and ANCMEF) in terms of the archived throughput is converging to a maximum throughput value. This SNR value is relatively intermediate or even high value and it is ranging between 11 dB as in Fig. 4.7c and higher than 15 dB as in Fig. 4.9c.

4.4.4 Average consumed energy for the proposed energy efficient schemes

Final property which is presented in Figs. 4.10, 4.11, and 4.12 is of great importance in this part of the study, i.e., as the proposed schemes here are for energy efficiency. Those results are of simulation outputs for various fading models in a parallel with the three satellite scenarios.

In the simulation, we first consider total energy consumption that has been calculated using both the power spectral density of the noise component level as $N_0 = -107$ dBm and the expected time needed to send 5 coded packets/dofs for each E_s/N_0 of each scheme. It is possible to note that the proposed schemes allow significant gains in terms of energy consumption with respect to the benchmark scheme (NC non-adaptive network coding scheme).

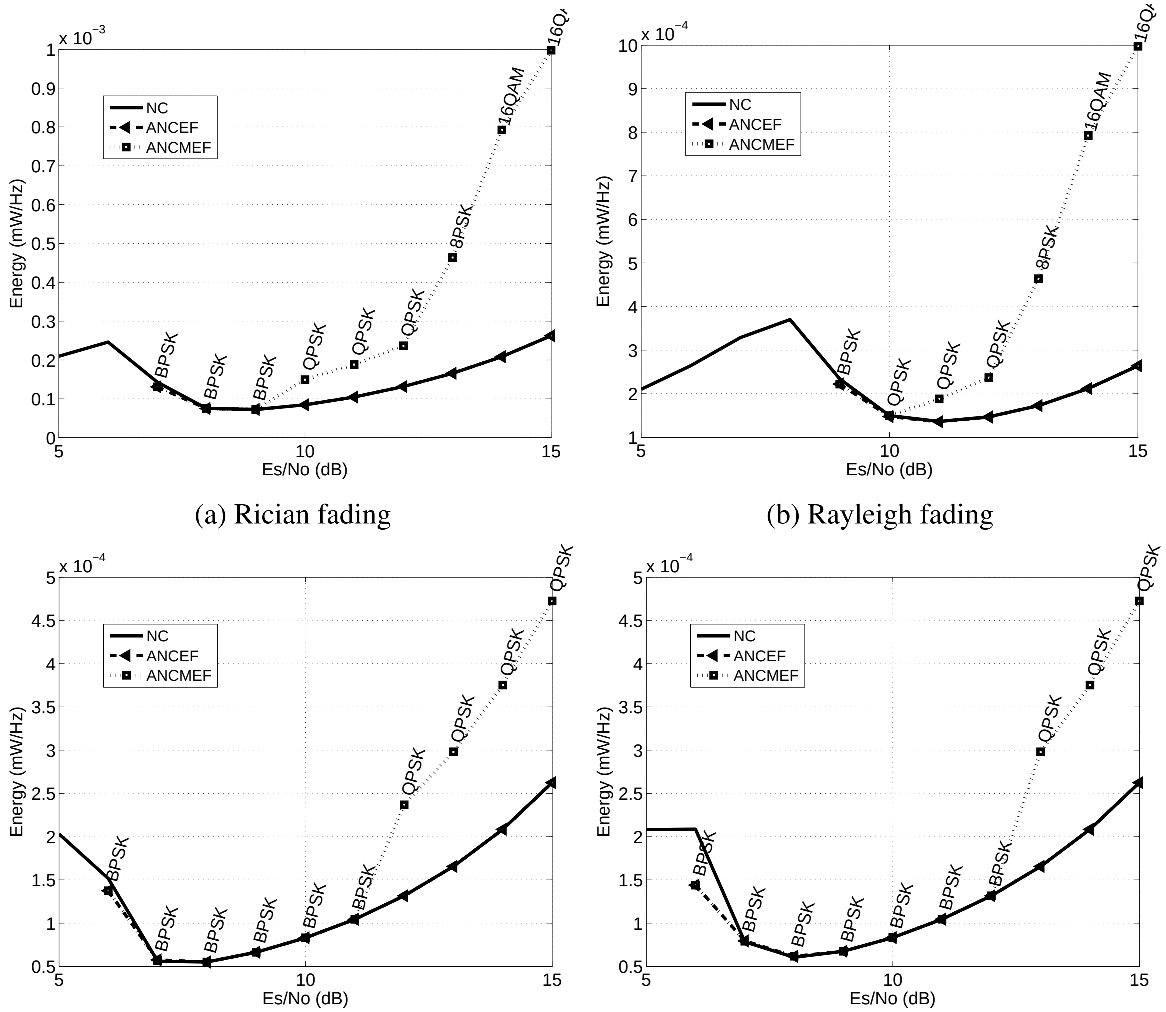

(a) Rician fading (b) Rayleigh fading

(c) LMS fading model with 1 m/s mobile speed (d) LMS fading model with 10 m/s mobile speed

Fig. 4.10 Average consumed energy in GEO satellite scenario for variable E_s/N_0 values and within various fading models.

It's clear that at the low SNR, i.e., precisely at $E_s/N_0 = 6$ dB in Figs. 4.10c, 4.10d, 4.11c, and 4.11d, we can see ANCEF and ANCMEF gain roughly $5 \times 10^{-5}\,\mathrm{mW\,Hz^{-1}}$ with respect to the NC scheme. Moreover, we consider to have one single beam with a transmitting power equal to 65 W and that the transmission bandwidth is 36 MHz. Hence, it is worth to see that ANCEF and ANCMEF reduce remarkably the energy consumption by calculating the overall energy that may consume by using one single beam for the considered operating bandwidth, Where

$$E \;=\; 5 \times 10^{-5} \;\times\; 36 \times 10^{6} \;=\; 1800\;[\mathrm{mW}] \tag{4.4}$$

so the schemes are gaining up to roughly with respect to the NC scheme 1.8 W out of 65 W that has been reserved to operate with transmitting using one single beam; such an amount might seem to be small, however, this represents very high figure in a large scale system with multiple receivers.

Furthermore, at the moderate and high SNR values, the ANCEF is better and more convenient than ANCMEF in terms of energy efficiency, i.e., at $E_s/N_0 \geq 9$ dB the ANCMEF will consume more energy than both NC and ANCEF and even exponentially due to the utilization of higher modulation orders, in which ANCMEF is associated with an increase in the transmitted message which necessarily increases the overall system energy consumption. Therefore, the ANCEF scheme beyond a certain SNR, will have a leakage in energy suggesting no further benefits out of increasing the SNR, when the number of packets converges to minimum, thus the energy consumption increases almost exponentially.

It is worth to mention that the ANCMEF energy consumption, during the selection of the order modulation type, pass through a sort of graded curve. Indeed, each grad level presents one of a type of modulation orders For example, in Fig. 4.10a the first three points at E_s/N_0 equals $7,\ 8,\ and\ 9$ dB use the basic modulation order (BPSK). Then it selects the modulation order QPSK for the next three points at E_s/N_0 equals $10,\ 11,\ and\ 12$ dB, in which the ANCMEF presents the second upper level of the energy consumption. While at E_s/N_0 equals 13 dB, and then at E_s/N_0 equals $14, and$ 15 dB illustrate the next upper two levels of the energy consumption by utilizing the modulation orders 8PSK and 16QAM, respectively.

Furthermore, ANCEF can be consider to be more intelligent scheme than the others, where at low SNR and because of the channel state of being with high erasure probabilities we can see that ANCEF plays an important rule due to the shorter batches of the packets length to be used according to method of energy efficiency. Then at high SNR, the ANCEF stay tuned in line with NC which means that there is no an added value of energy consumption, so this adaptive scheme can be nominated as an energy efficient scheme that can be ranging form low to high SNR values, and while passing through the moderated ones.

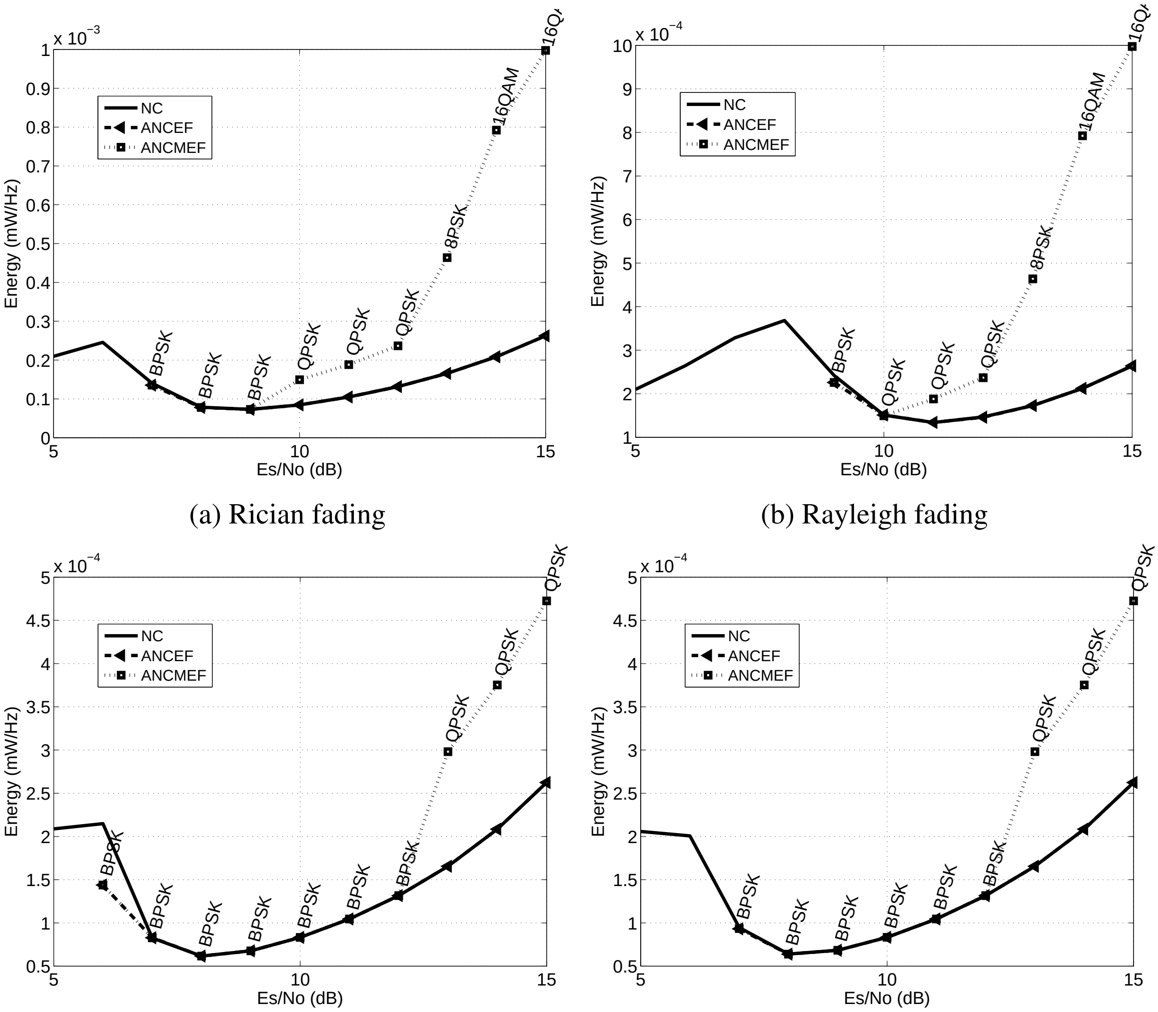

(a) Rician fading (b) Rayleigh fading

(c) LMS fading model with 1 m/s mobile speed (d) LMS fading model with 10 m/s mobile speed

Fig. 4.11 Average consumed energy in MEO satellite scenario for variable E_s/N_0 values and within various fading models.

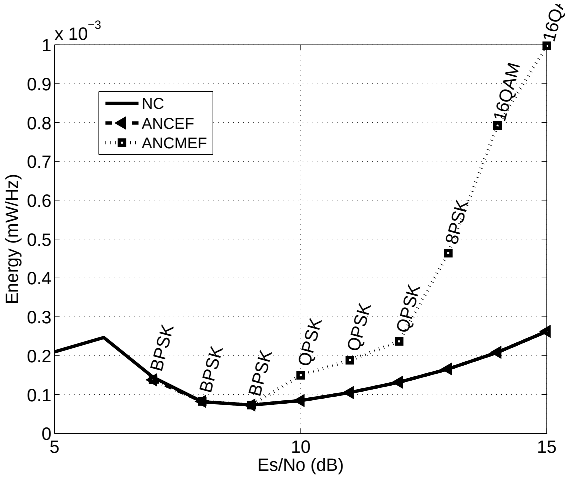

(a) Rician fading

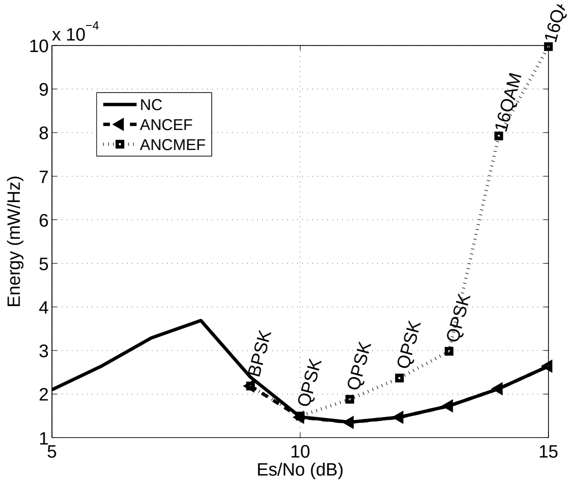

(b) Rayleigh fading

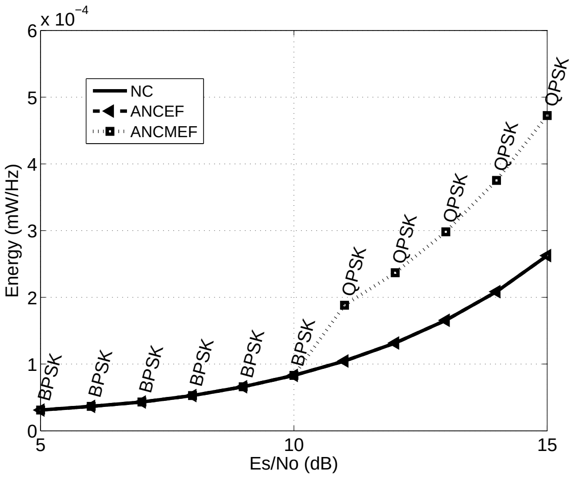

(c) LMS fading model with 1 m/s mobile speed

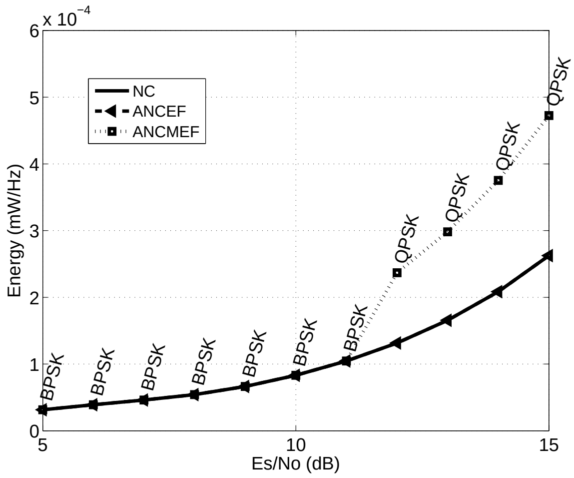

(d) LMS fading model with 10 m/s mobile speed

Fig. 4.12 Average consumed energy in LEO satellite scenario for variable E_s/N_0 values and within various fading models.

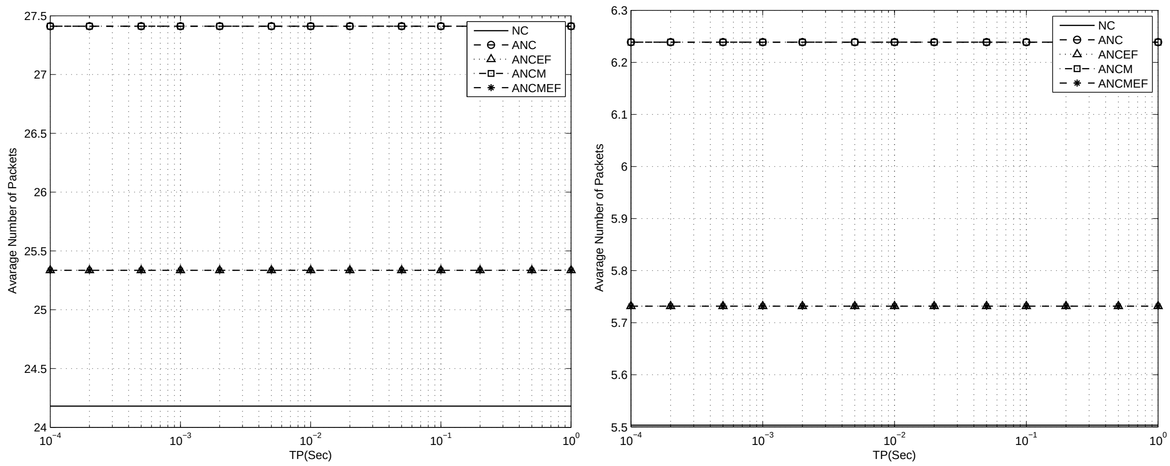

(a) Long batch size (12 packets)　　(b) Short batch size (3 packets)

Fig. 4.13 Average number of transmitted packets in a GEO Satellite scenario for variable T_P values with E_s/N_0 equal to 7 dB and $10\,\mathrm{m\,s^{-1}}$ mobile speed.

4.5 Packet length effect on rate-efficient and energy-efficient schemes

Finally, Figs. 4.13-4.16 illustrate the effects of packet length on the performance of our proposed schemes, by considering a fixed SNR value, that we have selected to be equal to 7 dB. In Fig. 4.13 the average number of packets as a function of T_p varying between 0.1 ms and 1 s is reported. It is possible to see that the average number of coded packets for each scheme has a fixed value along with the increase of packet length time, e.g., for long batch size (12 packets) the corresponding average number of coded packets is 24.2, 25.4, and 27.45 packets for NC, (ANCEF, ANCMEF), and (ANC, ANCM), respectively.

Fig. 4.14 shows the end to end delay as a function of T_p. It is possible to see that the packet length does not have a major impact on the delay when T_P is less than 50 ms. After that, the delay becomes more vulnerable to the packet length.

In particular, when the packet length is small the delay is mostly affected by the RTT, since the energy per bit is high enough to yet allow the mitigation of channel variations over time.

However, in case of larger packets the delay is not mainly affected by the RTT which occurs less frequently, but the lack of mitigation of channel variation over time. This suggests a clear impact of the length of the packet on the performance of the system.

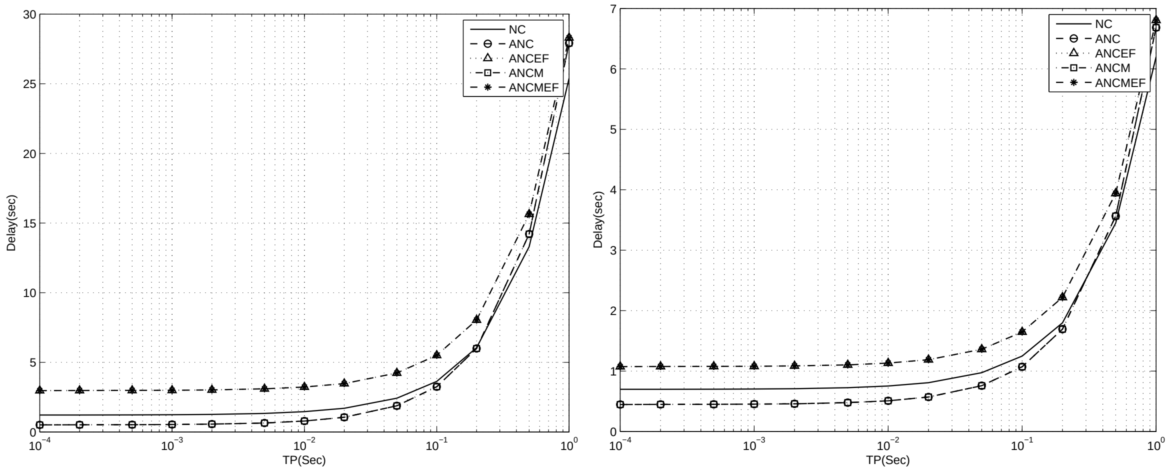

(a) Long batch size (12 packets)

(b) Short batch size (3 packets)

Fig. 4.14 Transmission delay in a GEO Satellite scenario for variable T_P values with E_s/N_0 equal to 7 dB and $10\,\mathrm{m\,s^{-1}}$ mobile speed.

Such result suggests a certain operating regime in terms of packet size at a certain satellite scenario, where if exceeded, it might be necessary not to use packet sizes of time lengths that meets higher orbit satellite waiting times.

Moreover, it is of particular importance to recall that each packet is associated to a single channel state, according to the model by [1], through which if the packet size exceeds the coherence time of the channel, which is roughly 50 ms, the estimates are stale and an appropriate packet length should not exceed that length.

The throughput as a function of T_p is shown in Fig. 4.15; also this case, similar to the delay, is distinguished by the throughput that is mostly affected by the relationship between RTT and the packet length. For small packet length the throughput is mostly affected by the RTT while that increased packet length the throughput is also affected by the reduced data rate introduced in case of larger packets.

Finally, Fig. 4.16 presents the energy consumed. It is possible to see that it has a behavior similar to the average number of transmitted packets, as expected, since the energy consumption is mostly affected by the sent packets irrespective to the relationship **with** packet length or RTT. However, ANC has the maximum energy consumed which is equal to 41 mW, while ANCEF and ANCMEF have the lowest energy consumed around 27.5 mW due to the low average number of transmitted packets.

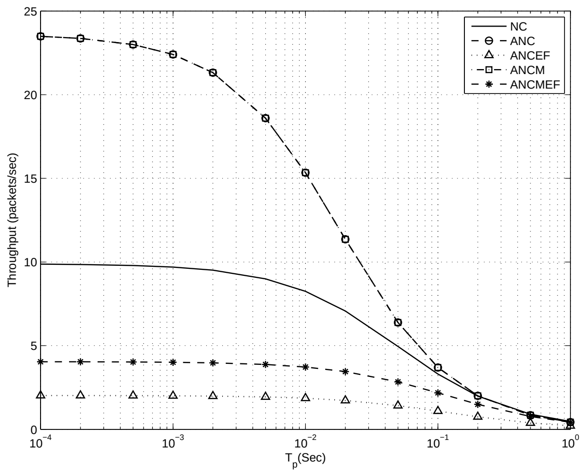

(a) Long batch size (12 packets)

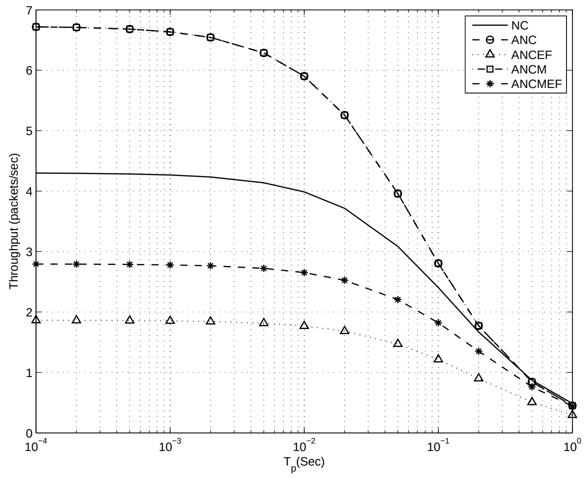

(b) Short batch size (3 packets)

Fig. 4.15 Throughput in a GEO Satellite scenario for variable T_P values with E_s/N_0 equal to 7 dB and $10\,\mathrm{m\,s^{-1}}$ mobile speed.

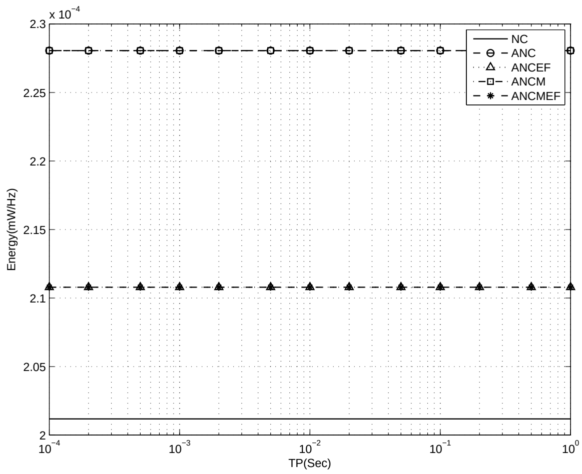

(a) Long batch size (12 packets)

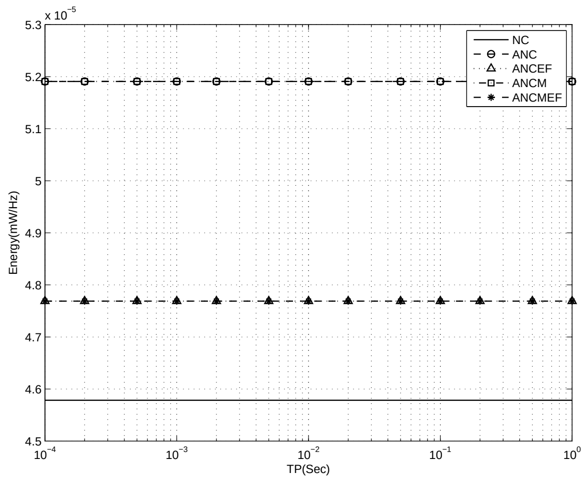

(b) Short batch size (3 packets)

Fig. 4.16 Average energy consumed in a GEO Satellite scenario for variable T_P values with E_s/N_0 equal to 7 dB and $10\,\mathrm{m\,s^{-1}}$ mobile speed.

Chapter 5

Adaptive network coding for multicast Sat. network

In this chapter, we are going to propose two novel schemes in order to solve the problem of finding the optimal number of coded packets, which in turns, are to multicast to a set of independent wireless receivers. The supposed receivers are suffering different channel conditions; this is a known open problem in the network coding literature.

In particular, we propose two virtual channel networks that allow for the representation of a group of receivers, and the intention here is to show the multicast group as a single receiver from the perspective of the satellite. Such approach allows for a transmission scheme not only adapted to per-receiver channel variation over time, but to the network-virtualized channel representing all receivers in the multicast group.

The first scheme capitalizes on a "Max erasure", which is a criterion that has been presented via the creation of a virtual reference channel of the network. The second scheme capitalizes on a "*Max CT*", a maximum completion time criterion by the use of the worst performing receiver channel as a virtual reference channel to the network. We apply such schemes to GEO satellite scenario. We demonstrate the benefits of the proposed schemes by comparing them to a per-receiver point-to-point adaptive strategy.

5.1 Introduction

Network coding is a key enabling technology for several communication network types. Within many, network coding offers a unique technique to multicast communications where a common information is shared among a set of receivers in a one-to-many fashion. Multicast communications are fundamental to many practical applications, including Satellite

TV broadcast, content delivery and interactive communications, such as in multimedia conferencing, across wired or wireless medium.

In wired networks, as mentioned before, network coding was shown to achieve the multicast capacity [22]. In particular, it is shown that an explicit construction of a code that achieves multicast network capacity is a linear network code [31]. Another proposal for multicast network is called Random Linear Network Coding (RLNC); which is to multicast in a distibuted network using network coding approach, the network suppose to have nodes that independently and randomly selecting linear coding coefficients from inputs onto output links over a Galois field, and then it achieves the capacity with very high probability.

The nature of wireless networks, and thus the broadcast and multicast on wireless links are suffering from different channel behaviors such as, the noise, the interference levels, and the variation over time. So, it becomes a challenge to find an explicit model that express a wireless network capacity. Moreover, the characterization of optimal approaches is of great importance that jointly minimize the system completion time to several entities.

In the multicast among a mesh of receiving nodes, the capacity was shown to be inversely proportional to the connection probability [47].

The authors in [62] characterize the expected number of transmissions per packet and quantify its gain with network coding analytically. They have also conjecture that network coding achieves a logarithmic gain in the expected number of transmissions/retransmissions to multicast compared to an ARQ scheme.

In this chapter, we try to provide an innovative way solutions to the question *how can we optimize jointly the coded transmission to a set of receivers in a multicast group?* In particular, we try to solve such an open problem due to lack of available models that express a correlated structure, by looking at the multicast approach through a virtual network that expresses an equivalent network to the min-cut. This network virtual link represents the multicast group time variant channel and can be exploited to design optimal or near optimal number of coded packets to transmit to all receivers in a multicast group.

This chapter goes in this direction by finding the optimal number of coded packets to transmit to all receivers of a multicast wireless network group. To the best of our knowledge, this work is the first to characterize schemes that can jointly design the number of coded packets to multicast to a set of multicast group receivers encountering different time variant channels.

5.2 System model

We consider a downlink multicast over a wireless channel. The source performs RLNC [32] and for GEO satellite scenario. The coefficients used to generate coded packets are chosen at random from a Galois finite field of very large size. With this, the probability of generating linearly dependent packets decreases with the field size increase. Therefore, we assume a very large field size that allows with almost probability 1 the decorrelation in generation.

However, it is worth to note that there yet exists a dependency in the probability of packet erasure due to channel variation over time which is inherently existing in the Land Mobile Satellite (LMS) channel model. Additionally, the probability of erasure in the acknowledgment is considered to be zero for simplicity.

After RLNC, the satellite multicasts to a group of K receivers that should receive a common content. Therefore, the per-receiver k will receive a vector modeled as:

$$y_k(t) = h_k(t) \cdot A \cdot x(t) + n_k(t), \tag{5.1}$$

where $x(t)$ and $y_k(t)$ correspond to transmit and receive symbols, respectively. By assuming a generalized fading model, that is time varying and follows the LMS model in a low height building environment [51], A is the transmitted signal amplitude from the GEO satellite, and $n(t)$ is the zero mean complex white Gaussian noise.

While t is considered to be within interval $\mathscr{T} = [0, \tau]$. Moreover, a set of K receivers $\mathscr{K} = \{1, \dots, K\}$, in the group of multicast, are associated to a vector of channel gains of length τ. We assume that there is no channel coding within the received packets. Thus, for each packet, every symbol needs to be received. Therefore, the corresponding packet erasure probability of channel gain $h_k(t)$ is expressed at time instant $t \in \mathscr{T}$ as:

$$P_e(h_k(t)) = 1 - (1 - P_b(h_k(t))^B, \tag{5.2}$$

where $P_b(h_k(t))$ is the bit error probability for a given modulation scheme, at a given channel gain $h_k(t)$, and B is the number of bits per coded packet.

In the following two subsections, we will present the utilization of a set of K completion times that will be associated to the receivers, suggesting a unifying approach that allow for a joint optimization of all the completion times of all the receivers. Given that such a problem is unsolvable, we propose two novel heuristic approaches that allows for near optimal joint optimization of the number of coded packets to multicast to all receivers.

5.3 Channel virtualization schemes

We propose two novel virtual channel schemes to address the multicast modeling problem with time variant channels. Such proposal inherently exploits the necessity to represent the wireless network in an equivalent form. Hence, it allows for characterizing the capacity of each wireless network by its min-cut [63]. A min-cut mimics the maximum delay or erasure that limits the information flow in a wireless network. Therefore, the solution, that can be proposed for a virtual network channel, should allow receiving with worst conditions to yet be able to decode the received information in a reliable way.

Due to the broadcast nature of wireless communications, and the impairments associated to their challenging environments, like the satellite communications addressed here, the interpretation of such approach for time variant channels is to represent all the wireless links as point-to-point. Moreover, those links should be with a reference of virtual channel that provides most possible losses in terms of packet erasures or in terms of completion time. Where both references are associated to resource wastage in retransmissions or within waiting times until content is delivered reliably.

We capitalize on the coded packet transmission model for time variant channel proposed in [1] to characterize per-receiver completion time. This model is used for characterizing, per-receiver, packet transmission adapted to its channel variation, also for network virtual and optimizing the batch size to be transmitted over it.

5.3.1 Maximum Packet erasure scheme (*Max Pe*)

In this scheme, we propose to represent the receivers' channels in the multicast group by their joint global "Max erasure" encountered by the considered receivers. This observation scans over each time slot within the time window of channel variation. In turn, the optimization problem of such scheme can be written as:

$$\begin{aligned}
\max_{P_e(h_k(t_1)),\dots,P_e(h_K(t_T))} \min_{N_1,\dots,N_i} T(i,h_j) &= \max_{P_e(h_k(t_1)),\dots,P_e(h_K(t_T))} \min_{N_1,\dots,N_i} T_d(N_i,h_j) \\
&+ \max_{P_e(h_k(t_1)),\dots,P_e(h_K(t_T))} \min_{N_1,\dots,N_i} \sum_{l=1}^{i} P^{N_i}_{(i,h_j)\rightarrow(l,h_{j+N_i})}\, T(l,h_{j+N_i+1}), \\
&\forall k=\{1,..,K\} \in \tau = \{1,\dots,T\} \quad (5.3)
\end{aligned}$$

So, the virtual channel can be produced by considering the packet erasure values $P_e(h_k(t_\tau))$ at each channel states $\tau = \{1,\dots,T\}$ of one receiver k, and then compare it with those of set other receivers $\{1,..,K\}$. By applying the above mentioned comparison and then take the maximum of packet erasures at the level of channel state and among the channels' receivers. So, we can obtain a joint maximum packet erasures of all channels' receivers. Thus, mathematically the obtained expression can be given by,

$$\max_{P_e(h_k(t_1)),\ldots,P_e(h_K(t_T))}.$$

Moreover, the joint maximum packet erasures for each number coded packets/dofs i at each channel state of each receiver will correspond with the minimal number of coded packets N_i.

As it is known that the optimization problem is combinatorial and hard, we resort to the heuristic Adaptive Network Coding (ANC) scheme in [1] to solve the problem of finding the number of coded packets to transmit to all receivers in the multicast group. Therefore the batch size that satellite multicast to all receivers with a guarantee to decode it under the design of worst case condition, so $N_1,\ldots,N_i$ is found by iterating over the vector of degrees of freedom as:

$$\sum_{s=j}^{N_i}(1-P_e(h_s)) = i, \qquad \forall P_e(s),\ s.t. \quad P_e(s) : \max\{P_e(h_k(t_1)),\ldots,P_e(h_K(t_T))\},$$
$$\forall k = \{1,..,K\} \in \tau = \{1,\ldots,T\} \quad (5.4)$$

5.3.2 Maximum Completion Time scheme (*Max CT*)

In this scheme, we propose to represent the receivers channels in the multicast group by the worst receiver's channel as a reference channel, which encounters "*Max CT*" or maximum completion time to receive and decode reliably all coded packets from the satellite within the observation time window of channel variation. In turn, the optimization problem of such scheme can be written as follows,

$$\max_k \min_{N_1,\ldots,N_i} T(i,h_j) = \max_k \min_{N_1,\ldots,N_i} T_d(N_i,h_j) + \max_k \min_{N_1,\ldots,N_i} \sum_{l=1}^{i} P^{N_i}_{(i,h_k)\to(l,h_{j+N_i})} T(l,h_{k+N_i+1}),$$
$$\forall k = \{1,..,K\} \quad (5.5)$$

As it is known that the optimization problem is combinatorial and hard, we resort to the heuristic ANC scheme in [1] to solve the problem of finding the number of coded packets to transmit to all receivers in the multicast group, therefore, the set of coded packets the GEO satellite will multicast with a guarantee that all receivers will be able to decode under the design for worst case condition $N_1,\ldots,N_i$ is found by iterating over the vector of degrees of

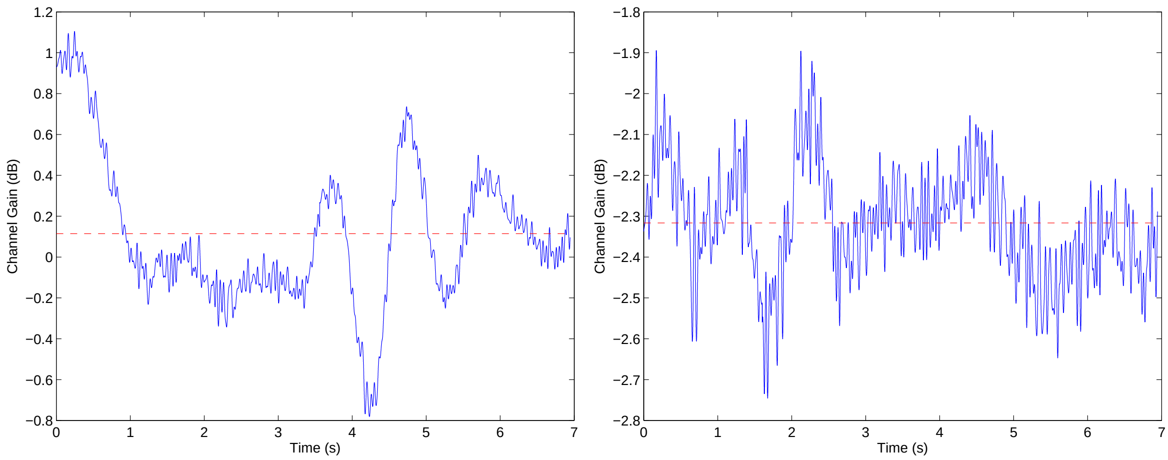

(a) Line of sight fading channel for receiver 2 (b) Deep fading channel for receiver 8

Fig. 5.1 Channel attenuation behavior in a Low height buildings environment.

freedom as follows,

$$\sum_{s=j}^{N_i}(1-P_e(h_s))=i, \qquad \forall P_e(s), \quad s.t. \quad P_e(s):\{P_e(h_k(t_1)),\ldots,P_e(h_k(t_T))\},$$
$$k:\max CT_k, \quad \forall k=\{1,...,K\} \quad (5.6)$$

A similar approach of *Max CT* was proposed to address the XOR network coding multicast scenario for receivers encountering similar erasures in [64], however, the way of completion time is modeled and measured lacks the consideration of packet erasures dependency which is something present in the model [1] with time variation, therefore, besides the difference in coding framework they used, such an assumption is absent in their work.

5.4 Properties of the proposed schemes

In order to clarify the characteristics that distinguish the proposed multicast schemes, we show the numerical results obtained through computer simulations for evaluating the performance of proposed techniques.

To this aim we suppose that the receivers are moving in a random direction with a constant speed equals $5\,\mathrm{m\,s^{-1}}$.

The performance is evaluated in terms of delay, throughput and average number of packets, by considering the on-board satellite transmitter multicasts a maximum batch of

Table 5.1 Summary table of the performance for GEO satellite results.

Rec No.	Ch. att. [dB]	Delay [ms]			Throughput [packet/ s]			Ave. No. of packets			Delay gain		Throughput gain	
		Without virtual.	MaxPe	MaxCT	Without virtual.	MaxPe	MaxCT	Without virtual.	MaxPe	MaxCT	MaxPe	MaxCT	MaxPe	MaxCT
1	0,29	293,83	287,04	287,04	36,35	37,07	37,07	16	17	17	6,79	6,79	0,72	0,72
2	0,11	297,35	292,30	292,30	35,96	36,57	36,57	16	18	18	5,05	5,05	0,61	0,61
3	0,16	295,78	288,31	288,31	36,16	36,93	36,93	16	18	18	7,47	7,47	0,76	0,76
4	-1,14	325,24	317,98	317,99	33,88	34,69	34,69	19	20	20	7,25	7,25	0,81	0,81
5	-0,79	313,15	309,51	309,51	34,72	35,21	35,21	18	19	19	3,64	3,64	0,49	0,49
6	-0,90	318,22	312,95	312,95	34,31	34,97	34,97	18	19	19	5,27	5,27	0,66	0,66
7	-2,22	344,04	340,08	341,48	32,30	32,63	32,56	21	21	21	3,95	2,56	0,33	0,27
8	-2,32	345,92	344,43	345,92	32,19	32,25	32,19	21	21	21	1,49	0,00	0,07	0,00
9	-2,20	342,76	340,21	341,56	32,35	32,60	32,54	21	21	21	2,56	1,20	0,26	0,19
10	-2,18	342,68	339,86	341,14	32,35	32,62	32,56	21	21	21	2,82	1,54	0,27	0,21

Table 5.2 Performance table of the proposed virtual channels for GEO satellite.

Virtual ch. scheme	Virt. rec. No.	Virt. rec. ch. gain [dB]		Non-adaptive Network Coding (NC)						Adaptive Network Coding (ANC)					
				Delay [ms]		Thr. [packet/s]		No. packets		Delay [ms]		Thr. [packet/s]		No. packets	
		Max.	Min.	Max.	Min.	Max.	Min.	Max.	Min.	Max.	Min.	Max.	Min.	Max.	Min.
MaxPe	1,...,10	-2,19	-2,49	1093,5	245,5	40,7	9,1	30	10	504,4	245,5	40,7	19,8	40	10
MaxCT	8	-2,08	-2,49	1116,7	245,5	40,7	8,9	30	10	504,4	245,5	40,7	19,8	40	10

$i = 10$ data packets or degrees of freedom (dof), each of size $B = 10^4$ bits. We consider a data packet of length 0.67 ms.

The application scenario considers one GEO satellite and ten mobile receivers moving on the Earth ground. Thus, each link is characterized by a Round Trip Time (RTT) equal to 0.2388 s.

The receivers are randomly positioned in the reception area so that each one could experience a different channel quality. To this aim we suppose that the receivers are moving in a random direction with a constant speed equal to $5\,\mathrm{m\,s^{-1}}$. In addition, the receivers are supposed to be located within a Low Height Building scenario [51], that considers the presence of three propagation states: line of sight, moderate and deep fading. To this aim, we also suppose that the users are equally distributed within the three states.

The proposed coded multicast schemes are evaluated, and the results are compared with two benchmark schemes: the per-receiver ANC scheme, and per-receiver non-adaptive NC scheme, for time variant channels, proposed in [1].

First, the behavior of channel attenuation is shown with respect to the time by focusing on a time window lasting 7 s. The Fig. 5.1 illustrates an example of channel attenuation for two receivers 2 and 8; one of them is passing through a direct line of sight fading as the case of receiver 2 shown in Fig. 5.1a, while the other passing through deep fading environment as the case of receiver 8 shown in Fig. 5.1b. For ease explanation purposes, we also intend to draw the average attenuation for each channel as a general reference.

As expected receiver 8 suffers from a higher attenuation due to the hypothesis of being in a deep fading environment, while the receiver 2 suffers less attenuation due to less fading

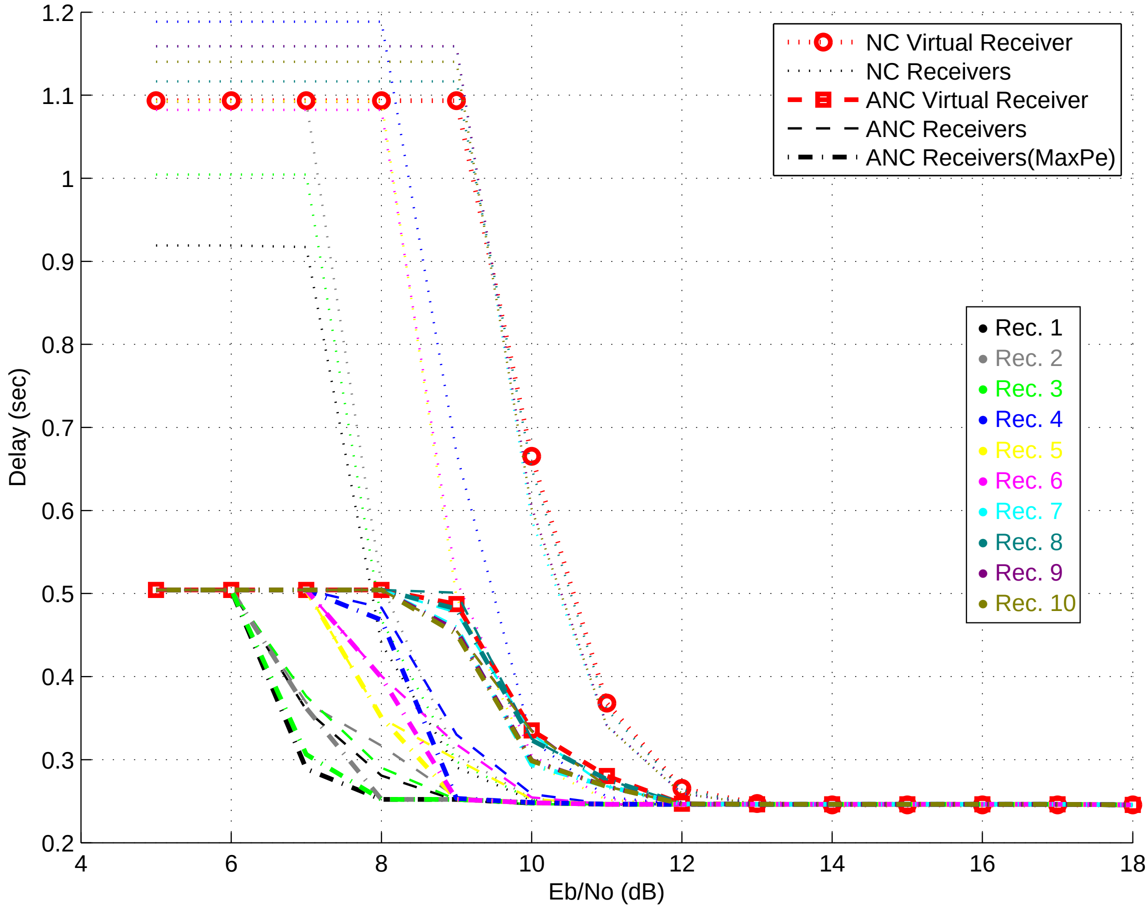

Fig. 5.2 Performance in terms of delay for the Maximum Erasure scheme by considering 10 receivers at different E_b/N_0 values.

within the line of sight channel. In Tab. 5.1, among other numerical values, we can see the average attenuation in the second column suffered by each receiver in the multicast group.

5.4.1 Maximum Packet erasure scheme (*Max Pe*)

In this scheme, we consider a virtualization of the maximum erasure in the system along time. We consider an adaptation of the worst channel conditions among all the receivers at any time instant. This corresponds to a virtual channel composed of behavior instantaneously having the higher attenuation. Such virtual channel can be seen as associated to all receivers suffering the worst channel conditions.

Notice that in the figures, a similar color is used to express a certain receiver, and the same line type is used to express the scheme: dotted with/without circle represents the non-adaptive

NC, dashed with/without rectangle for the ANC, and the dotted-dashed represents the joint ANC with *Max Pe* scheme for coded multicast.

In Fig. 5.2, the performance in terms of delay is shown for ANC and NC under two types of environment; the receivers of the first group are under line of sight fading and moderate shadowing, and the second group of receivers are under deep fading. The saturated values of delay or throughput at the moderate SNRs are resorted to limiting the transmission/retransmission window to a certain threshold of maximum coded packets in the adaptive schemes. The proposed schemes are mainly driven by more transmissions when the channels are worse, unlike silent schemes which main target is energy efficiency, see [37, 36].

As shown in Fig. 5.2, the first group has better performance than those under moderate channels, and so on for the last four receivers. However, it is clear that NC encounters higher delays than ANC for all receivers, and close to the virtual receiver.

The minimum observed delay for the ANC scheme without virtualization is associated to receiver 1, since its associated channel maintains the highest average channel gain among the others, and equals 0.42 dB, as shown in Tab. 5.1.

However, the worst delay performance among receivers multicast group is reported to the receiver 8 that is suffering worst channel. It plays an important role to be a reference of the following *Max CT* scheme.

As anticipated, we can see how the *NC Virtual Receiver* and *ANC Virtual Receiver* experience the highest delay among all NC and ANC receivers, as shown in the first row in Tab. 5.2. Furthermore, it is interesting to see the comparison between ANC receivers, exploiting a per-receiver ANC technique, and ANC receivers with *Max Pe* that are adapting ANC to the virtual receiver channel, also highlighted in the figure.

The following our main observations:

- Receivers under line of sight and moderate fading, are gaining the most in terms of delay. For instance, Tab. 5.1 emphasizes the gain of receiver 6 equals 7.29 ms.
- The receivers under deep fading, i.e., receivers 7 to 10, are still enjoy gains compared to the case without the virtualization scheme albeit in a limited way.

As an example, Fig. 5.3b shows the receiver 8 is gained very little compared to ANC, but for Fig. 5.3b the receiver 2 is gaining a bit more of 50 ms at $E_b/N_0 = 8$ dB.

Therefore, we can see generally that by adapting to a virtual receiver channel, we can gain with respect to the per-receiver schemes.

In Fig. 5.4, the throughput performance is shown; as this figure includes all ten receivers having throughput relatively higher than virtual schemes. Because of the hypothesis for

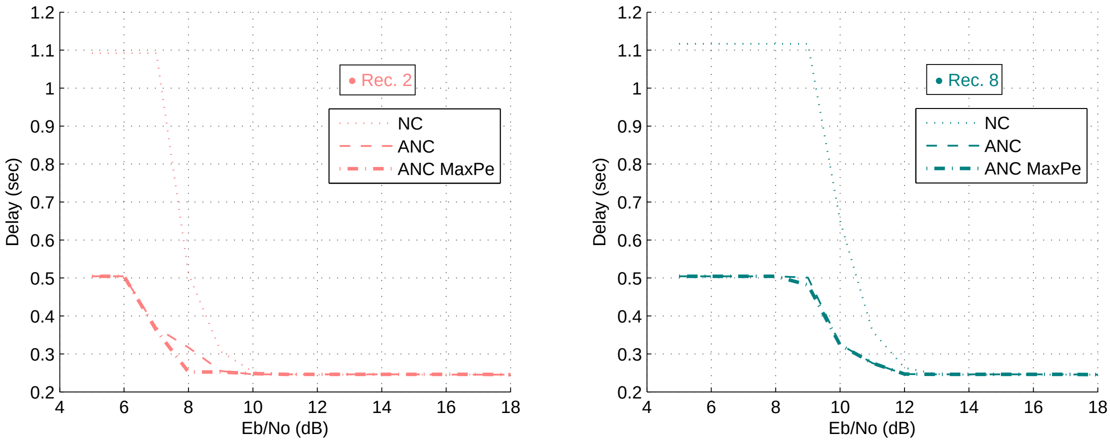

(a) Receiver 2

(b) Receiver 8

Fig. 5.3 Extracted delay performance from Fig. 5.2.

combining the highest erasures probabilities which produces a virtual channel with worst condition.

Receiver 2, by exploiting *Max Pe*, gains roughly up to 8 packet/s at $E_b/N_0 = 8$ dB compared to the mere utilization of ANC scheme. Hence, the maximum throughput gain using the virtual channel is reported at moderate SNR, i.e., at 8 dB. However, Tab. 5.1 show the general behavior and demonstrates the average of throughput gain for receiver 2 is equal to 0.61 packet/s for the SNR range, i.e., $E_b/N_0 = [5\ 18]$ dB. On other hand, receiver 8, suffering deep fading, shows negligible average throughput gain that equals 0.07 packet/s.

Even the Fig. 5.5a show three schemes applied to receiver 2, the Tab. 5.1 has some gains obtained by comparing between only two schemes ANC and *Max Pe*.

However, the second class of receivers suffering deeper fading such as receiver 8 in Fig. 5.5b, the throughput has neither loss nor gain for low SNR, and still gain a bit in moderate SNR.

In general, the throughput performance of *Max Pe* receivers shows some gain with respect to the per-receiver ANC scheme at the moderate SNR values. Of particular relevance is to observe that the receivers with smallest attenuation obtain better in resource allocation for packet transmission. Even for the throughput it is possible to note that there is still some gain for the receivers suffering from deeper fading, even it is limited.

Finally, the performance for average number of packets is shown in Fig. **??**. The reason of results shown in Fig. 5.3a and Fig. 5.5a, in terms of delay and throughput at moderate SNR can be seen as a result of an increase in the average number of transmitted packets.

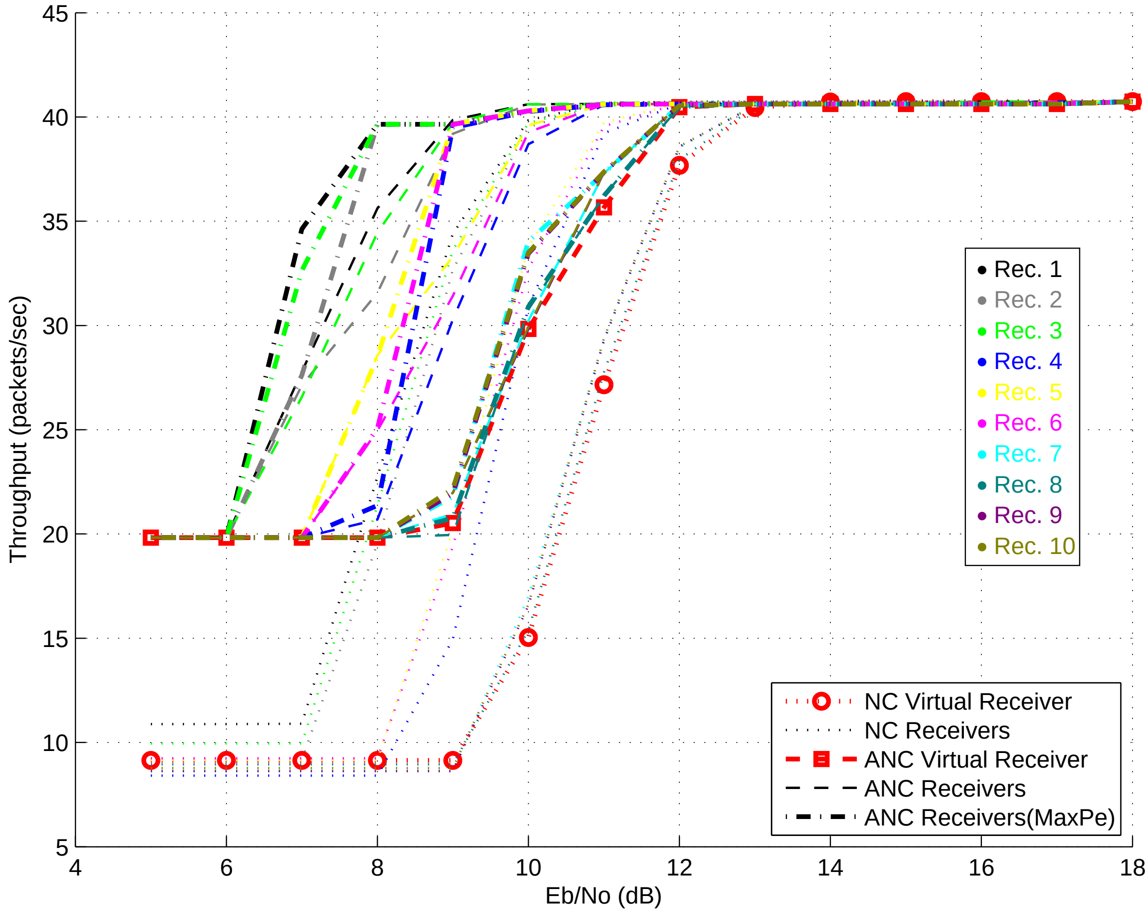

Fig. 5.4 Performance in terms of throughput for the Maximum Erasure scheme by considering 10 receivers at different E_b/N_0 values.

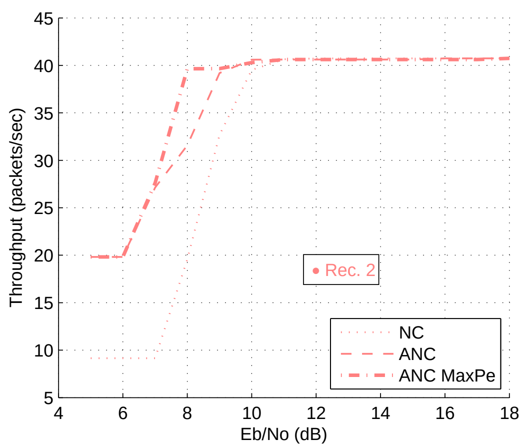

(a) Receiver 2

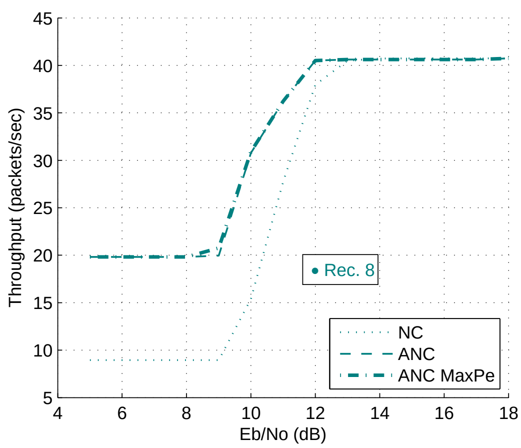

(b) Receiver 8

Fig. 5.5 Extracted throughput performance from Fig. 5.4.

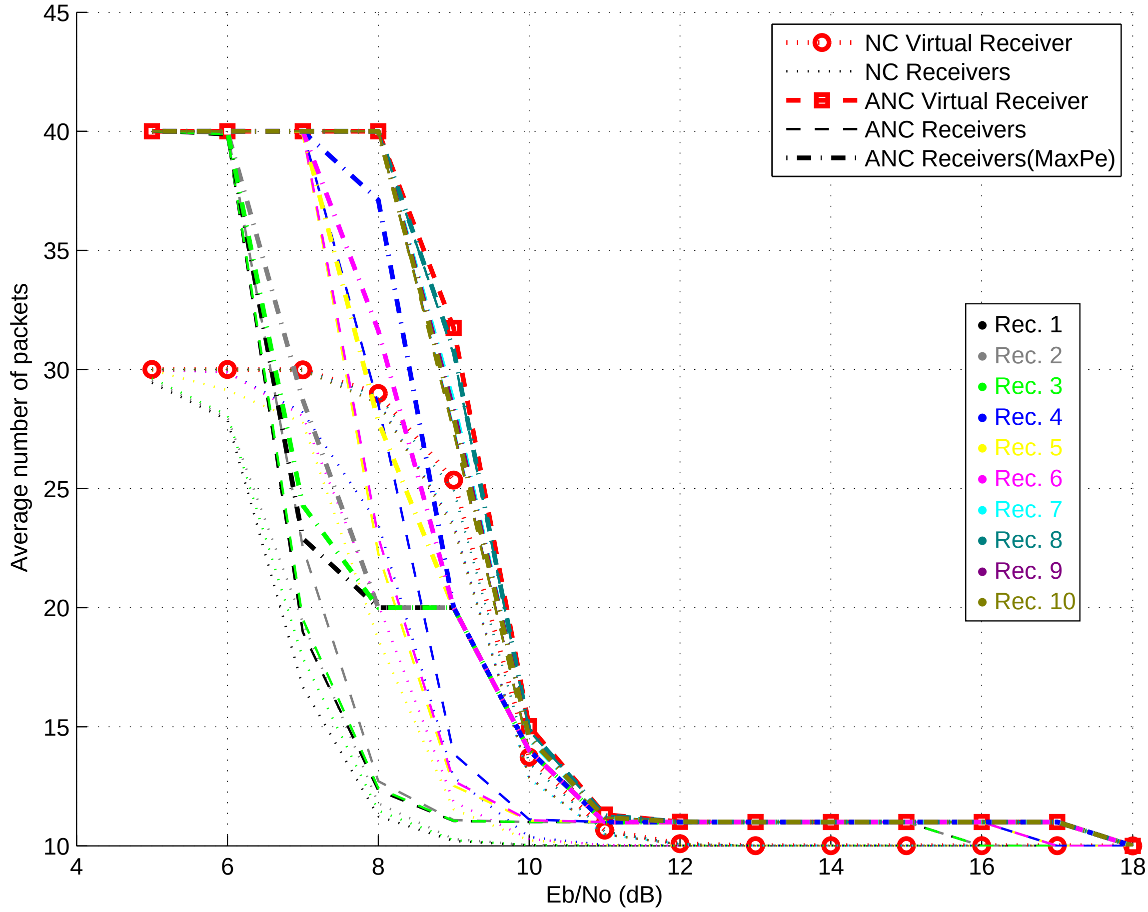

Fig. 5.6 Performance in terms of average number of transmitted packets for the Maximum Erasure scheme by considering 10 receivers at different E_b/N_0 values.

While in Fig. 5.7b shows no such increment as deep fading channel itself doesn't allow for much improving neither delay nor throughput.

It is worth to observe that the increment in average number of packets due to the proposed schemes could be negligible, suggesting that the system behaves almost equivalently in terms of cost transmission (resources) when it is designed for worst case condition.

5.4.2 Maximum Completion Time scheme (*Max CT*)

The performance results of the maximum completion time scheme is shown, where the virtualization is applied by using the channel of that receiver suffering the maximum completion time among all receivers in the multicast group. This channel is considered as the network virtual channel and this receiver becomes a reference receiver to all other receivers

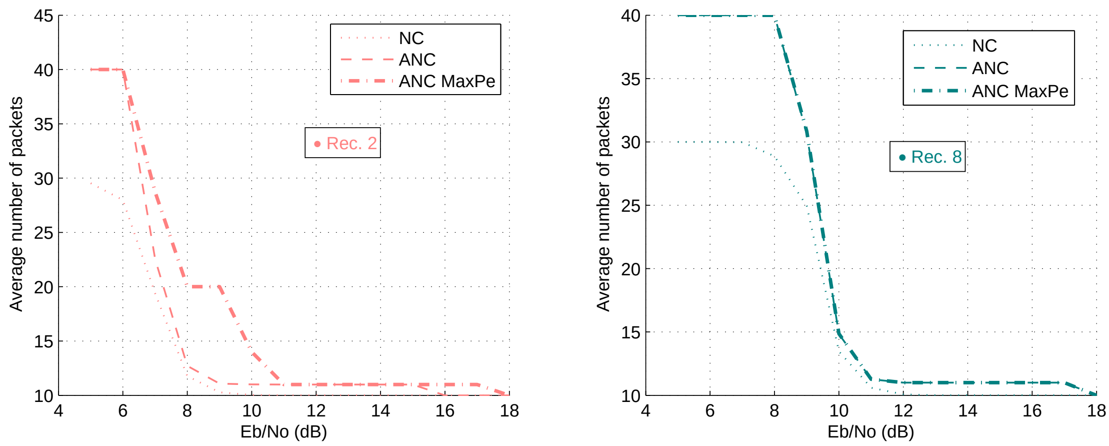

(a) Receiver 2 (b) Receiver 8

Fig. 5.7 Extracted average number of transmitted packets from Fig. 5.6.

in the multicast group to which the system coded transmission will be designed or adapted accordingly.

Tab. 5.1 illustrates that receiver 8 suffers higher completion time compared to other receivers and its average delay equals 608.2 ms. Hence, other receivers are supposed to utilize the ANC transmission strategy of receiver 8 and optimize their transmission of coded packets according to its virtual channel. The performance of the max CT scheme is compared with per-receiver NC and ANC benchmark schemes as was done earlier.

The performance is compared for the NC and ANC applied on a per-receiver basis by each receiver and the application of maximum completion time approach by all the receivers

In Fig. 5.8, illustrates the delay performance of the proposed *max CT* scheme and the benchmark schemes. Moreover, receiver 8 is been utilized as the reference receiver with its channel as the multicast group virtual channel. Similar to the previous set of results, we consider the first group of receivers suffers line of sight and moderate fading, and the second group suffers from deep fading conditions.

The previous section has addressed two examples from the first and third categories, i.e., receivers 2 and 8, respectively. While, here it also good to see the behavior of an example from moderate shadowing. It is possible to note from Fig. 5.11a which presents delay performance of receiver 4. This category has almost the best conditions among the others. Hence, using such scheme has affected delay performance making the receiver to gain 50 ms, i.e., comparing *ANC MaxCT* to ANC scheme.

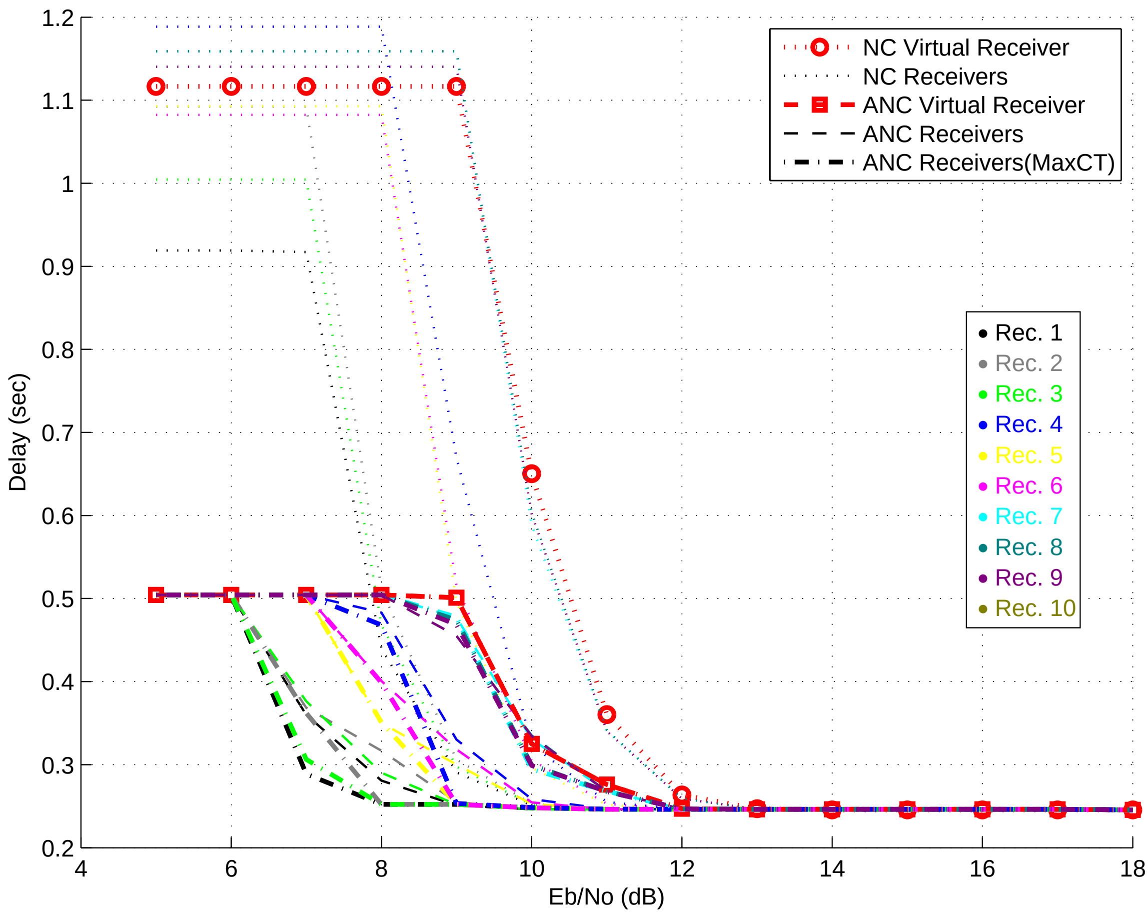

Fig. 5.8 Performance in terms of delay for the Maximum Completion Time scheme by considering 10 receivers at different E_b/N_0 values.

While the values in Tab. 5.1 show the average improvements regarding to this scheme. Actually, Tab. 5.1 presents general overview since its contents are average results and more glance view could be compensated using the extracted figures.

In general, it is possible to note that by using such scheme all the receivers are gaining with respect to the per-receiver application of the ANC. This is even more clear by looking to the values in Tab. 5.1 where the results including delay and throughput gains are shown for each receiver. In turn, the reference gains are limited to the application of ANC scheme on its real channel.

Similarly, in Fig. 5.9, it is possible to see that by using the *Max CT* scheme it is possible to gain with respect to the per-receiver ANC in terms of throughput. However, the performance of receiver 4 in both Tab. 5.1 and Fig. 5.11b show a considerable improvements that can be noted at $E_b/N_0 = 9$ dB.

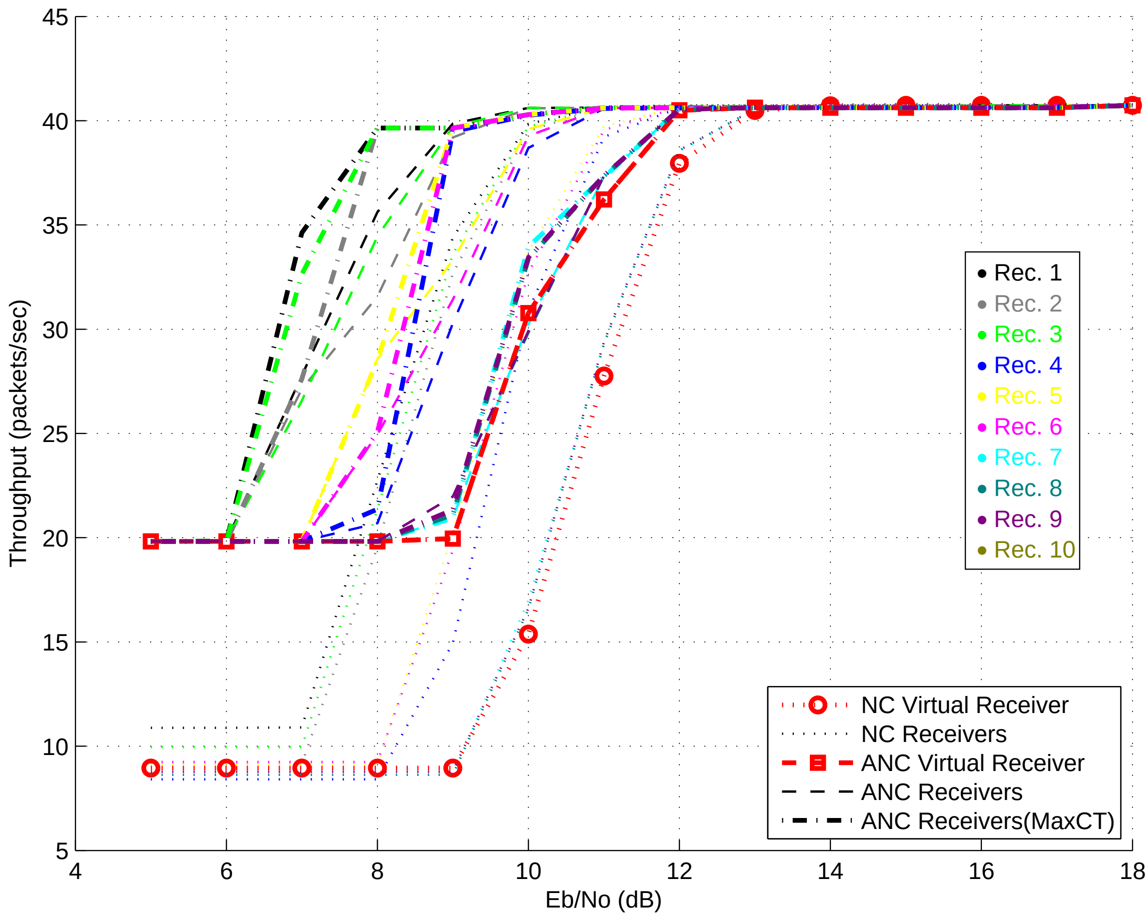

Fig. 5.9 Performance in terms of throughput for the Maximum Completion Time scheme by considering 10 receivers at different E_b/N_0 values.

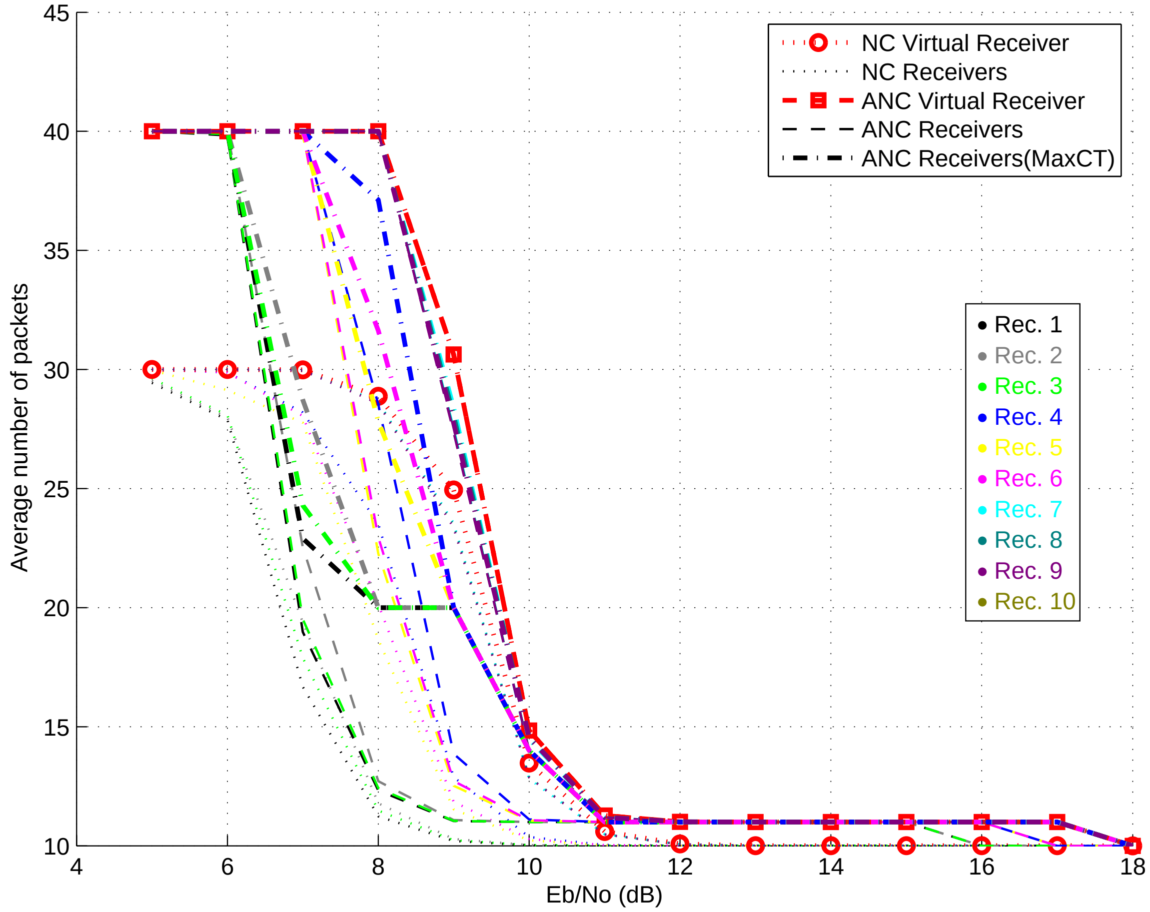

Fig. 5.10 Performance in terms of average number transmitted packets for the Maximum Completion Time scheme by considering 10 receivers at different E_b/N_0 values.

In terms of the average number of sent packets, as shown in Fig. 5.10, it is possible to observe that for the *Max CT* scheme their increases are negligible, suggesting that the system behaves almost the same in terms of costs for transmission (resources) when it is designed for worst case conditions.

5.4.3 Comparison between Maximum Packet erasure and Maximum Completion Time virtualization schemes

Comparing non-adaptive schemes to adaptive ones using *Max Pe* and *Max CT*, we can see a gain of 589.13 ms and 612.3 ms on the max mean completion time, respectively. This bear witness on the gains introduced from making a careful design of the adaptive coded packets, while guaranteeing through both virtualizaton schemes to have the receivers able to decode reliably.

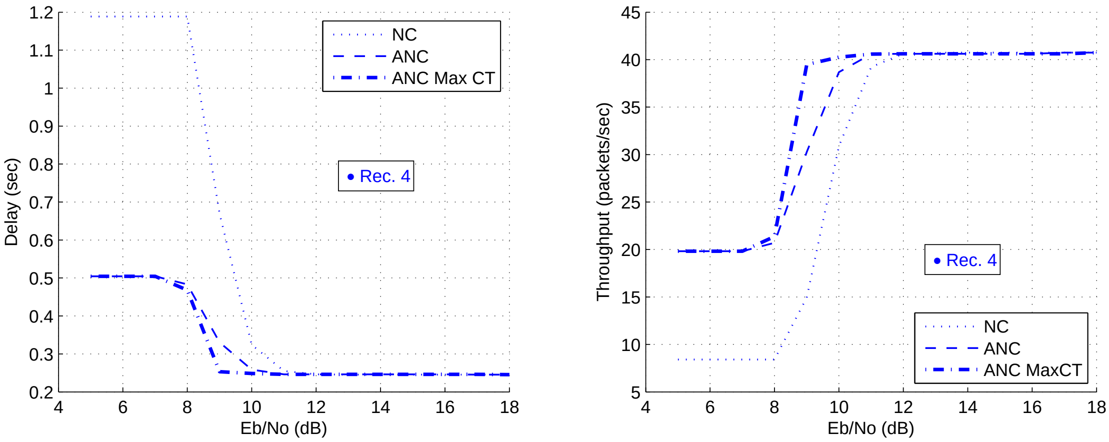

(a) Delay extracted from Fig. 5.8 (b) Throughput extracted from Fig. 5.9

Fig. 5.11 Extracted performance figures of the receiver 4 using *Max CT* scheme .

The maximum erasure scheme takes into account the instantaneous variations at the packet level. In addition, this scheme considers all the receivers' channels over time, and produces a virtual channel to be used by all the receivers involved in the multicast communication. Hence, this scheme allows to improve the performance of all the receivers, especially those suffering higher error rates, and this is the reason why maximum erasure scheme *Max Pe* outperforms the *Max CT* for the case of deep fading.

On the contrary, the maximum completion time scheme considers one receiver having the highest completion time among all the receivers as reference one; this does not take into account instantaneous deep fades that can occur for certain receivers, while working more on a long term horizon.

It is of particular relevance to observe the applicability of the two proposed schemes into systems beyond the satellite application, where receivers on the edge of a cell, or with worst coverage can yet be able to receive reliably the distributed content when the system is adapted to it.

Chapter 6

Conclusions and future research

6.1 Conclusions

This work addresses network coding over time varying channels. We proposed novel schemes that adapted and characterized by physical layer aware. The aim is to optimize packet transmission over time variant channels. The strategy of schemes is based on taking into account the lost degrees of freedom by tracking the packet erasures over time. In addition, defining transmission strategies that allows for gains in packet rate or energy efficiency and finding an optimal coded packets transmission to allow for such conflicting objectives is of particular interest.

To the final aim, in the first part of the work we dealt with rate efficient adaptive network coding schemes by compensating lost degrees of freedom during channel variation over time. A novel adaptive network coding and modulation scheme is proposed.

The second part of this work addresses energy efficient adaptive network coding schemes with time varying channel. Two novel adaptive physical layer aware and energy efficient schemes have been proposed for coded packet transmission over various channel fades. Those schemes compensate for the lost degrees of freedom by tracking the packet erasures over time.

The novelty of such schemes is expressed by the allowance due to smart silence/transmission periods to significant energy savings. At the end of second part, we have underlined that, at SNR values high enough for reliable transmission, the schemes can be switched off to allow more for a reduction in the processing power at the transmitter side.

The novelty of first and second part schemes is expressed by their remarkable rate enhancements and energy savings due to adaption to various factors such as channel quality, that inherently express different sources of variation, shadowing, fading, and mobile speed.

The numerical results have been carried out under different conditions, by considering the impact of packet characterization such as, duration and size of large and small regimes of batch transmissions/retransmissions and also under various fading channels such as, Rician, Rayleigh, and land mobile satellite systems with different SNR values.

In the final part, we propose two network channel virtualization schemes to address the network coding for multicast with time variant channels. The proposed schemes rely on representing the multicast network with a worst performing virtual line network in packet erasure or completion time. The proposed virtualization schemes prove improvements when compared to per-receiver optimization, with and without adaption, while assuring reliable reception by all receivers in the multicast group. Future research will consider dual correlation structure of the underlying multicast.

Moreover, at SNR values, high enough for reliable transmission, the schemes can be switched off to allow for a reduction in the processing power at the transmitter side.

6.2 Future research

Future research will consider complexity analysis of acknowledgment packet erasures and its implication on the overall modeling process, as well as the proposed schemes performance in terms of delay, throughput, and energy consumption.

References

[1] S. A. M. Ghanem, "Network coding mechanisms for Ka-band satellite time varying channel," in *Proc. of 2013 IEEE 24th Annual International Symposium on Personal, Indoor, and Mobile Radio Communications (PIMRC)*, London, UK, Sep. 2013, pp. 3291–3296.

[2] S. Watts and O. G. Aliu, "5g resilient backhaul using integrated satellite networks," in *2014 7th Advanced Satellite Multimedia Systems Conference and the 13th Signal Processing for Space Communications Workshop (ASMS/SPSC)*, Sept 2014, pp. 114–119.

[3] B. G. Evans, "The role of satellites in 5g," in *2014 7th Advanced Satellite Multimedia Systems Conference and the 13th Signal Processing for Space Communications Workshop (ASMS/SPSC)*, Sept 2014, pp. 197–202.

[4] N. Panwar, S. Sharma, and A. K. Singh, "A survey on 5g: The next generation of mobile communication," *Physical Communication*, vol. 18, Part 2, pp. 64 – 84, 2016, special Issue on Radio Access Network Architectures and Resource Management for 5G. [Online]. Available: http://www.sciencedirect.com/science/article/pii/S1874490715000531

[5] T. Spathopoulos, O. Onireti, A. H. Khan, M. A. Imran, and K. Arshad, "Hybrid cognitive satellite terrestrial coverage - a case study for 5g deployment strategies," in *CrownCom*, 2015.

[6] N. Courville, H. Bischl, E. Lutz, A. Svigelj, P. M. Chan, E. Papapetrou, and R. Asorey-Cacheda, "Hybrid satellite/terrestrial networks: State of the art and future perspectives," in *QShine 2007 Workshop: Satellite/Terrestrial Interworking*, ser. IWSTI '07. New York, NY, USA: ACM, 2007, pp. 1:1–1:7. [Online]. Available: http://doi.acm.org/10.1145/1577776.1577777

[7] R. K. Miranda, J. P. C. L. d. Costa, F. Roemer, F. Raschke, T. Eishima, Y. Nakamura, and G. D. Galdo, "Implementation of improved software defined radio modulation scheme and command and telemetry software interface for small satellites in 5g systems," in *ICOF 2016; 19th International Conference on OFDM and Frequency Domain Techniques*, Aug 2016, pp. 1–7.

[8] G. Araniti, I. Bisio, M. D. Sanctis, A. Orsino, and J. Cosmas, "Multimedia content delivery for emerging 5g-satellite networks," *IEEE Transactions on Broadcasting*, vol. 62, no. 1, pp. 10–23, March 2016.

[9] X. Cui, T. A. Gulliver, J. Li, and H. Zhang, “Vehicle positioning using 5g millimeter-wave systems,” *IEEE Access*, vol. 4, pp. 6964–6973, 2016.

[10] B. Sklar, “Rayleigh fading channels in mobile digital communication systems .i. characterization,” *IEEE Communications Magazine*, vol. 35, no. 7, pp. 90–100, Jul 1997.

[11] F. Al-Ogaili and R. M. Shubair, “Millimeter-wave mobile communications for 5g: Challenges and opportunities,” in *2016 IEEE International Symposium on Antennas and Propagation (APSURSI)*, June 2016, pp. 1003–1004.

[12] F. Guidolin and M. Nekovee, “Investigating spectrum sharing between 5g millimeter wave networks and fixed satellite systems,” in *2015 IEEE Globecom Workshops (GC Wkshps)*, Dec 2015, pp. 1–7.

[13] A. Karttunen, C. Gustafson, A. F. Molisch, R. Wang, S. Hur, J. Zhang, and J. Park, “Path loss models with distance-dependent weighted fitting and estimation of censored path loss data,” *IET Microwaves, Antennas Propagation*, vol. 10, no. 14, pp. 1467–1474, 2016.

[14] R. Maaskant, D. J. Bekers, M. J. Arts, W. A. van Cappellen, and M. V. Ivashina, “Evaluation of the radiation efficiency and the noise temperature of low-loss antennas,” *IEEE Antennas and Wireless Propagation Letters*, vol. 8, pp. 1166–1170, 2009.

[15] P. Liu, M. D. Renzo, and A. Springer, “Line-of-sight spatial modulation for indoor mmwave communication at 60 ghz,” *IEEE Transactions on Wireless Communications*, vol. 15, no. 11, pp. 7373–7389, Nov 2016.

[16] T. Hatsuda, Y. Iwamori, M. Kuroda, K. Imai, M. Sasaki, Y. Tsushima, N. Yosimura, T. Zakoji, and K. Kawasaki, “Unique attenuation characteristics of ku-band lune-q antenna for satellite retransmission of terrestrial digital broadcasting signal,” in *2007 IEEE Antennas and Propagation Society International Symposium*, June 2007, pp. 2017–2020.

[17] (ITU), “International telecommunication union’s,radio regulations, section iv. radio stations and systems,” article 1.166.

[18] (Sue, M.K), “"radio frequency interference at the geostationary orbit". nasa. jet propulsion laboratory. retrieved 6 october 2011.” https://ntrs.nasa.gov/archive/nasa/casi.ntrs.nasa.gov/19810018807.pdf.

[19] M. Allman, D. Glover, and L. Sanchez, “Enhancing TCP Over Satellite Channels using Standard Mechanisms,” RFC 2488 (Best Current Practice), Internet Engineering Task Force, January 1999. [Online]. Available: http://www.ietf.org/rfc/rfc2488.txt

[20] M. G. Matossian, *A Teledesic Space Infrastructure Overview*. Dordrecht: Springer Netherlands, 1998, pp. 153–156. [Online]. Available: http://dx.doi.org/10.1007/978-94-011-5088-0_14

[21] L. Wood, Y. Lou, and O. Olusola, “Revisiting elliptical satellite orbits to enhance the o3b constellation.” *CoRR*, vol. abs/1407.2521, 2014. [Online]. Available: http://dblp.uni-trier.de/db/journals/corr/corr1407.html#WoodLO14

[22] R. Ahlswede, N. Cai, S. Y. R. Li, and R. W. Yeung, "Network information flow," vol. 46, no. 4, pp. 1204–1216, Jul. 2000.

[23] P. Torres Compta, F. H. P. Fitzek, and D. E. Lucani, "Network coding is the 5G key enabling technology: effects and strategies to manage heterogeneous packet lengths," *Transactions on Emerging Telecommunications Technologies*, vol. 26, no. 1, pp. 46–55, Jan. 2015.

[24] Y. Chen, S. Kishore, and J. Li, "Wireless diversity through network coding," in *Proc. of 2006 IEEE Wireless Communications and Networking Conference (WCNC 2006)*, vol. 3, Las Vegas, NV, USA, Apr. 2006, pp. 1681–1686.

[25] S. Gollakota and D. Katabi, "Zigzag decoding: combating hidden terminals in wireless networks," in *Proc. of the ACM SIGCOMM 2008 conference on Data communication*. Seattle, WA, USA: ACM, Aug. 2008, pp. 159–170.

[26] S. Katti, D. Katabi, W. Hu, H. Rahul, and M. Medard, "The importance of being opportunistic: Practical network coding for wireless environments," in *Proc. of 43rd Annual Allerton Conference on Communication, Control and Computing*, vol. 2, Monticello, IL, USA, Sep. 2005, pp. 756–765.

[27] M. Xiao and M. Skoglund, "On network coding with finite channel state information," in *2011 8th International Symposium on Wireless Communication Systems (ISWCS)*, Aachen, Germany, Nov. 2011, pp. 487–491.

[28] B. Shrader, A. Babikyan, N. Jones, T. Shake, and A. Worthen, "Rate control for network-coded multipath relaying with time-varying connectivity," vol. 29, no. 5, pp. 1106–1117, May 2011.

[29] D. Lucani and J. Kliewer, "On the delay and energy performance in coded two-hop line networks with bursty erasures," in *2011 8th International Symposium on Wireless Communication Systems (ISWCS)*, Aachen, Germany, Nov. 2011, pp. 502–506.

[30] C. Fragouli, J. Widmer, and J. Y. L. Boudec, "A network coding approach to energy efficient broadcasting: From theory to practice," in *Proc. of 25th IEEE International Conference on Computer Communications (IEEE INFOCOM 2006)*, Apr. 2006, pp. 1–11.

[31] S. Y. R. Li, R. W. Yeung, and N. Cai, "Linear network coding," *IEEE Transactions on Information Theory*, vol. 49, no. 2, pp. 371–381, Feb 2003.

[32] T. Ho, M. Medard, R. Koetter, D. R. Karger, M. Effros, J. Shi, and B. Leong, "A random linear network coding approach to multicast," *IEEE Transactions on Information Theory*, vol. 52, no. 10, pp. 4413–4430, Oct 2006.

[33] D. C. Adams, J. Du, M. Médard, and C. C. Yu, "Delay constrained throughput-reliability tradeoff in network-coded wireless systems," in *2014 IEEE Global Communications Conference*, Dec 2014, pp. 1590–1595.

[34] M. Xiao, M. Medard, and T. Aulin, "Cross-layer design of rateless random network codes for delay optimization," *IEEE Transactions on Communications*, vol. 59, no. 12, pp. 3311–3322, December 2011.

[35] J. Cloud and M. Médard, "Network coding over SATCOM: Lessons learned," in *Wireless and Satellite Systems: 7th International Conference, WiSATS 2015, Bradford, UK, July 6-7, 2015. Revised Selected Papers*, P. Pillai, Y. F. Hu, I. Otung, and G. Giambene, Eds. Cham, Switzerland: Springer International Publishing, 2015, pp. 272–285.

[36] A. E. Gharsellaoui, S. A. M. Ghanem, D. Tarchi, and A. Vanelli-Coralli, "Adaptive network coding schemes for satellite communications," in *2016 8th Advanced Satellite Multimedia Systems Conference and the 14th Signal Processing for Space Communications Workshop (ASMS/SPSC)*, Sept 2016, pp. 1–7.

[37] A. Gharsellaoui, S. A. M. Ghanem, D. Tarchi, and A. Vanelli-Coralli, "Energy efficient adaptive network coding schemes for satellite scenarios," in *8th EAI International Conference on Wireless and Satellite Systems (formerly PSATS)*, Cardiff, UK, Sep. 2016.

[38] S. Katti, H. Rahul, W. Hu, D. Katabi, M. Médard, and J. Crowcroft, "XORs in the air: Practical wireless network coding," in *Proceedings of the 2006 Conference on Applications, Technologies, Architectures, and Protocols for Computer Communications*, ser. SIGCOMM '06. New York, NY, USA: ACM, 2006, pp. 243–254.

[39] S. Chachulski, M. Jennings, S. Katti, and D. Katabi, "Trading structure for randomness in wireless opportunistic routing," in *Proceedings of the 2007 Conference on Applications, Technologies, Architectures, and Protocols for Computer Communications*, ser. SIGCOMM '07. New York, NY, USA: ACM, 2007, pp. 169–180.

[40] J. Krigslund, J. Hansen, M. Hundeboll, D. E. Lucani, and F. H. P. Fitzek, "CORE: COPE with MORE in wireless meshed networks," in *2013 IEEE 77th Vehicular Technology Conference (VTC Spring)*, Dresden, Germany, Jun. 2013.

[41] C. Fragouli, J.-Y. Le Boudec, and J. Widmer, "Network coding: An instant primer," *SIGCOMM Comput. Commun. Rev.*, vol. 36, no. 1, pp. 63–68, Jan. 2006.

[42] P. A. Chou, Y. Wu, and K. Jain, "Practical network coding," 2003. [Online]. Available: http://citeseer.ist.psu.edu/viewdoc/summary?doi=10.1.1.11.697

[43] T. De Cola, D. Tarchi, and A. Vanelli-Coralli, "Future trends in broadband satellite communications: information centric networks and enabling technologies," *International Journal of Satellite Communications and Networking*, vol. 33, no. 5, pp. 473–490, 2015.

[44] "The role of satellites in 5G," NetWorld2020 ETP - SatCom WG, White paper, Jul. 2014. [Online]. Available: http://www.networld2020.eu/wp-content/uploads/2014/02/SatCom-in-5G_v5.pdf

[45] R. W. Yeung, "Avalanche: A network coding analysis," *Communications in Information & Systems*, vol. 7, no. 4, pp. 353–358, 2007. [Online]. Available: http://projecteuclid.org/euclid.cis/1211574971

[46] M. Wang and B. Li, "R2: Random push with random network coding in live peer-to-peer streaming," vol. 25, no. 9, pp. 1655–1666, Dec. 2007.

[47] G. Altay, "Broadcast multicast capacity of network coding for random wireless networks," *IET Communications*, vol. 4, no. 12, pp. 1495–1503, Aug. 2010.

[48] F. Alagoz and G. Gur, “Energy efficiency and satellite networking: A holistic overview,” *Proceedings of the IEEE*, vol. 99, no. 11, pp. 1954–1979, Nov. 2011.

[49] D. E. Lucani and J. Kliewer, “On the delay and energy performance in coded two-hop line networks with bursty erasures,” in *Proc. of 2011 8th International Symposium on Wireless Communication Systems (ISWCS)*, Nov. 2011, pp. 502–506.

[50] D. E. Lucani, M. Stojanovic, and M. Medard, “Random linear network coding for time division duplexing: When to stop talking and start listening,” in *IEEE INFOCOM 2009*, April 2009, pp. 1800–1808.

[51] F. P. Fontan, M. Vazquez-Castro, C. E. Cabado, J. P. Garcia, and E. Kubista, “Statistical modeling of the LMS channel,” *IEEE Transactions on Vehicular Technology*, vol. 50, no. 6, pp. 1549–1567, Nov. 2001.

[52] C. Loo, “A statistical model for a land mobile satellite link,” *IEEE Transactions on Vehicular Technology*, vol. 34, no. 3, pp. 122–127, Aug. 1985.

[53] X. Wang, W. Wang, Y. Zhang, K. Sun, and L. Li, “On orbit satellite fuel consumption optimization with analytic hierarchy process method,” in *2016 22nd International Conference on Automation and Computing (ICAC)*, Sept 2016, pp. 440–443.

[54] E. Kieffer, A. Stathakis, G. Danoy, P. Bouvry, E. G. Talbi, and G. Morelli, “Multi-objective evolutionary approach for the satellite payload power optimization problem,” in *2014 IEEE Symposium on Computational Intelligence in Multi-Criteria Decision-Making (MCDM)*, Dec 2014, pp. 202–209.

[55] H. Fenech, S. Amos, A. Tomatis, and V. Soumpholphakdy, “High throughput satellite systems: An analytical approach,” *IEEE Transactions on Aerospace and Electronic Systems*, vol. 51, no. 1, pp. 192–202, January 2015.

[56] J. Barros, R. A. Costa, D. Munaretto, and J. Widmer, “Effective delay control in online network coding,” in *IEEE INFOCOM 2009*, April 2009, pp. 208–216.

[57] Y. E. Sagduyu and A. Ephremides, “On broadcast stability of queue-based dynamic network coding over erasure channels,” *IEEE Transactions on Information Theory*, vol. 55, no. 12, pp. 5463–5478, Dec 2009.

[58] R. Dougherty, C. Freiling, and K. Zeger, “Insufficiency of linear coding in network information flow,” *IEEE Transactions on Information Theory*, vol. 51, no. 8, pp. 2745–2759, Aug 2005.

[59] T. Ho, R. Koetter, M. Medard, D. R. Karger, and M. Effros, “The benefits of coding over routing in a randomized setting,” in *IEEE International Symposium on Information Theory, 2003. Proceedings.*, June 2003, pp. 442–.

[60] A. Fiandrotti, V. Bioglio, M. Grangetto, R. Gaeta, and E. Magli, “Band codes for energy-efficient network coding with application to p2p mobile streaming,” *IEEE Transactions on Multimedia*, vol. 16, no. 2, pp. 521–532, Feb 2014.

[61] S. Ferguson, M. Miller, B. Sievers, R. Utz, B. Wynne, J. Reed, and B. Kutter, “Fuel cell power system development for lox/lh/2 upper stage,” in *2016 IEEE Aerospace Conference*, March 2016, pp. 1–9.

[62] M. Ghaderi, D. Towsley, and J. Kurose, “Network coding performance for reliable multicast,” in *MILCOM 2007 - IEEE Military Communications Conference*, Orlando, FL, USA, Oct. 2007.

[63] R. Koetter, M. Effros, and M. Medard, “A theory of network equivalence – Part I: Point-to-point channels,” vol. 57, no. 2, pp. 972–995, Feb. 2011.

[64] A. Douik, S. Sorour, M. S. Alouini, and T. Y. Al-Naffouri, “Completion time reduction in instantly decodable network coding through decoding delay control,” in *2014 IEEE Global Communications Conference*, Austin, TX, USA, Dec. 2014, pp. 5008–5013.